SPATIAL PATTERNS AND IMPACTS OF SLOPE FAILURES IN FIVE CANYONS OF THE TETON MOUNTAINS, GRAND TETON NATIONAL PARK, WYOMING

by

WILLIAM DAVID BUTLER

B.S., Texas State University, 2010

A THESIS

submitted in partial fulfillment of the requirements for the degree

MASTER OF ARTS

Department of Geography
College of Arts and Sciences

KANSAS STATE UNIVERSITY
Manhattan, Kansas

2013

Approved by:

Major Professor
Dr. Richard Marston

ABSTRACT

Slope failures play a significant role as a mass movement hazard in the deglaciated mountain canyons in Grand Teton National Park. The park's geologic and glacial histories are unique in comparison to other areas in the Rocky Mountain range. However, few detailed maps and statistical analyses of slope failures as hazards exist for park officials and visitors. The purpose of this study is to produce a comprehensive map of slope failures in five of the most accessible and commonly used canyons of the park: Cascade, Death, Garnet, Granite, and Paintbrush.

This project combined fieldwork, LiDAR imagery, and GIS mapping to document five main categories of slope failures—rock slides, rock/debris flows, rock falls, and snow avalanches, as well as complex slope failures involving a combination of these categories. Summary statistics, maps, and histograms of average slope gradient, aspect, and curvature conditions as well as precipitation conditions at the "source" area of slope failures were generated for individual canyons as well as the entire study area. Snow avalanche source areas where debris flows were not readily present occurred most commonly on north and northeast facing slopes, slopes averaging a 40% gradient, and slightly convex slopes. Debris flow source areas occurred most commonly on south and southeast facing slopes, slopes with an average 42% gradient, and on slightly convex slopes. Rock fall source areas were most common on north facing slopes, slopes of an average 55% gradient, and a mostly flat curvature. Rock slide source points were most common on north facing slopes, slopes of an average 54% gradient, and flat to slightly concave slopes. Rock Mass Strength (RMS) values were sampled at a rate of every 0.5

kilometers on the hiking trail of each canyon to provide an introductory insight into rock stability conditions in each canyon.

Slope failures not only impact the physical landscape of canyons in Grand Teton National Park but can affect human structures as well. Physical attributes and locations of slope failures were compared to locations of camping zones and hiking trails in the Park to determine areas of common human usage that were most susceptible to past movement events.

TABLE OF CONTENTS

LIST OF FIGURES

Appendix

LIST OF TABLES

ACKNOWLEDGEMENTS

I would first of all like to thank my primary advisor Dr. Richard Marston for his expert guidance, support, and constant interest in my progress despite a hectic two years for him working at the US State Department and as head of the KSU Department of Geography. He helped provide me the inspiration to turn a wonderful trip to the UW-NPS Research Center into a thesis project and took care of the logistics to make the trip possible. I would also like to thank my fellow field assistant Brandon Weihs for his assistance and collaboration throughout the course of this project. Thanks to my other advisors, Dr. Bimal Paul for providing his expertise on statistics and natural disasters and Dr. Shawn Hutchinson for his providing his expertise in everything GIS-related. Thank you to other non-committee faculty members who provided instruction, advice, and support throughout my time at KSU.

The next group of people I need to thank is everyone at the University of Wyoming – National Park Research Center. Thanks to Kathy Mellander and Celeste Havener for their assistance in providing data and logistical support throughout this project, the National Park Service Rangers at Jenny Lake and Moose, as well as Hank Harlow and the entire UW-NPS Research Center staff for providing a world-class research facility to base this project out of.

Thanks to all of the grad students, classmates, officemates, and friends involved in keeping me on track and occasionally providing a bit of much-needed sanity throughout this process: Amy Hathaway, Jedidiah Riley, Savannah and Gaelan McKillip, Miles Valliant, Alexandria Cook, Brittni Taylor, Dalton Sweat, Alexandra Schorn, and Rachel Cavin.

Finally, and most importantly, thanks to my parents, Dr. David Butler and Dr. Janet Butler, for providing a constant, loving, much-needed supply of support throughout my time at KSU. Without your help, this thesis would not have been possible.

CHAPTER 1 - INTRODUCTION

Approximately 2.7 million people visited Grand Teton National Park in 2010 (National Park Service, 2010), and thousands of these visitors made use of the numerous hiking trails that ascend into the glacially carved, parabola-shaped canyons of the park. Slope failures occur in these canyons regularly, and these failures can have profound impacts on hikers and on human-built structures such as hiking trails and campgrounds. Grand Teton National Park is, therefore, an important place to study interactions between the natural environment and humans as well as human-built structures.

A main purpose of this study is to map slope failures—debris and rock flows, rock falls, rock slides, and snow avalanches, as well as complex slope failures that exhibit two or more of these processes—that are present in the Park using both GIS technology and *in situ* fieldwork. These previously occurring slope failures have encroached into areas of human activity (such as campsites and hiking trails) in the Park, and this study locates where these events have taken place. Another aim of this research is to document the geomorphologic conditions in locations where slope failures have occurred. Knowing what conditions are common in the vicinity of slope failures in Grand Teton National Park (GTNP) may help to provide a better understanding of what areas might be at risk of experiencing a future slope failure event. Finally, this predictive model can be compared to current locations of human structures, and we can note which of these structures may be at the most potential risk.

The human impacts of snow avalanches, debris flows, and rock falls are potentially enormous. Snow avalanches have caused up to $2 million in property damages and killed up to 90 people in individual events in the United States (Armstrong and Williams, 1986); debris flows have caused millions of dollars in damages in western states such as Utah and California (Jakob

and Hungr, 2005b, p. 37); and rock falls, while often not as spatially extensive as debris flows or snow avalanches, can also be potentially dangerous: 10 people have been killed and 20 people have been injured in Yosemite National Park alone from rock falls from 1857-2002 (Guzzetti et al., 2003). The nearby 1925 Gros Ventre slide, while not within the borders of GTNP, moved 50 million tons of material and dammed up the Gros Ventre River to form Lower Slide Lake (Forest Service, n.d.). Two years later, the dam burst and flooded the valley, killing six people (Forest Service, n.d.). Grand Teton National Park has also experienced slope failures that have wreaked havoc on Park staff and visitors; these incidents are covered in more detail in section 3.1c.

The products from this project are: maps of the slope failures located in five specific canyons in the GTNP (produced in ArcMap 9.3 and 10); a preliminary analysis of potential *hot spots* of future slope failure activity; and an analysis of human structures, specifically hiking trails and camping *zones* where hikers can camp for the night in any area off the trail.
Two desired outcomes of this research are to increase the scientific community's knowledge base of the spatial distribution of slope failures in GTNP and to assist the National Park Service in formulating park policies that address slope failure events and their potential threats toward park visitors by conveying these distributions. By addressing these questions, this research will hopefully be considered useful to geomorphologists and other interested parties in academia, park officials, visitors, and others considered beyond the purview of traditional academic circles.

Three research questions and seven hypotheses have been incorporated into this study in order to address the components of GIS mapping, slope failure geomorphic characteristics, field work examining local rock stability, and human-environment interactions between slope failures and human structures in the five canyon study area of Grand Teton National Park. The seven hypotheses have been listed in the form of a null hypothesis.

1.1 Research Questions and Hypotheses

The primary research questions in this study are:

1. Where do slope failures occur in deglaciated parabolic canyons in Grand Teton National Park?
2. What are the local characteristics of geomorphological variables that may affect the distributions of slope failures?
3. How do slope failure events currently and potentially impact human activities in the five-canyon study area?

The hypotheses for this study are as follows:

1. Results for chi-square analysis of slope gradient data (deg.) for slope failures located in watersheds in Cascade, Death, Garnet, Granite, and Paintbrush canyons will not be significant at the $p = .05$ level in explaining slope failure distributions.
2. Results for chi-square analysis of slope aspect data (deg.) for slope failures located in watersheds in Cascade, Death, Garnet, Granite, and Paintbrush canyons will not be significant at the $p = .05$ level in explaining slope failure distributions.
3. Results for chi-square analysis of slope curvature data for slope failures located in watersheds in Cascade, Death, Garnet, Granite, and Paintbrush canyons will not be significant at the $p = .05$ level in explaining slope failure distributions.
4. Results for chi-square analysis of average annual precipitation data (in./y.) for slope failures located in watersheds in Cascade, Death, Garnet, Granite, and Paintbrush canyons will not be significant at the $p = .05$ level in explaining slope failure distributions.

5. Results for chi-square analysis of rock type data for slope failures located in watersheds in Cascade, Death, Garnet, Granite, and Paintbrush canyons will not be significant at the p = .05 level in explaining slope failure distributions.
6. Results for chi-square analysis of distance from the Teton Fault data for slope failures located in watersheds in Cascade, Death, Garnet, Granite, and Paintbrush canyons will not be significant at the p = .05 level in explaining slope failure distributions.
7. Results for chi-square analysis of trimline position data for slope failures located in watersheds in Cascade, Death, Garnet, Granite, and Paintbrush canyons will not be significant at the p = .05 level in explaining slope failure distributions.

1.2 Thesis Outline

The following parts of this project include:

- A literature review chronicling past research on characteristics of slope failures, past slope failures in Grand Teton National Park, and the dearth of current research on slope failures in the Park.
- A methods section detailing the field work, GIS and slope failure mapping, statistical analyses, and human-environment interactions components of this project.
- A results and discussion chapter split into sections addressing GIS mapping of slope failures in Grand Teton National Park, statistical analysis of geomorphic characteristics of slope failures in GTNP, RMS (field work) results and analysis, and mapping of interactions between slope failures and human structures.

- A conclusions chapter summarizing the results and how they address the hypotheses and research questions in Chapter 1, as well as suggested future research/recommendations and potential improvements to this study.

CHAPTER 2 – LITERATURE REVIEW

2.1 What is a slope failure?

Multiple terms have been used to describe a large movement of natural materials moving down a slope: landslides, mass movements, and slope failures are among the most commonly (and sometimes interchangeably) used in the literature. Gerrard (1994, p. 221) defined a landslide as "a major world-wide hazard…greatest in areas of weak rock and steep slopes. An external trigger, such as heavy rainfall, slope undercutting, or seismic activity initiates the process." A widespread seismic event can destabilize slopes across an entire region if the event is large enough and can increase the possibility of future slope failures (Keefer, 1994). The word *landslide* is often used in the literature as a catch-all term to describe any type of natural material—rocks, soil, general debris—moving *en masse* down a slope, but this term is somewhat of a misnomer because of the singular mechanism of movement—sliding—that is implied within the word. Varnes (1958) noted that materials can not only slide but fall or even flow down a hill and took the first step toward making a more accurate classification system of these types of events by introducing terms such as debris flows, rock falls, soil creep, debris avalanches, etc. Table 3.1 in the Methods section shows a more advanced and organized slope failure classification system developed by Varnes (1978), and this will be the main reference point for classifying three main types of slope failures that would normally fall under the *landslides* term: debris flows, rock falls, and rock slides.

Snow avalanches also may be classified as a type of slope failure where snow is the primary material being transported *en masse* down a slope (Luckman, 1977; Armstrong and Williams, 1986; Alexander, 1993; also see "Definitions of Types of Slope Failures, Snow Avalanches" section); however, they are not considered to be a type of *landslide*. Whereas soil,

rocks, and debris such as trees can be moved down a slope during a snow avalanche (Armstrong and Williams, 1986), the predominant nature of the mass movement of snow during an event precludes snow avalanches from being included with the traditional definition of landslides in the literature. Snow avalanches also impact landscapes in vastly different ways from flows, falls, or slides (see "Definitions and Physical Identifiers of Slope Failures – Snow Avalanches" section) so they are often treated as a separate type of phenomenon in most of the literature. However, for the sake of convenience of providing a look at all slope failures in the five-canyon study area in GTNP, snow avalanches, falls, flows, and slides will be combined together in this study and designated an individual type of slope failure.

2.2 Definitions and Physical Identifiers of Slope Failures

2.2a Debris Flows

Debris flows occur in many mountainous regions and national parks in the American west (VanDine, 1985; Butler and Malanson, 1996; Vaughn, 1997; Walsh and Butler, 1997; Butler et al., 1998), and Grand Teton National Park is no exception. One of the first definitions for debris flows comes from the Stiny (1910, p. 106) monograph in *Die Muren* (Debris Flow), which describes them as "a flood in a mountain torrent, carrying suspended load, and transporting quantities of bedload. At a certain limit (of sediment carried by the flow), it has changed into a viscous mass consisting of water, soil, sand, gravel, rocks, and wood mixed together, which flows like a lava into the valley." Johnson (1970) classified debris flows as "gravity-induced mass movement" that is "intermediate between landsliding and waterflooding," differentiating the slurry that a debris flow creates from water-dominated and rock-dominated downward movements. A modern definition of debris flows by Abanco et al. (2012, p. 4871) posits that they are "fast movements formed by a mixture of water, solids (sand, boulders, gravel,

and silt) and, on some occasions, woody debris." A slight change from Stiny's definition of debris flow behavior was offered by Johnson and Rodine (1984) who stated that a debris flow's behavior is similar to that of liquid concrete. Varnes (1978) stated that the soil texture of debris flows is predominantly coarse, although they are obviously finer in comparison to other mass movements such as rock falls or slides.

Despite occasional differences in the minutiae of debris flow details—such as particle size, debris type, and flow behaviors during movement—a general acceptance exists in the literature that a debris flow takes solid earthen materials and a liquid catalyst in order to travel down a steep slope. The debris flow travels down the slope in a coarse, viscous mixture thicker than water or mud. Table 2.1 lists the myriad definitions of debris flows that have been published in the literature.

Table 2.1: Various definitions of debris flows adapted from the literature

Definition of Debris Flow	Source
A flood in a mountain torrent, carrying suspended load, and transporting quantities of bedload. At a certain limit (of sediment carried by the flow) it has changed into a viscous mass consisting of water, soil, sand, gravel, rocks, and wood mixed together, which flows like a lava into the valley	Stiny (1910)
A gravity-induced mass movement involving a body of granular solids, water, and air.	Johnson (1970)
A form of rapid mass movement involving a body of granular solids, water, and air.	Varnes (1978)
A moving mass of mud, soil, and rock with more than half of the particles greater than sand size.	Bates and Jackson (1984)
They are initiated by the sudden collapse of bank material and consist of a mixture of fine material, coarse material, and water that moves downhill, often in surges, caused by gravity.	Corominas et al. (1996)
They involve complex processes including fluidization, liquefaction, remoulding, cohesionless grain flow, and possibly air lubrication and are transitional between streamflow and rockfall	Thomas and Goudie (2000)
Debris flow was defined as a slurry, or mixture, of soil, water, rock, and other debris that is transferred downhill by the force of gravity.	Wilkerson (2004)
Fast movements formed by a mixture of water, solids (sand, boulders, gravel, and silt) and, on some occasions, woody debris.	Abanco et al. (2012)

2.2b Snow Avalanches

Snow avalanches are the most frequent catastrophic mass movement in the United States (Walsh et al., 1990, p. 615), and they are certainly present in deglaciated canyons in Grand Teton National Park as well (Patten and Knight, 1994). Alexander (1993) defined the movement of snow avalanches as the result of snow packs on slopes experiencing structural instability to the point of snow movement. Hopfinger (1983, p. 5) attributes this instability to "weak substratum layers consisting of coarse crystals with very weak intergranular bonds," otherwise known as depth hoar. The most common *trigger* of an avalanche is cited by Hopfinger (1983, p. 52) as an avalanche's accumulation of snow or *bed* on a slope, increasing in weight during a snowstorm and eventually experiencing a release that causes the bed to cascade downward.

Figure 2.1: Examples of snow avalanche paths in Cascade Canyon, Grand Teton National Park, Wyoming. Note the stark contrast of low-growth, light-colored vegetation of the avalanche paths in comparison with the high-growth conifer forests next to the paths.

Other release mechanisms for snow avalanches include "ski loads, falling cornices, earthquakes, and artificial triggering caused by human activity" (Hopfinger, 1983, p. 51). Snow avalanches can erode and transport various materials such as snow, vegetation, rocks, and soil across a landscape, although they are not always as effective of a geomorphic agent as a debris flow or rock fall (Butler et al., 1992). That said, with enough speed and mobility to reach a valley bottom, a snow avalanche can scour the landscape and create erosional landforms such as boulder holes, tarns, and impact pools (Luckman, 1978; Butler et al., 1992). A variety of snow avalanche definitions are available in Table 2.2.

Vegetation patterns in Grand Teton National Park are changed and fragmented by snow avalanches increasing the diversity of vegetation regimes present, and these changes in vegetation regimes known as *avalanche paths* are the easiest way to determine the locations of past snow avalanche events (Patten and Knight, 1984).

Table 2.2: Various definitions and descriptions of snow avalanches from the literature

Definition of Snow Avalanche	Source(s)
Snow avalanches "commonly release due to warming and reduction of the strength of the snowpack or because some combination of increased loading and decreased snowpack strength."	Mears (1975, p. 521)
"Rapid downslope movements resulting from the failure of an unstable snow cover."	Luckman (1977, p. 31)
An avalanche is a mass of snow—sometimes containing ice, water, soil, rock, and trees—which slides down a mountain side.	Armstrong and Williams (1986, p. 4)
"The principal morphological features by which avalanches are classified are the form of motion, the free-water content in the snow cover, the location of the lower boundary of the flow, the track geometry, and the type of rupture of the snow cover."	Hopfinger (1983, p. 49)
Snow avalanches in subalpine terrain typically occur within well-delineated paths that pass vertically through the surrounding forested environment, producing distinct swaths of nonforested, supple vegetation.	Butler and Malanson (1992, p.77); Malanson and Butler (1984, 1986); Butler, 1989; Erschbamer (1989)
Snow packs experience structural instability on slopes to the point of snow movement.	Alexander (1993)

Patten and Knight's (1994) dendrochronological study of tree cores in Cascade Canyon found that 53% of avalanche paths were covered by small-conifer vegetation regimes. Other significant materials found in avalanche paths in Cascade Canyon include talus (16%), aspen shrubland (*Populus tremuloides;* 8%), low shrubland (6%), and aspen-conifer vegetation (*Populus tremuloides, Abies lasiocarpa;* 6%), with significant talus deposits being caused by other types of slope failures. One can therefore spot snow avalanche paths and sites of past avalanches on satellite imagery and/or Google Earth® by finding *scars* of small trees or brush on a landscape where fully grown trees should be.

2.2c Rock/Debris Slides

Large rock slides may be considered *deep, rapid landslides*, which distinguish themselves from flows by sliding down a slope without the assistance of moisture (Cruden and Varnes, 1996) and are composed primarily of large rocks instead of a mixture of debris (Varnes, 1978). Rock slides can either be rotational or translational in movement (see Table 2.3) and are different from rock falls because the parent material in slides stays close to the ground while traveling downslope (Cruden, 1976, p. 4).

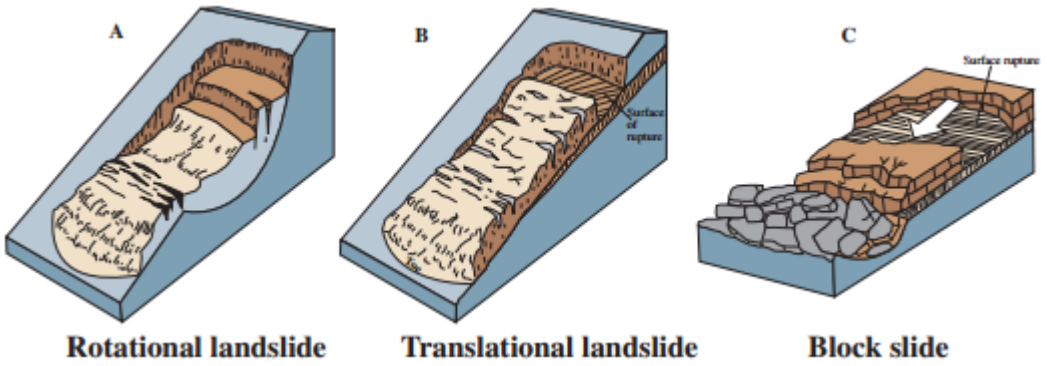

Figure 2.2: Graphic of the three major types of landslide movement (USGS, 2004).

Debris slides, which are less common in GTNP than rock slides (Case, 1989), has the same mechanism of movement as a rock slide but is transporting debris such as soil and

vegetation instead of purely rocks (Varnes, 1978). Curiously, a debate is relatively lacking about the official definition of rock slides in comparison to other slope failures such as debris flows or snow avalanches; the work of Cruden (1976), Varnes (1978), and Cruden and Varnes (1996) seem to be the widely accepted studies denoting what a rock slide is. Indeed, the U.S. Geological Survey slope failure fact sheet that lists the definition of rock slide exclusively relies on Varnes (1978) and Cruden and Varnes (1996) for their sources of information! Table 2.3 lists the definitions of rock slides from these publications.

Table 2.3: Relevant definitions of rock slides in the literature

Definition of Rock Slide	Author
The parent material of rock slides travel at ground-level while moving down a slope.	Cruden, 1976
Landslides that slide down a slope without the assistance of moisture.	Cruden and Varnes, 1996
A zone of weakness separates slide material from stable, underlying material. Rotational slides have a surface of rupture that is curved concavely upward and the slide movement that *rotates* along an axis that is parallel to the ground surface and transverse across the slide. Translational slides have a mass that moves along a roughly planar surface with little rotation or backward tilting. Block slides are translational slides with a single unit or closely related units of rupture material that move together as a relatively coherent mass downslope.	USGS (2004), p.1

2.2d Rock Falls

Rock falls are mass movements that *occur through the air* from exposed rocks that are jointed and fractured on the edges of cliffs (Alexander, 1993; National Atlas of the U.S., 2011). Rather than sliding or flowing down a slope like the three other types of process-oriented slope failure classifications used in this study, rock falls involve a detachment of large slabs of bedrock from a bare rock face or cliff (Cruden and Varnes, 1996; National Atlas of the U.S., 2011). These slabs fall through the air to the ground as they first go into a free fall, then bounce and roll, and then finally settle in a depositional pile at the base of the face or cliff (National Atlas of the U.S., 2011). Cruden (1976, p. 4) differentiated rock falls and rock slides by using the earth's surface as

a mechanism of comparison: the *rock mass leaves the rupture surface* during a fall instead of remaining in contact with the surface, as in the case of a rock slide.

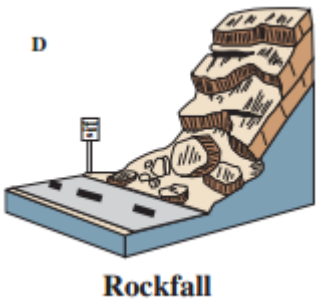

Figure 2.3: Graphic of rock fall movement (USGS, 2004).

Rock falls are one of the most common types of slope failures in mountainous areas across the world (Porter and Orombelli, 1981; Whalley, 1984; Flageollet and Weber, 1996; Parise, 2002) and can often follow rock slides or topples (Cruden and Varnes, 1996; Parise, 2002). Despite their common nature and widespread signage of potential rock falls occurring in areas of "high local relief" and "steep terrain" (Butler, 1990, p. 81), Parise (2002) stated that rock falls often get less attention from researchers than other more *notable* slope failures, possibly because of the smaller likelihood of a rock fall transporting a large volume of material in comparison to slides, snow avalanches, and flows.

Apparently, only a few small differences are in the minutiae and semantics of the various definitions of rock falls in the literature; some definitions use a steep slope as the main origin point for a rock fall, some use a cliff, and some use both. Some definitions specifically address the detachment of rocks from their origin points, whereas some definitions are a little less specific about the beginning of rock fall movements. All of the definitions are in agreement about the type of movement a rock fall experiences—falling, bouncing, and rolling. Table 2.4 displays the various definitions of rock falls in the literature.

Table 2.4: Relevant definitions of rock falls in the literature

Definition of Rock Fall	Author
Areas with steep terrain and high relief are subject to rock fall hazards.	Butler (1990)
"A detachment of rock from a steep slope along a surface in which little or no shear displacement takes place. Movement is rapid to very rapid. Except when the displaced mass has been undercut, falling will be preceded by small sliding or toppling movements that separate the displacing material from the undisturbed mass."	Cruden and Varnes (1996, p. 53)
A rock detaches from a steep slope and descends through the air via falling, bouncing, or rolling.	Parise (2002)
"Falls are abrupt movements of geologic materials, such as rocks and boulders, that become detached from steep slopes or cliffs. Separation occurs along discontinuities such as fractures, joints, and bedding planes, and movement occurs by free-fall, bouncing, and rolling."	National Atlas of the U.S. (2011)

2.3 Causes and Physical Identifiers of Slope Failures

2.3a Debris Flows

The terminus of a debris flow can be seen as a lobe-shaped depositional fan known as a debris fan or colluvial fan or cone (Butler and Walsh, 1994; Jakob and Hungr, 2005a). A variety of subclassifications of debris flows exists, such as earth flows, mud flows, and debris floods, (Jakob and Hungr, 2005a), but for the purpose of this study all of these will fall under the catch-all term of *debris flows* because it was not possible to investigate all of these slope failures *in situ*.

Multiple accounts in the literature describe the ideal conditions needed for debris flows to occur. A general account of optimal debris flow conditions was given by Costa (1984, p. 269): "Prerequisite conditions for most debris flows include an abundant source of unconsolidated

fine-grained rock and solid debris, steep slopes, a large but intermittent source of moisture, and sparse vegetation." He also noted that smaller basins with higher slope gradients are able to transport higher percentages of eroded material through mass wasting in comparison to larger and shallower basins. Sidle and Ochiai (2006) observed debris slides and flows as moving at a rapid pace, having a shallow depth, and occurring at a slope gradient $\geq 25^{o}$. Debris slides and flows initiate on concave or linear slopes and are often started by quick rates of snowmelt, tectonic activity, and rainstorms. Jakob and Hungr (2005a) stated that debris flows generally occur on a steep slope of 20 to 45^{o}. Steep slopes can be counted as a primary causal factor for debris flow occurrences and recurrences, whereas precipitation amounts and basin size can play roles in determining how much material is transported downslope.

Commonly cited criterion in debris flow occurrence rates are the frequency of previous debris flow events (Johnson et al., 1990; Ellen and Mark, 1993) as well as the magnitude of the event (Hampel, 1977; Ikeya, 1981; Takahashi, 1981; Ikeya and Mizuyama, 1982; Kronfellner-Kraus, 1982; Mizuyama, 1982; Thurber Engineering, 1983; Hungr et al., 1984; Johnson et al., 1990), otherwise known as the amount of debris supply transported in each event (Johnson et al., 1990). Debris supply conditions can explain variances in debris flow samples of up to 15% in debris flows with an unlimited supply of debris for transport (Bovis and Jakob, 1999), and debris flow magnitude and frequency rates are dependent on debris channel recharge rates (Jakob et al., 2005). Determining magnitude data for debris supply requires discharge and volume data of the debris deposit, and debris flow frequency conditions are often determined using the dendrochronological technique of measuring each event's impact on tree rings via reaction wood (Bovis and Jakob, 1999; Stoffel et al., 2005).

The general consensus among literature from geomorphologists is that debris flows are most likely to occur in channels where previous debris flows have already occurred (Butler and Walsh, 1994, 1997; Coe et al., 2003) The primary methods for predicting debris flow probability at a certain point on a mountainous landscape have been focused around predicting recurrence rates of flows at sites that have already been established to have previously experienced debris flow events (Walsh and Butler, 1997; Coe et al., 2003), although methods have varied for developing regression models for future debris flow prediction. Walsh and Butler (1997) used three primary components in developing their regression model to predict the most dangerous sites for debris flows in Glacier National Park: the maximum elevation of a debris flow, an index of potential snowpack values for each debris flow area, and the Euclidean distance to the snow-patch that was in closest proximity upslope of a debris flow. They stated that the most hazardous sites for debris flows in their study area are for "those areas at higher elevations with concave slopes, marked by couloirs and gullies capable of capturing and retaining snow and possessing a greater colluvium depth" (Walsh and Butler, 1997, p. 9). Coe et al. (2003) took a different approach by using stratigraphic records and historical records of past debris flows on 19 debris flow fans in the Front Range of Colorado to estimate mean recurrence intervals. While these studies have more detailed data and information about individual debris flows than is available for this project, the principle that sites of previous debris flows are the primary *hot spots* for potential debris flows in the future has proven to be valuable in this study (see Chapter 3, section "Analysis – Debris Flows and Snow Avalanches").

Case (1989) mapped the locations of debris flow deposits in GTNP, and debris flow deposits are highly visible in maps, satellite imagery, and *in situ* observations in the five canyons of this study.

Figure 2.4: Example of a debris flow deposit in Granite Canyon, Grand Teton National Park, Wyoming. Note the lobate shape of the deposit and coarse soils that spread out from the source point upslope.

A wealth of literature exists for the geologic and geomorphologic conditions both past and present in GTNP (see *Geomorphology of Grand Teton National Park*, Chapter 3), but a notable lack of additional information on debris flows exists for the area. This study will contribute to literature on debris flows in Grand Teton National Park by updating maps of debris flows in the park to a more current temporal period as well as listing and mapping the hazards that flow events pose to Park visitors and employees.

2.3b Snow Avalanches

As is the case with debris flows, precipitation and climate play an integral role in catalyzing the occurrence of snow avalanches (Luckman, 1977; Butler, 1986; Lacroix et al., 2012). Three different types of snow avalanches with differing physical characteristics and movement types are often classified by researchers studying snow avalanches: dry snow avalanches, wet snow avalanches, and slab avalanches (Luckman, 1977; Butler, 1986). The type of snow avalanche that may occur on a given slope can be very much dependent on meterological and climatological data (Luckman, 1977; Butler and Malanson, 1985; Butler, 1986; Butler and Walsh, 1990; Lacroix et al., 2012); reliable climatic data inside the canyons of the study area for this research was not available at the time of this study, however.

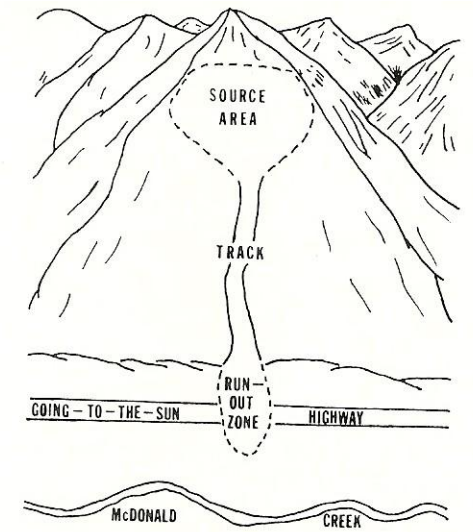

FIG. 1.Morphometric components of snow avalanche paths.

Figure 2.5: Morphology of a snow avalanche path shown in a diagram. Source: Walsh et al., 1990.

Slope gradient is a conspicuous control of avalanche occurrence rates (Butler and Walsh, 1990; Alexander, 1993). Small avalanches commonly occur at angles of 35 to 75^{o}, occasionally from 25 to 35^{o}, and rarely to nonexistent for gradients below 25^{o} and above 75^{o}, whereas large avalanches commonly occur at gradients of 25 to 50^{o}, less commonly from 50 to 70^{o}, and rarely

to nonexistent for gradients below 25^{o} or above 70^{o} (Alexander, 1993). Walsh et al. (1990, p. 615) noted that "steep gullies" and "open slopes" are natural avalanche paths; whereas ridges, outcrops, and terraces are natural avalanche barriers, suggesting that overly convex structures impede avalanche formation.

Figure 2.6: Example of a snow avalanche path on aerial imagery from Glacier National Park, Montana. "1" is the starting zone, "2" is the track, and "3" is the run out zone. Source: Butler and Walsh, 1990.

They also defined three main components of an avalanche path: a source area, track, and runout zone (Figures 2.5 and 2.6).

Snow avalanches in GTNP occur at higher frequencies at higher elevations (Patten and Knight, 1994). Avalanche path locations are well established as noted by the consistent presence of low- to medium-growth vegetation patterns such as small conifers (*Abies lasiocarpa)* and aspen shrubs (*Populus tremuloides)* in the same locations every year (Patten and Knight, 1994). In essence, any avalanche path that is visible on maps, satellite imagery, or *in situ* can be considered a potential site of future avalanches; whereas more stable areas of high-growth conifer plant regimes can be assumed to be at lower risk of future avalanche occurrences. While low-risk areas in the Tetons are not completely exempt from potentially devastating snow avalanche events (Butler and Malanson, 1992; Patten and Knight, 1994), they are not considered to have a significant effect on the comprehensive vegetation mosaic of the landscape.

2.3c Rock/Debris Slides and Rock Falls

When shear stress is greater than shear strength, the likelihood of a rock fall or rock slide occurring is high (Hungr, 2007; Harvey, 2012). The threshold at which shear stress can surpass or surpasses shear strength is a subject that has been attempted to be quantified in countless *landslide* hazard studies around the world—Guzzetti et al. (2003); Topal et al. (2012); Youssef and Maerz (2012)—are just a few recent examples. This threshold can be slowly reached over time by certain shear stressors: steep slopes, a geological structure that alternates weak and strong rocks to create shear planes amongst the weaker rocks, and concentrations of groundwater or steep gradients to the water table can tip the balance in favor of a higher shear stress than shear strength (Harvey, 2012). After this threshold has been reached, a trigger is needed to make a rock fall or rock slide occur. Common factors that have been triggers to cause new rock falls

and slides include erosion of basal material on a hillslope, rainstorms of high intensity and/or long duration that saturates the rocks and increases pore pressure, melting of permafrost, and earthquake shocks and aftershocks (Harp et al., 1981; Keefer, 2002; Bromhead, 2004; Hungr, 2007; Harvey, 2012).

These aforementioned influences are triggers common to rock falls and slides (as well as debris flows in some cases), but falls and slides do have certain unique conditions that are necessary for one to occur instead of the other. Rock falls are most prone to occur at locations where slope gradients are steep, the parent material has been sufficiently weathered to possessing large cracks and joints, and little to no vegetation is present to keep rocks anchored to their present location (Cruden and Varnes, 1996; National Atlas of the U.S., 2011; Harvey, 2012). They may also follow rock slides or topples, as previously mentioned in section 2.2d. Rock slides, while prone to occur on steep slopes themselves, require a strong underlying parent material and a weaker upper layer of strata (USGS, 2004). The presence of water in the weathering and/or sliding processes can also be important; a heightened moisture level at the plane of contact between the strong parent material and the weak upper strata can facilitate the sliding process after shear stress exceeds shear strength (Bromhead, 2004; Hungr, 2007).

Rock falls and slides also have distinguishing features from each other that makes it possible to identify one or the other in aerial photography and during *in situ* observations. Both types of slope failures appear to have coarse, rocky material in their deposits when viewed in an aerial photograph or on Google Earth®. However, rock fall deposits are often far from their source material because of the high gradient of slope present at the fall's origin; and as a result, many falls can travel a long way down a path (Parise, 2002). Rock slide deposits have clearly

traveled as a somewhat well-organized block whilst sliding down a slope (USGS, 2004), and they often have a concave, *slumping* local relief within them.

2.4 Slope Failure Hazards to Humans

Searches of the literature failed to reveal reliable data documenting deaths and injuries caused by rock falls, rock slides, and debris flows in Grand Teton National Park, but casualty data for snow avalanches has been provided by the Colorado Avalanche Information Center and the American Avalanche Association website (2013) from 1998-2013. Table 2.5 lists for individual avalanche accident events the number of deaths, number of injuries, location, and date on which each accident took place. Three deaths occurred during this time period within the five canyon study area used in this project, specifically Garnet and Granite canyons.

Table 2.5: GTNP Avalanche Casualty Figures

Location	Date	Deaths	Injuries
Survey Peak	January 27, 2013	1	0
Prospectors Mountain, Apocalypse Couloir	January 3, 2013	1	1
Ranger Peak, Waterfall Canyon	March 7, 2012	2	0
Garnet Canyon	April 16, 2011	2	0
South Teton	February 21, 2010	1	0
Granite Canyon	February 23, 2001	1	0
	Total	8	1

CHAPTER 3 – STUDY AREA

3.1 Grand Teton National Park

Grand Teton National Park (GTNP) is situated in the northwest corner of Wyoming, encompassing the central and east sides of the Teton Range and parts of the Jackson Hole basin to the east (Fig. 2). Yellowstone National Park is immediately north of and adjacent to GTNP, Idaho sits adjacent to the park's western boundary, and the Bridger-Teton National Forest sits to the northeast (Jobes, 1992).

3.1a Geomorphology of GTNP

The Teton Range, at approximately 10 million years old, is the youngest mountain range in Wyoming and is one of the youngest in the country (Lageson and Spearing, 1991). It has undergone three major glaciations: the Buffalo glaciation at approximately 200,000 years ago, the Bull Lake glaciation from 200,000-130,000 years ago, and the Pinedale glaciation that occurred between 70,000 and 13,000 years ago (Lageson and Spearing, 1991). The range itself is a product of an uplifted normal fault block with the adjacent Jackson Hole basin being the lowered fault block, making the Tetons unique from other regional mountain ranges produced by reverse faulting (Lageson and Spearing, 1991). The Teton Fault, a north-south oriented normal fault located at the base of the Teton Range, was once the epicenter for widespread seismic activity (White et al., 2009); but in recent times, the fault has only produced small earthquakes along the base of the Teton Range that do not seem to have a visible effect on recent slope failure rates (Smith et al., 1976; White et al., 2009). However, significant seismic activity is prevalent to the north, south, and east of the Teton Fault (White et al., 2009), and the potential for a major seismic event directly along the Teton Fault may exist in the future if the central and northern regions of the fault are locked and storing strain energy (Smith et al., 1976; White et al., 2009).

Figure 3.1: Location of Grand Teton National Park relative to Wyoming and Yellowstone National Park. Image courtesy of the National Park Service (http://www.nps.gov/grte/planyourvisit/images/wy.gif.)

Glacial erosion can be a major driver in the erosion of alpine mountain ranges (Hallet et al., 1996; Montgomery, 2002; Stroeven et al., 2009), although the effect of glacial erosion may be minimized in certain mountain ranges already well-carved by fluvial forces (Brocklehurst and Whipple, 2002). In the case of the Teton Range, the cause of most of its erosion to date is thought to be from glacial forces (Foster et al., 2010) because of its relative youth, steepness, and lack of major fluvial carvings (Lageson and Spearing, 1991), thus explaining the parabola-like shape of this study's five canyons. It is also currently subject to post-glacial erosional processes—mainly those from fluvial forces and mass movements—that have recently eclipsed the rate of crustal uplift, thus keeping the range in a perpetual *cycle of erosion* (Schumm and Lichty, 1965).

3.1b Climate and Vegetation of GTNP

The modern vegetation regime in Grand Teton National Park is of a montane coniferous forest variety (Vankat, 1979). Studies of vegetation regimes in the Park note a reforestation of the alpine areas of GTNP since the Pinedale glaciation, with limber pines (*Pinus flexilis*) and firs (*Abies lasiocarpa, Pseudotsuga menziesii*) present at lower elevations (~ 1700-2000 m), lodgepole pines *(Pinus contorta)* and spruce varieties *(Picea engelmannii, Picea pungens)* at sites of moderate to high elevations (~ 2100-2700 m), and whitebark pine (*Pinus albicaulis*) at very high elevations (~ 2750-2900 m) (Whitlock, 1993). Whitlock's post-glacial reconstruction of vegetation regimes shows that changes in vegetation zones are unsurprisingly reliant on elevation.

The type of climate is purely continental, and temperatures can be highly variable. Mean minimum winter temperatures can range from -12ºC to 3ºC (Mahaney, 1990), but wind chills can reach as low as -51ºC (Dirks and Martner, 1982). The area averages over 200 cm of precipitation per year (Foster et al., 2010); and local testimony given from Kelley, WY, stated that rates of annual snowfall commonly pass 500 cm. Data collected from local weather stations note the direct effect that elevation has on a location's temperature in GTNP (Dirks and Martner, 1982).

3.1c Slope Failures in GTNP

In addition to the slope failure inventory map of Case (1989), a wealth of evidence is available to suggest a high activity level of slope failures in GTNP as well as the potential hazards they pose to park visitors and staff. Hikers and tourists have been injured or killed by slope failures in the Park's canyons within the last 10 years (and presumably before then). A look at GTNP's online news archives that date back to 2006—stories from 2003 to 2005 are listed but are inaccessible because of broken links—show that rock falls and snow avalanches

have negatively impacted visitors to the Park's mountainous areas within the past 6 years. A snow avalanche in Granite Canyon injured a backcountry skier in February 2011 (National Park Service, 2011a), and another snow avalanche in March 2012 took the lives of two expert backcountry skiers at the northern edge of the Teton Range (National Park Service, 2012a,b). A rock fall injured a man climbing the Grand Teton on 6 July 2012 (National Park Service, 2012c). The National Park Service also put out a warning dated 17 June 2011 of potential late season snow avalanche activity, citing unseasonably cool and wet conditions as the potential causes for large avalanche events (National Park Service, 2011b). Patten and Knight (1994) noted the ability of snow avalanches to change vegetation patterns in the large canyons of GTNP. Debris flows are known to have occurred in GTNP in "larger canyons at 7500 to 8500 feet altitude, beneath talus slopes at the base of couloirs in canyon walls" (Fryxell and Horberg, 1943, p. 457).

Talus and landslide deposits mapped by Love et al. (1992) are cited by Love et al. (2003, p. 13) as evidence that "the land surface (in GTNP) is restless" and that those deposits result from "the ever-changing piles of rock debris that mantle the mountain slopes, the creeping advance of rock glaciers, the devastating snow avalanches and the thundering rock falls." Relevant to the study area are a large number of deposits from the Love et al. (1992) map that are concentrated in Paintbrush and Granite Canyons.

3.2 Study Sites

The five canyons under examination in this study are, moving from north to south, Paintbrush Canyon, Cascade Canyon, Garnet Canyon, Death Canyon, and Granite Canyon (Fig. 3). Each canyon exhibits a parabolic shape consistent with glacial carving and recession and has multiple slope failure mass movement events readily observable on the landscape. These five canyons were specifically selected over others in the park because of ease of access and high

levels of use by park visitors. Each canyon has a trailhead accessible by road, and all of the canyons have high levels of hiker activity because of well-maintained trails, the presence of campgrounds, or both.

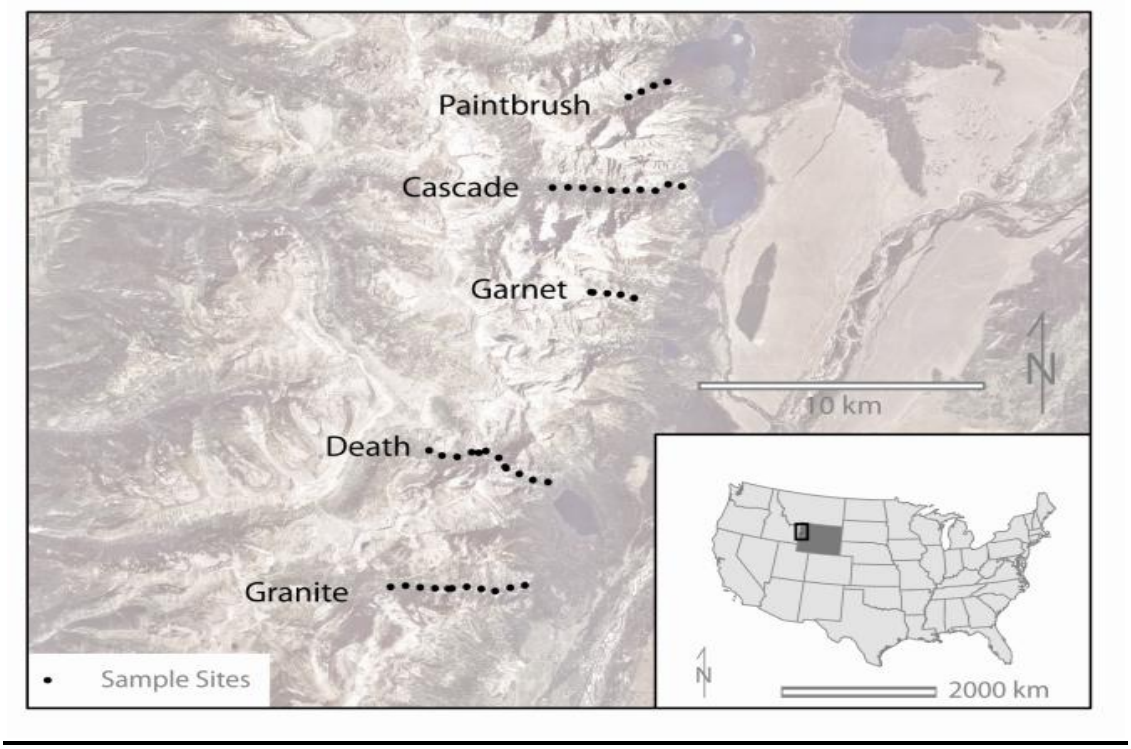

Figure 3.2: Location of the five study canyons in relation to Grand Teton National Park.

Section 3.2a: Individual Canyon Characteristics

Cascade Canyon is a north-south oriented canyon towards the north end of the Park boundary. It features a wide, flat bottom with increasing slope gradients as one travels towards the tops of the canyon walls, especially on the northern and southwestern edges. Its average annual precipitation gradient goes from relatively low values (~30 in/y.) in the eastern portion to moderate values on the canyon bottom as one travels west. The northern and especially southern edges of the canyon can receive close to 60-70 inches/year of precipitation. Surface rock types are dominated by alluvial fan and glaciations deposits with large deposits of Mount Owen Quartz Monzonite in the northwest and southwest areas of the canyon as well as significant deposits of

layered gneiss and migmatite in the northeast and southeast areas. This canyon experiences high levels of debris flow and snow avalanche activity with a modicum of rock fall deposits followed by rock slide and complex deposits.

Granite Canyon has many physical characteristics in common with Cascade Canyon as they are oriented in a north-south direction, a slope gradient regime that steadily increases as elevation increases towards the edge of the canyon walls, and an active regime of debris flow activity. However, Granite Canyon's overall steepness is gentler than Cascade Canyon and is the least steep of the five canyons in terms of slope gradient. Paths apparently exclusive to snow avalanches and not debris flows are relatively rare here as well. Granite Canyon's geology is also unique in that it is home to significant deposits of Rendezvous Metagabbro and lesser deposits of members of the Gros Ventre formation. Most of the canyon bottom and extreme southwest edge of the canyon is comprised of quaternary talus deposits. Precipitation values increase from east to west and from the canyon bottom to the top of the canyon walls, especially on the northern end.

Death Canyon has a general northwest to southeast orientation but contains a significant curve in its middle that causes a brief shift to a northeast to southwest orientation. Its steepest gradients occur on the southwest and southeast walls of the narrowest part of the canyon just before the curve. Death Canyon's precipitation regime is lowest (~30 in/y.) at its southeast edge and increases significantly into 50-60 in/y. in the western portion of the canyon. Precipitation values also increase towards the high 60/low 70 in/y. ranges at the northeast and southwest edges of the canyon walls. The predominant rock type in this canyon is layered gneiss and migmatite with some quaternary talus deposits at the bottom of the canyon and areas where gneiss contains pods and lenses of metagabbro at its northern and western edges. A wide variety of all different

types of slope failures occur in this canyon, with debris flows and avalanches having occurred towards the center and eastern edges of the canyon whereas rock falls tended to occur in the central to western portions of the canyon. Complex deposits occurred in relatively high numbers in all parts of the canyon.

Garnet Canyon is a steep, narrow, short canyon where slope failure activity is relatively very high. Rock falls and slides are common in Garnet Canyon, debris flows less so, and snow avalanches are rare. Garnet Canyon has a high level of gradient steepness on the narrow, exposed canyon walls that account for a high level of talus and debris that cover the canyon floor. The orientation of the canyon is from northwest to southeast and its precipitation gradient is of similar orientation with precipitation levels decreasing from 70-80 in./y to the 40-50 in./y range as one travels from northwest to southeast. The canyon is intersected by a seemingly heterogeneous mix of layered gneiss and migmatite, quaternary talus, and Mount Owen quartz monzonite and pegmatite deposits.

Paintbrush Canyon is another short canyon with a high level of slope failure activity taking place in a small area, but its slope failure regime is different from that of Garnet Canyon. Debris flows and especially snow avalanches are common while complex deposits and slides are rare in the canyon. The canyon also has more of an open bottom area with higher levels of vegetation and less talus and debris in comparison to Garnet canyon. Paintbrush Canyon's orientation is from northeast to southwest and its precipitation gradient is similar in orientation, with values increasing from northeast to southwest. Deposits of augen gneiss dominate the portion of the canyon on which slope failures were document in this study, and large deposits of layered gneiss and migmatite are located to the southwest further into the canyon.

CHAPTER 4 - METHODS

Three primary components comprise the methods of this project: field work, mapping, and statistical analysis. *In situ* data pertaining to the rock stability of canyon walls was taken in the hiking trails in each canyon and is outlined in section 4.1. Mapping the locations of slope failures and the source points of these failures in the five-canyon study area is the focus of sections 4.2a and 4.2b. Slope failure locations were superimposed over the locations of human-built structures, specifically hiking trails and camping zones, and are described in further detail in section 4.2c. The analysis section (4.4) takes a preliminary look at locations where slope failures might or might not be prone to occur in the future. Finally, these zones of potential hazard will be compared with the locations of hiking trails and campgrounds in the Park to show these structures' potential level of risk in experiencing a potentially damaging slope failure in the future (section 4.4c).

4.1 Field Work

The purpose of collecting rock mass strength (RMS) data from the five-canyon study area is to provide a preliminary perspective of rock stability within each canyon. The following section explains the details of collecting RMS data, the proper use of a Schmidt hammer in collecting RMS data, and the methodology for which RMS data was collected in this study. Field research was undertaken in July of 2010 under the direction of Dr. Richard Marston and the assistance of KSU PhD student Brandon Weihs.

4.1a Rock Mass Strength

An integral component in determining rock strength is the Schmidt rock hammer (Goudie, 2006; Viles et al., 2011). B.P. Moon and R.J. Selby played an integral role in transitioning the Schmidt hammer from a tool solely for the use of the concrete industry to a

dynamic research instrument used to measure rock mass strength (RMS), a measure of rock stability. The technique was originally pioneered by Selby (1980) and subsequently used by Selby (1982) in the central Namib Desert and by Moon and Selby (1983) in locations across southern Africa. The RMS uses both intact rock strength measured by the Schmidt hammer and data about the joints and weathering of a rock (see Fig. 4.1) to determine rock stability, which can be used to determine the angle at which the slope of a given landform is at equilibrium. Moon further refined the RMS technique in 1984 by adding further subdivisions for intact rock strength and joint spacing. Viles et al. (2011) discussed the current debate over sampling methodology for Schmidt hammer measurements in geomorphic studies. Owen et al. (2007) studied chemical weathering rates of rock in Norway by using the Schmidt hammer, and they found that periglacial (physical) erosion after the Little Ice Age canceled out all changes to topographic relief caused by chemical weathering.

Table 40 Geomorphic rock mass strength classification and ratings

Criteria	*(1)* Very strong	*(2)* Strong	*(3)* Moderate	*(4)* Weak	*(5)* Very weak
Intact rock# strength	100–60	60–50	50–40	40–35	35–10
Rating	*20*	*18*	*14*	*10*	*5*
Weathering	Unweathered	Slightly weathered	Moderately weathered	Highly weathered	Completely weathered
Rating	*10*	*9*	*7*	*5*	*3*
Joint spacing	>3 m	3–1 m	1–0.3 m	0.3–0.05 m	<0.05 m
Rating	*30*	*28*	*21*	*15*	*8*
Joint orientation	>30° into slope	<30° into slope	Horizontal and vertical	<30° out of slope	<30° out of slope
Rating	*20*	*18*	*14*	*9*	*5*
Joint width	<0.1 mm	0.1–1 mm	1–5 mm	5–20 mm	>20 mm
Rating	*7*	*6*	*5*	*4*	*2*
Joint continuity	None continuous	Few continuous	Continuous, no infill	Continuous, thin infill	Continuous, thick infill
Rating	*7*	*6*	*5*	*4*	*1*
Groundwater outflow	None	Trace	Slight	Moderate	Great
Rating	*6*	*5*	*4*	*3*	*1*
Total rating	100–91	90–71	70–51	50–26	<26

Source: Modified from Selby (1980), and Moon (1984)
Note: # N-type Schmidt hammer rebound values

Figure 4.1: Selby system for rock mass strength (RMS) from Selby (1980) and Moon (1984).

4.1b Data – Uses and Limitations

The Selby system and Schmidt rock hammer measurements were taken at a rate of every 0.5 km upon entering the canyon. The specific Selby data categories used in the statistical analysis category for RMS were rock joint width, joint spacing (m), joint orientation, joint continuity, amount of groundwater present, the amount of local landform weathering, and Schmidt rock hammer ratings. Additionally, the geology of the rock was recorded but was deemed to be inappropriate to use in context with the aforementioned Selby system data. Schmidt hammer measurements were used from rocks either immediately adjacent to the trail or within a distance of about 50 m. Other Selby measurements were used from a scale more oriented toward the local canyon profile. Pictures of both the north- and south-facing slopes of the canyon to document these profiles are available in the Appendix (section: Study Site Photographs). Latitude and longitude coordinates as well as site elevation measurements were also recorded to document the locations of the study sites via a Garmin GPSmap 60CSx handheld GPS device.

The Selby system measurements at each site are an estimate of the local geomorphologic conditions at the rock faces sampled. Therefore the RMS values from each sample site can be considered estimates to the best of the researchers' knowledge—it was not possible to physically extract RMS values from each rock face because of time constraints.

4.2 GIS Mapping of Slope Failures

Case (1989) mapped all mass movement hazards as shapefile polygons in Grand Teton National Park in his "Landslide Map of Wyoming." USGS quadrangles for the whole state of Wyoming were compiled and all "landslides" (slope failures) were drawn in for all parts of the state. For Grand Teton National Park, a 1:24,000 topographic map was heads up digitized using

aerial color satellite imagery and georeferenced into a data set usable in ArcMap versions 9.3 and 10. The data layer can overlay a modern-day orthorectified (NAIP) image of GTNP. Case mapped all potential mass movement hazards in the entire park, including different types of *landslides* and *sediment and landform units*. This map is considered to be the most recent slope failure hazards map of GTNP and Teton County. The Case classification system for *landslides* is primarily based on the morphology of a mass movement.

This study therefore builds upon Case's (1989) preexisting slope failure map to specifically inventory and map five primary types of slope failures: debris flows, rock falls, rock slides, snow avalanches, and complex slope failures that embody multiple processes. The classification system used in this study is primarily based on a slope failure's dominant process or, in the case of complex failures, processes. Falls encountered in GTNP are composed of bedrock, flows are primarily composed of predominantly coarse soils, and slides are a combination of bedrock and coarse-soil debris. Varnes (1978) created an easy to use mass movement classification system to differentiate different types of slope-failure–induced movements, which can be seen in Table 4.1.

Table 4.1: Mass movement classification system adapted from Varnes (1978) and taken from http://nationalatlas.gov/articles/geology/a_landslide.html; the dominant slope failure types used in this project have been bolded

Type of Movement		**Type of Material**		
		Bedrock	**Engineering Soils**	
			Predominantly Coarse	Predominantly Fine
	FALLS	**Rock fall**	Debris fall	Earth fall
	TOPPLES	Rock topple	Debris slide	Earth slide
SLIDES	ROTATIONAL	**Rock slide**	Debris slide	Earth slide
	TRANSLATIONAL			
	LATERAL SPREADS	Rock spread	Debris spread	Earth spread
	FLOWS	Rock flow	**Debris flow**	Earth flow
		(deep creep)	(soil creep)	
	COMPLEX	Combination of two or more principal types of movement		

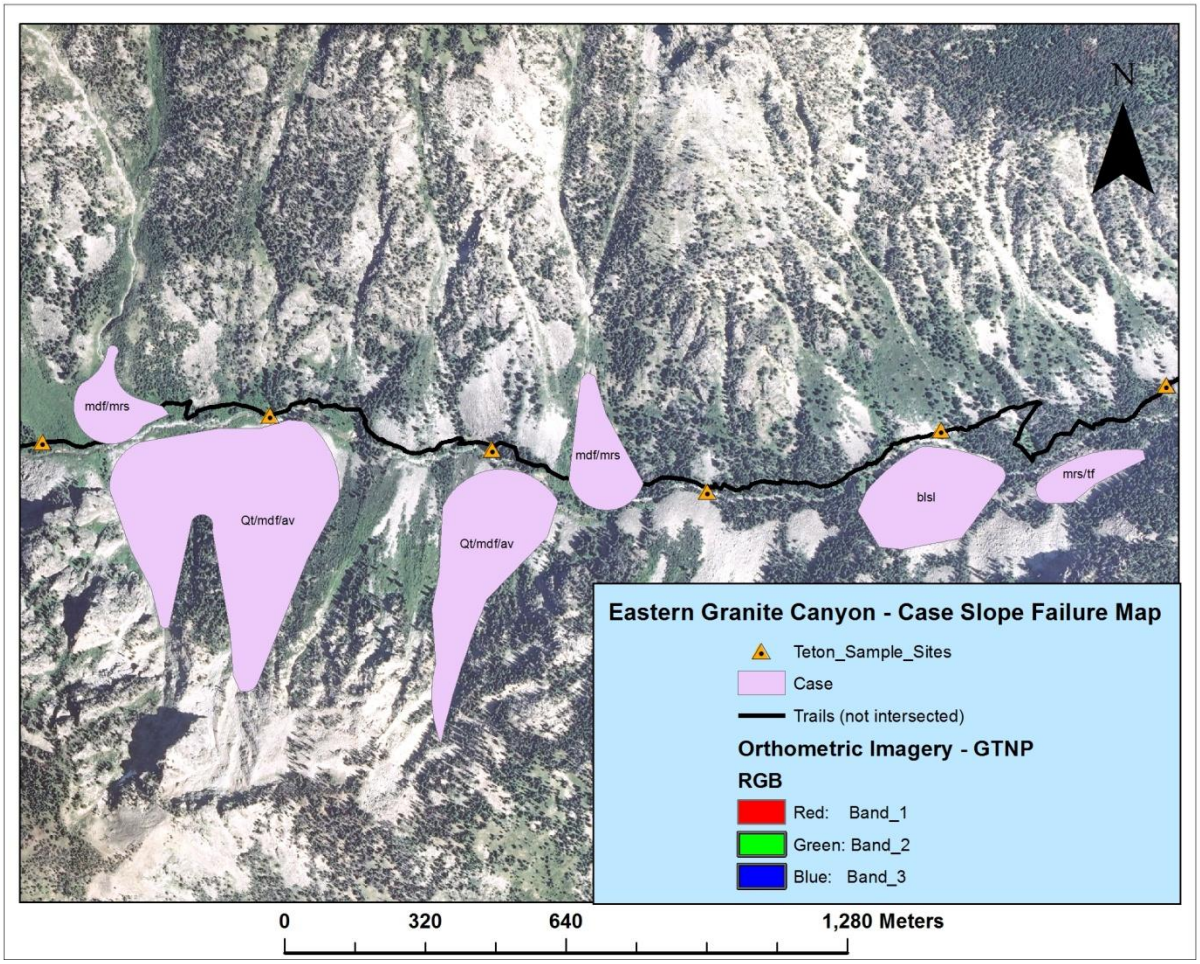

Figure 4.2: Slope failures mapped by Case (1989) in the eastern portion of Granite Canyon.

The boundaries of each slope failure were drawn manually as individual polygon shapefiles in ArcMap 9.3/10 atop a full color orthorectified (NAIP) 1 x 1 meter two dimensional satellite image of the Park in 2010. Google Earth® IKONOS-2 full color imagery from July 4, 2009 was used to provide a three-dimensional perspective of each slope failure, determine which type of slope failure was present in a given location, and further denote the respective boundaries of each slope failure. This imagery was particularly useful in situations where a slope failure's full extent may have been obscured by shadowing, excessive light, or areas where slope profile wasn't immediately clear on two-dimensional satellite imagery. Google Earth® IKONOS-2 and orthorectified NAIP satellite imagery were also used in determining the source points of each

slope failure. Multiple locations in the study area required significant additions or revisions of the Case (1989) map, such as eastern Granite canyon as noted in Figures 4.2-4.4.

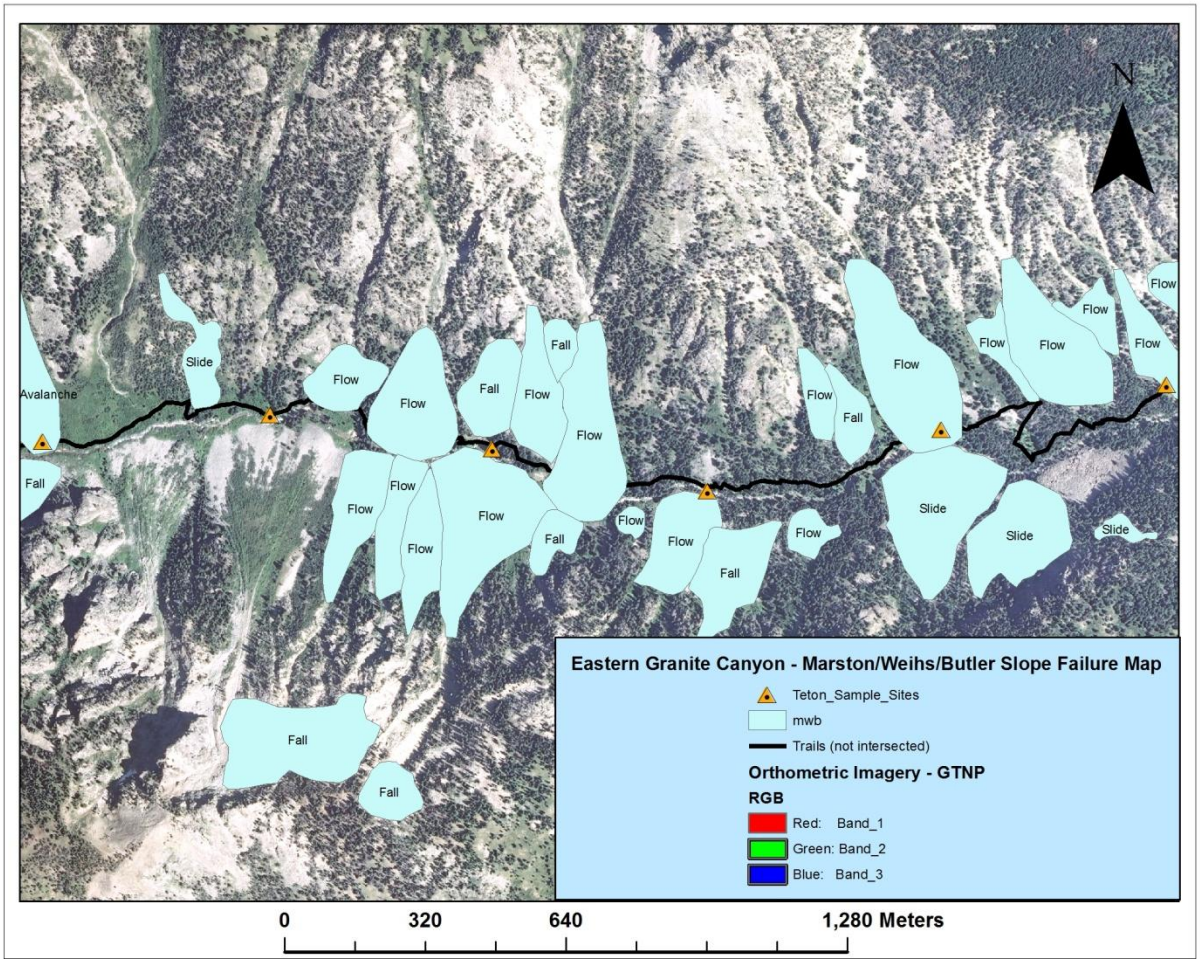

Figure 4.3: Slope failures mapped by Marston, Weihs, and Butler (2011) in the eastern portion of Granite Canyon.

Note that in the eastern two-thirds of Granite Canyon only six slope failure polygons were present on the Case (1989) map, but the Marston, Weihs, and Butler (2011) map added 32 new slope failure polygons, three of which were revisions and/or additions to the extents of previously drawn Case (1989) polygons.

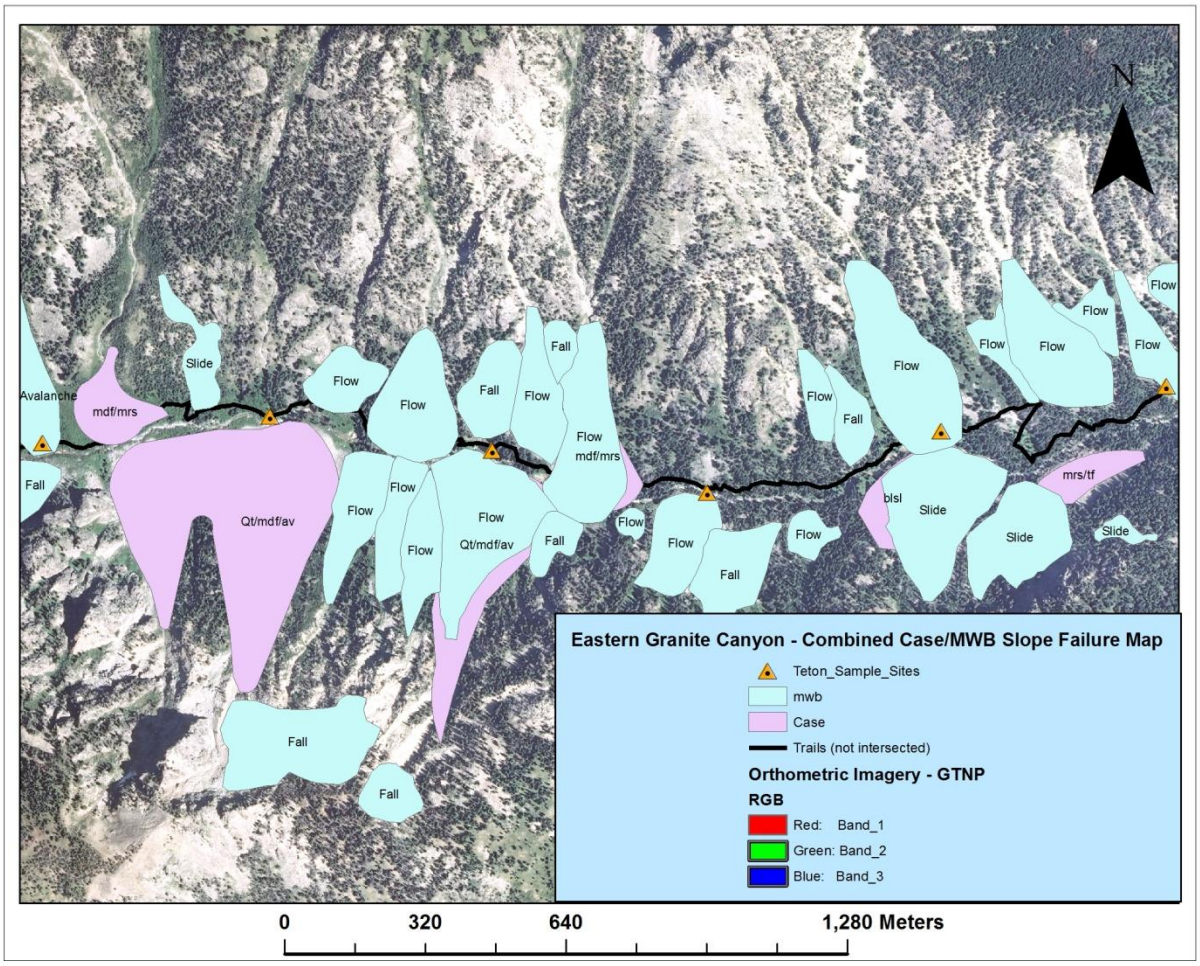

Figure 4.4: Slope failures mapped by Case (1989) and Marston, Weihs, and Butler (2011) in the eastern portion of Granite Canyon.

4.2a Documenting Slope Failure Deposits in Google Earth®/GIS

All slope failure deposits were recorded in ArcMap 9.3/10 via polygon shapefiles. Six primary categories of shapefiles were created: snow avalanche deposits, snow avalanche tracks, debris flow deposits, rock fall deposits, rock slide deposits, and complex slope failure deposits. Snow avalanche deposits were noted on satellite imagery by a clear path or scar of lightly colored vegetation that denotes small conifers and shrubs. Preceding these deposits are the avalanche *tracks*, where snow has traveled downslope in a narrow, concentrated path. Figure 4.5 provides an example of a snow avalanche path as seen in NAIP satellite imagery of the park.

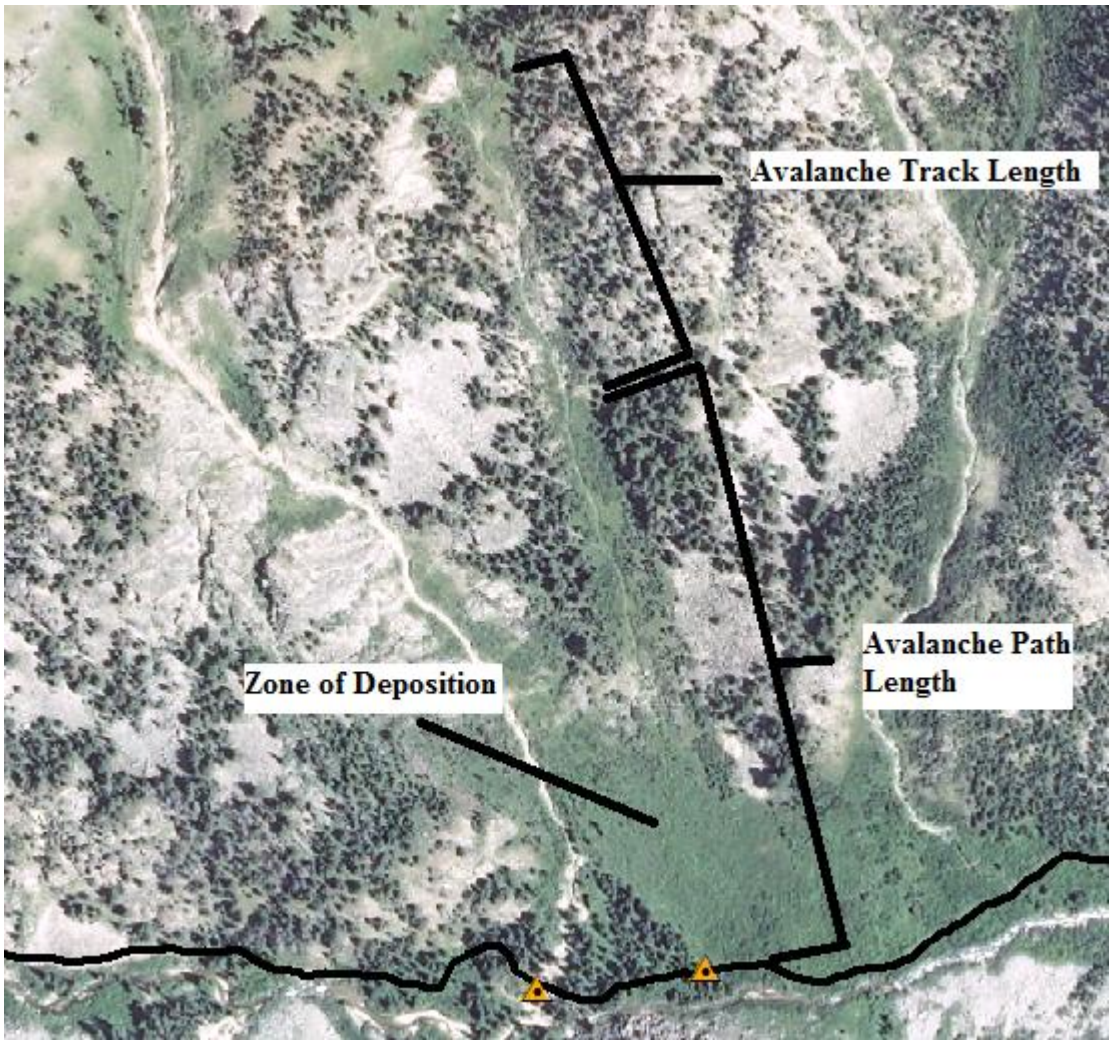

Figure 4.5: Diagram of a snow avalanche deposit in Granite Canyon on NAIP satellite imagery. Note the scarring of the local landscape where low-lying vegetation is present instead of thicker vegetation such as trees.

Debris flows were identified by finer soils, a telltale stream channel, and a lobate outward flow of material at the bottom of the flow structure. Figure 4.6 notes all of these features in a diagram of a debris flow as seen from NAIP satellite imagery. Snow avalanches and debris flows often overlapped in the same paths because of their sharing of similar physiographic landscape conditions necessary for their occurrence.

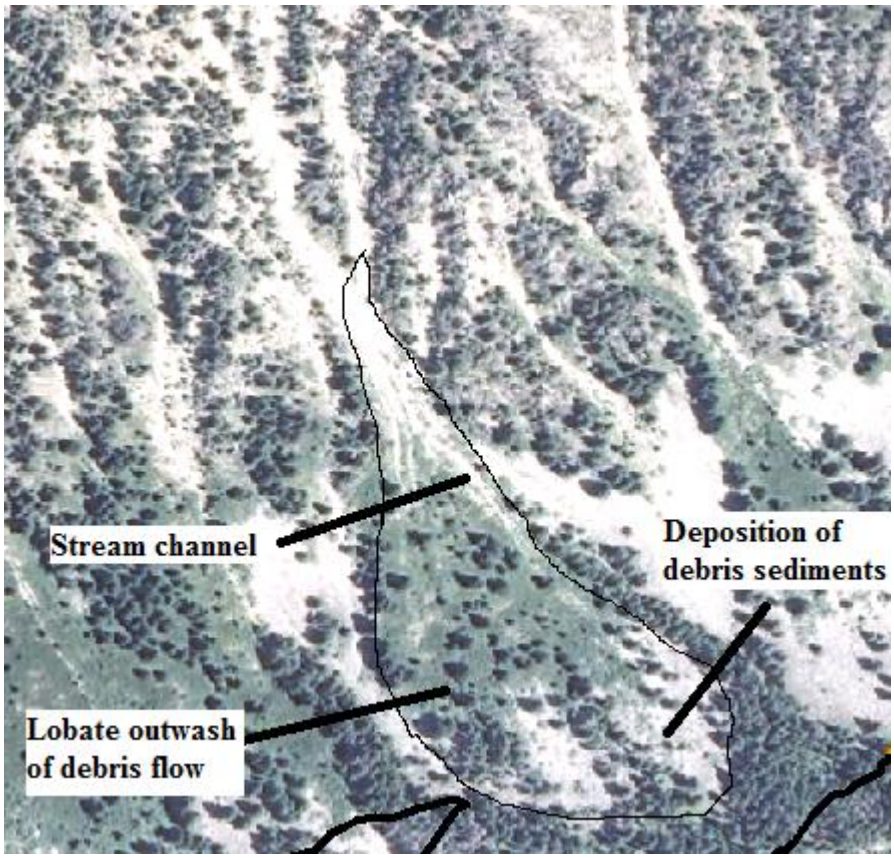

Figure 4.6: Diagram of a debris flow deposit in Granite Canyon on NAIP satellite imagery. Note that this image has been outlined to show the extent of the debris flow deposit. Three primary elements were observed in order to classify a debris flow in satellite imagery: a stream channel in which debris can travel, a lobate zone of outwash of the flow from the narrower channel, and a clear deposition of fine-grained debris sediments and materials.

Rock falls were noted by deposits of coarse talus near the base of a steep face of bare rock. Rock slides also were denoted by deposits of coarse talus, but were located on less steep topography and often in concave surfaces of rupture. Figures 4.7 and 4.8 show example diagrams of a rock fall and rock slide, respectively, as seen from NAIP satellite imagery. Google Earth® imagery was crucial in deciphering whether a slope failure was a rock fall or rock slide since having a three dimensional perspective allowed for visualizing slope profiles and whether the local topography is conducive to multiple rocks detaching and falling from a cliff or a block of rocks detaching and sliding down a slope.

Figure 4.7: Diagram of a rock fall deposit in Granite Canyon on NAIP satellite imagery. Note that this image has been outlined to show the extent of the rock fall deposit. Two primary elements were used in determining rock fall deposits: A steep, exposed rock face from which rocks could detach and fall to the ground and a clear spatial extent of coarse-grained rock deposits in contrast to local vegetation.

The color coding of each slope failure event on the GIS maps is arbitrary: snow avalanches are denoted in blue, debris flows in green, rock falls in red, and rock slides in purple. Complex slope failures, a combination of one or more of the aforementioned categories, have a color code of yellow.

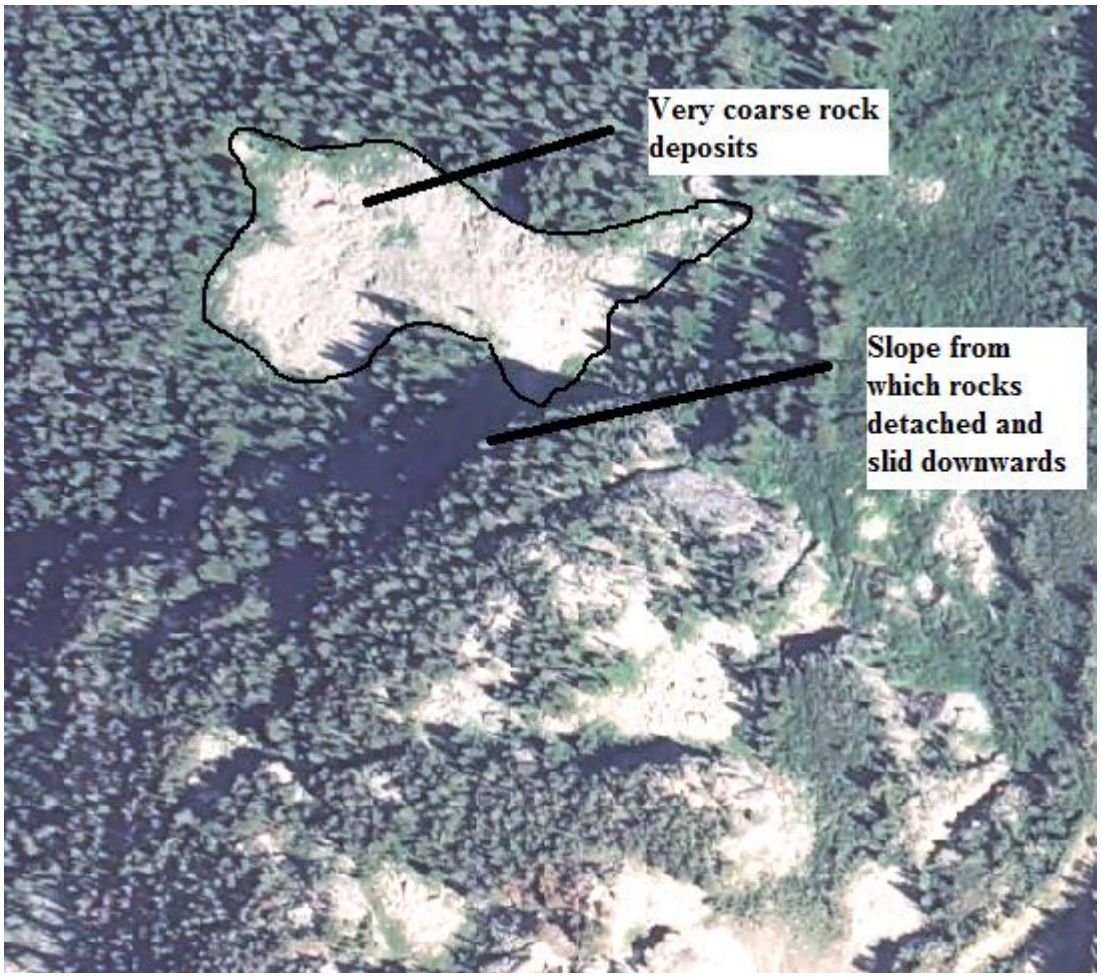

Figure 4.8: Diagram of a rock slide deposit in Cascade Canyon on NAIP satellite imagery. Note that this image has been outlined to show the extent of the rock slide deposit. Two primary elements were used in determining rock slide deposits: A steep, exposed rock face from which a block could detach and slide downwards and a clear spatial extent of very coarse-grained rock deposits in contrast to local vegetation.

4.2b Determining Source Points for Slope Failures in ArcMap 9.3/10

Snow avalanches were assigned source points at terrain that facilitated a downward movement of snowpack with little resistance. Origin points for rock falls were delineated at the center of a rock or cliff face where the material from the failure originated. Source points for debris flows were created within channels where the transport of soil, debris, and liquid materials were most likely to start flowing downhill. These locations are often identifiable on satellite

imagery as the start of a channel at the top of a slope. Rock slide origin points were created where the sliding block of material detached from the stable block. Source points for complex slope failures are denoted by the initial type of slope failure that occurred at the zone of movement: for example, a complex slope failure that started out as a rock slide and morphs into a debris flow downslope will have a rock slide source point classification.

4.2c Determining Human Impacts of Slope Failures in ArcMap 9.3/10

Shapefiles of all GTNP hiking trails and camping zones were imported into ArcMap 9.3/10 and clipped to solely denote human structures within the five-canyon study area. Statistics extracted from slope failure shapefiles intersecting with human structure shapefiles include the number of camping zones directly intersected by a past slope failure, the distance and relative percentage of trail segments intersected by past slope failure deposits out of all trails in the study area, the distance and relative percentage of trail segments with slope failure deposits coming within 100 m of them, and the percentage of area within the camping zones that have been directly intersected by a past slope failure deposit.

4.3 Data Gathered for Slope Failures in ArcMap 9.3/10

Attribute data were collected and extracted for polygons and source points to produce similar, but not entirely identical, data layers. Data categories that are present in both the polygon and source point attribute tables are listed in detail in Table 4.2, whereas elements unique to polygons and source points are described in Tables 4.3 and 4.4, respectively. Only elements that are relevant to statistical analysis are listed in these tables; attributes used to identify individual polygons or points were omitted.

Table 4.2: GIS attributes shared by source points and slope failure polygons

GIS Element	Explanation
Slope aspect	Compass bearing for the element in question. For slope failure polygons, the aspect was manually taken by estimating the full polygon's downslope orientation to the nearest 22.5^{o} interval. For source points, a slope aspect map was generated using ArcMap 9.3/10, and the aspect value for each point was extracted from this map.
Elevation	The elevation of the source point or the centermost point of a polygon.
Above or below trimline	Whether the polygon or source point occurs above or below the glacial trimline in the canyon the element occurred in. Some polygons are oriented both above and below the glacial trimline.
Canyon	The canyon where the element is present (Cascade, Death, Garnet, Granite, Paintbrush).
Slope gradient	For source points, the steepness of the slope where the point is present. For debris flow and snow avalanche polygons, the overall slope gradient from top to bottom as determined by elevation over distance. No slope gradient value for rock falls or rock slides are present.

Table 4.3: GIS attributes unique to slope failure deposit polygons (snow avalanches)

GIS Element	Explanation
Shape area	The area of the slope failure deposit (m^2).
Shape length	The total perimeter of the slope failure deposit (m).
Top of polygon	The elevation at the very top of a snow avalanche or debris flow polygon.
Bottom of polygon	The elevation at the very bottom of a snow avalanche or debris flow polygon.

Table 4.4: GIS attributes unique to slope failure source points

GIS Element	Explanation
Geology	The parent geology present at the source point.
Slope curvature	The curvature of the slope where the source point is present. Determined using a slope curvature map in ArcMap 9.3/10.

4.3a Data Uses and Limitations

These data can only be used to determine the average slope, geological, and geomorphological conditions present at a site of slope failure and are not necessarily predictive. Precipitation conditions are vital in causing snow avalanches and debris flows, and groundwater conditions can play an integral role in causing rock falls and rock slides (see section 2.3), and obtaining these data proved to be impossible because few reliable ways exist to measure these conditions over the entire five-canyon study area. However, by providing the average geomorphological conditions at all sites of slope failure in this project's study area and extracting any patterns from these data, gleaning information on the most common conditions where slope failures have occurred in the past becomes possible. More suggestions on how the results from this project can be used in tandem with future studies are discussed in Chapter 7 – Conclusions.

4.4 Analysis of Slope Failure Locations and Geomorphic Conditions

4.4a Statistical Analyses

Analytical statistics for characteristics of source points were generated using the Summary Statistics function in ArcMap 9.3/10. The products generated from these analyses include mean value, standard deviations, median, minimum values, maximum values, and histograms. The individual characteristics for each of the four categories of source points include slope gradient, slope curvature, elevation, and slope aspect. Additionally, the rock types present at each slope failure point were manually analyzed in Excel to determine how many times they

occur at a failure site as well as whether different categories of slope failures occurred more often under certain rock types than others. Characteristics for slope failure polygons that were analyzed include slope failure area (m^2) and slope aspect and, for snow avalanches, their individual slope gradients (see Table 4.3).

4.4b Slope Aspect, Gradient, and Curvature Maps

Raster sets for slope aspect, slope gradient, and slope curvature in Grand Teton National Park were created using the *aspect*, *slope*, and *curvature* tools, respectively, from the *surface* toolset in the "Spatial Analyst Tools" series in ArcMap 9.3/10. The method for which the slope tool calculates degree values for a given cell value is to determine the maximum change in elevation over the distance between the cell and its eight nearest neighbors. Slope aspect is calculated in ArcMap 9.3/10 by identifying the downward direction of the maximum rate of change in slope value from an individual cell to its nearest neighbors. The slope curvature tool is the 2^{nd} (z) dimension of slope, or, in layman's terms, "slope of the slope." The total curvature form was used in ArcGIS 9.3/10 in order to include the full analysis of the z-component of the slope gradient layer. Slope gradient, aspect, and curvature calculations were based off of multiple 10 m resolution digital elevation models downloaded from the USGS National Map Seamless Server and combined into a mosaic overlaying Grand Teton National Park in ArcMap 9.3 thanks to the assistance of KSU Ph.D student Brandon Weihs.

Slope failure polygonal deposits and source points were overlaid atop these map layers to provide a spatial context of the local slope conditions where previous events occurred. Specifically, any patterns that were manually observed—such as one type of slope failure occurring more or less often in a certain range of slope aspect values—were compared against the summary statistics described in section 4.4a.

4.4c Precipitation and Geology Maps

The most comprehensive precipitation grid for Grand Teton National Park in ArcMap 9.3/10 is the Lindstrom (2005) geospatial dataset for average annual precipitation in the park. Local maps of the area were scanned, georeferenced, and heads-up digitized to create polygons symbolizing ranges of average annual rainfall. Each grid cell represents 300 x 300 meters and average annual precipitation values are measured in inches per year from 1971-2002. The most comprehensive map of rock types in the Park was the revised 1992 geospatial dataset created by Geonex Program Development, Inc. This data layer features polygonal extents of various rock types in the park that were observed and recorded in the field via USGS guidelines. The field data was then transferred to 7.5 minute USGS topographic maps and later converted to a 1:62,500 scale map for GTNP, heads up digitized, and converted into a format beneficial for ArcMap usage.

4.4d Trimline Position and Slope Failure Distance from the Teton Fault

Vector lines denoting the position of trimlines in each canyon were overlaid on the orthorectified NAIP image of the park in ArcMap 9.3/10. Each slope failure source point and deposit was noted as to whether they were above the trimline, below the trimline, or, in the case of some deposit polygons, traversed both sides of the trimline. The location of the Teton Fault was provided by Kathy Mellander of the National Park Service as a line shapefile, and the distance of each slope failure source point from the fault was computed in ArcMap 9.3/10.

4.4e Chi-square analysis

The local geomorphic conditions in the study area for each variable listed above were analyzed via chi-square statistical testing for the purpose of determining whether slope failures occurred under geomorphic characteristics unique in comparison the overall geomorphic makeup

of the nearby landscape. In this study, "nearby landscape" can be defined as the catchment areas extracted and/or created by Marston, Weihs, and Butler (2011) from the National Hydrology Dataset. Each catchment area included drainages directly pertaining to the sample sites in each canyon and within 50 meters of the beginning and end of each canyon's sample sites. Observed values for slope gradient, slope aspect, slope curvature, average annual precipitation, rock type, trimline position, and distance from the Teton Fault were compared with the expected geomorphic composition of the catchment areas for each characteristic. Expected values were computed via cell count of raster surfaces for the catchment areas of for individual canyons and all canyons combined. The standard formula of $\chi = \Sigma (O-E)^2/E$ where O = observed values and E = expected values was used for each chi-square test.

4.4f Hazards vs. Human Structures

The locations of slope failure deposits as drawn by Case (1989) and Marston et al. (2010) were analyzed against the locations of National Park Service camping zones and trails in ArcMap 9.3/10. The length (m) and percentage of trail directly intersected by past slope failures in the five-canyon study area were determined using the *Clip* tool in ArcMap. Because past slope failure deposits can show where potentially new slope failures may occur (see section 2.3), determining the length of trail that is potentially in danger of being impacted by a future slope failure event was necessary. The length of trail that was directly intersected by a slope failure deposit was thus extracted using the *Clip* tool in ArcMap.

Camping zones are large areas prescribed by the National Park Service as legal to camp in. Multiple camping zones exist throughout the five-canyon study area, and in ArcMap 9.3/10 they are represented as a polygon layer provided by the National Park Service electronic archives. Three key components of past and potential slope failure hazards to these areas were

determined: the number and names of camping zones that have been previously intersected by a slope failure deposit, the percentage of area intersected in camping zones by previous slope failure deposits, and the number of camping zones where slope failure deposits have occurred within 100 m of them.

CHAPTER 5 – RESULTS AND DISCUSSION

Section 5.1 features four types of maps for each canyon in the study area. The first map includes the locations of all slope failure deposits, tracks, and source points, as well as the park trails and sample sites for this study. These elements were superimposed over an orthorectified image of Grand Teton National Park in ArcMap 10. For the following four maps, raster layers of local slope gradient, slope aspect, slope curvature, and estimated precipitation values were employed as the base layers rather than the orthorectified park imagery. Slope failure source points, trails, and sample sites were superimposed over the base layers.

Histograms, tables, and statistical analysis of the data extracted from the maps of sections 5.1 are displayed in section 5.2. Sub-sections 5.2a through 5.2c contain histograms for slope gradient, slope curvature, and estimated precipitation values data for each type of slope failure in all canyons, as well as tables listing the median, average, minimum, and maximum values for these data. Slope aspect values are shown in *radar* charts showing the most common orientations for source points. These charts are accompanied by tables listing all aspect frequencies and summary statistics. Sub-section 5.2d displays statistics of the area and percentage of the extent of camping zones directly intersected by slope failure deposits, the length and percentage of hiking trails directly intersected by slope failure deposits, and the length and percentage of hiking trails within 100 m of a slope failure deposit.

Slope curvature values are expressed as positive and negative values in ArcMap; positive values represent convex slopes, negative values represent concave slopes, and flat surfaces are represented as zero. Slope aspect values were divided into compass orientations from zero to 360 degrees: North = 337.5-22.5º, Northeast = 22.5 – 67.5º, East = 67.5 – 112º, Southeast = 112.5 – 157.5º, South = 157.5 – 202.5º, Southwest = 202.5 – 247.5º, West = 247.5 – 292.5º, Northwest =

292.5 – 337.5º. Slope gradient values range between a flat slope of 0º and a completely perpendicular slope of 90º. Average annual precipitation values are expressed in inches per year and are taken from the digitized GIS precipitation grid created by Lindstrom (2005).

Chi-square analyses of all seven types of geomorphic characteristics tested in this study for each type of slope failure and individual canyon are detailed in Sections 5.3a and 5.3b, respectively. Section 5.3c discusses the chi-square test results in comparison to the descriptive statistics results from Sections 5.1 and 5.2 and their overall significance to the hypotheses proposed for this project.

The locations of slope failures in reference to hiking trails and camping zones within the study area are featured in section 5.4. Each canyon features two types of maps: a map of the segments of hiking trails that have been directly intersected by past slope failure deposits, and a map depicting the locations of camping zones as well as the spatial extent of each zone that has been directly intersected by a past slope failure.

5.1: Slope Failure Maps

5.1a: Cascade Canyon

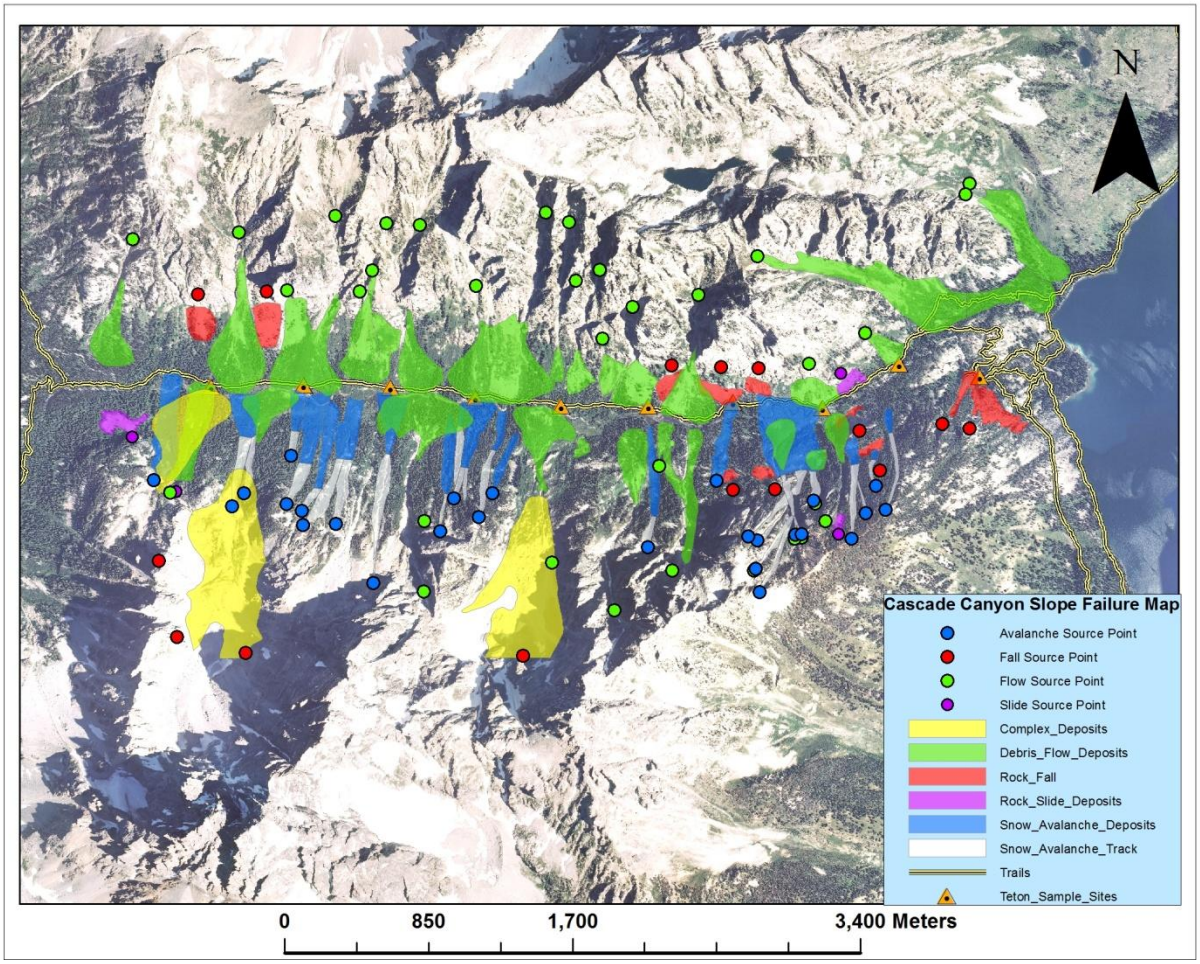

Figure 5.1: Locations of slope failure source points, tracks, and deposits superimposed over an orthorectified image of Cascade Canyon, Grand Teton National Park.

Table 5.1: Slope Failure Inventory for Cascade Canyon, Grand Teton National Park

	Avalanches	Falls	Flows	Slides	Complex	Total
SF deposits	18	13	28	3	3	65
SF source points	25	15	34	4	-	78

Cascade Canyon is dominated by debris flows and snow avalanches. The comparatively gentle slope profile of this canyon provides for more long-track movements than slope failures caused by cliff/rock face detachments. Also worth noting are the relatively few complex

(multiple) failure deposits present in this canyon.

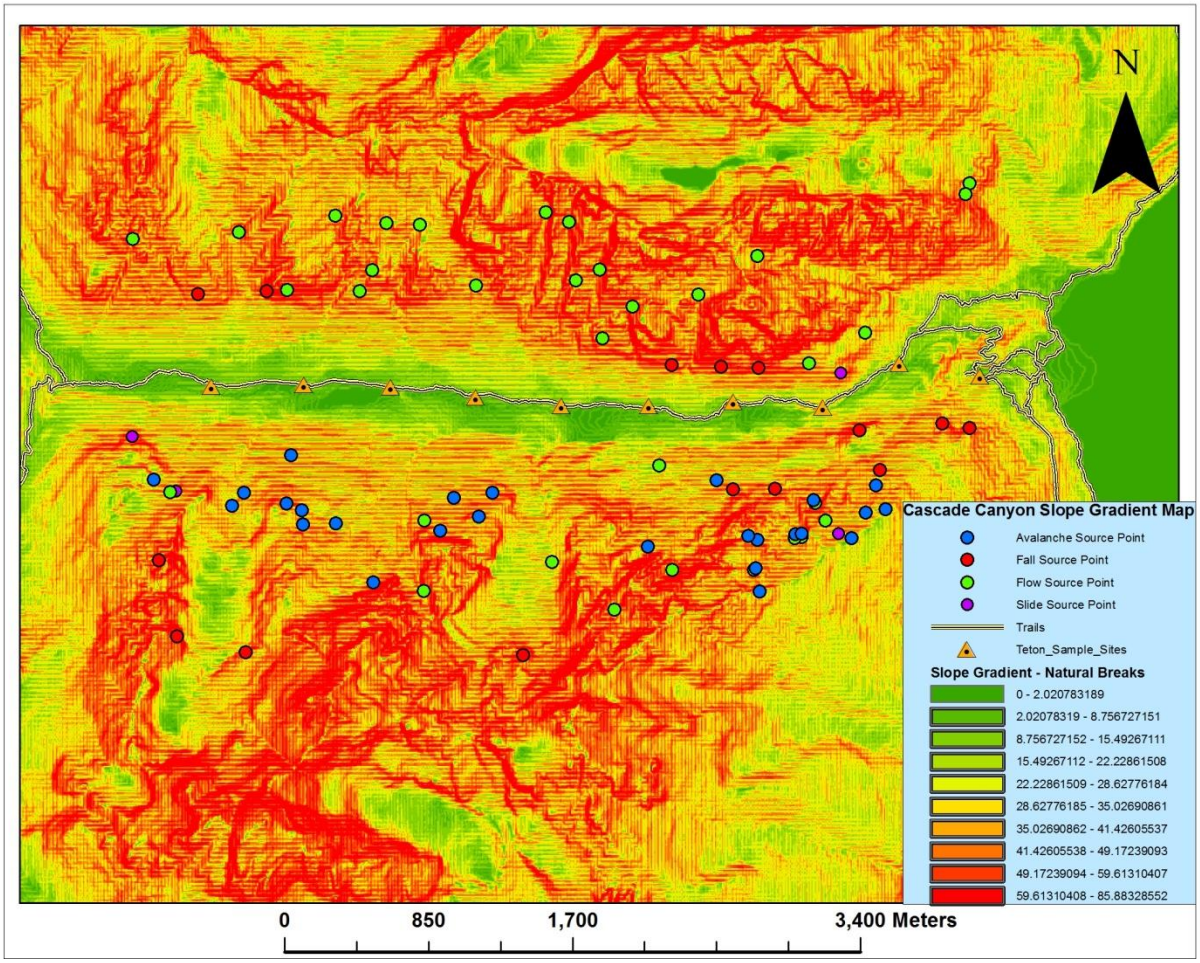

Figure 5.2: Slope gradient map with slope failure source points in Cascade Canyon, GTNP

Table 5.2: Summary statistics for slope gradient values for all source points in Cascade Canyon

	Count	Mean	Median	Minimum	Maximum	St. Dev.
Avalanches	25	37.44	38.13	16.55	60.29	11.00
Falls	15	59.67	60.72	32.23	76.11	10.69
Flows	34	41.94	43.27	20.37	73.39	14.58
Slides	4	54.53	59.45	31.50	67.73	14.32

Although the actual count of fall and slide source points only adds up to 19, they exhibit a much higher slope gradient than their avalanche and flow counterparts. Fall slope gradient median and mean values are close to 60º, slide gradient mean and median values span the mid to high 50s, whereas avalanches occurred on average at around 38º and debris flows near 42º.

Debris flows and rock slides exhibited the highest variability out of the slope failure categories, although rock slide variability values in Cascade Canyon should be treated with skepticism because of the low sample size.

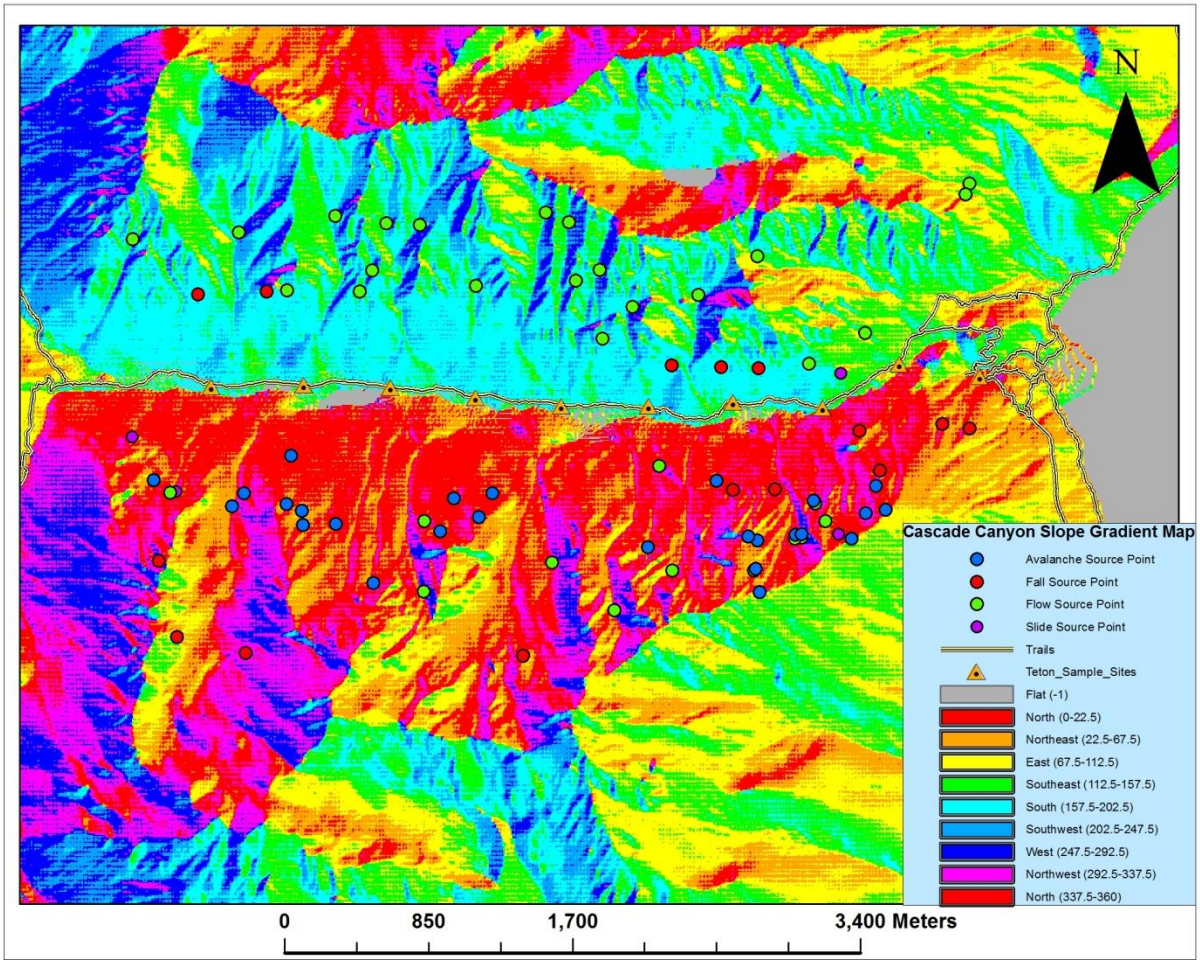

Figure 5.3: Slope aspect map with slope failure source points in Cascade Canyon, GTNP

Table 5.3: Slope aspect distribution table for all slope failure source points in Cascade Canyon

	Total	North	NE	East	SE	South	SW	West	NW
Avalanches	25	15	8	1	0	0	0	0	1
Falls	15	7	1	0	0	4	1	0	1
Flows	34	6	3	1	2	12	4	5	1
Slides	4	3	0	0	0	1	0	0	0

A pattern was present in avalanche and flow aspect values: snow avalanches primarily occurred at north or northeast orientations, though in contrast debris flows occurred more often

at southern orientations. However, north-oriented source points comprised the second highest aspect value of debris flows in Cascade Canyon. Rock falls occurred primarily on north-oriented aspects with some southern/southwest orientations also present.

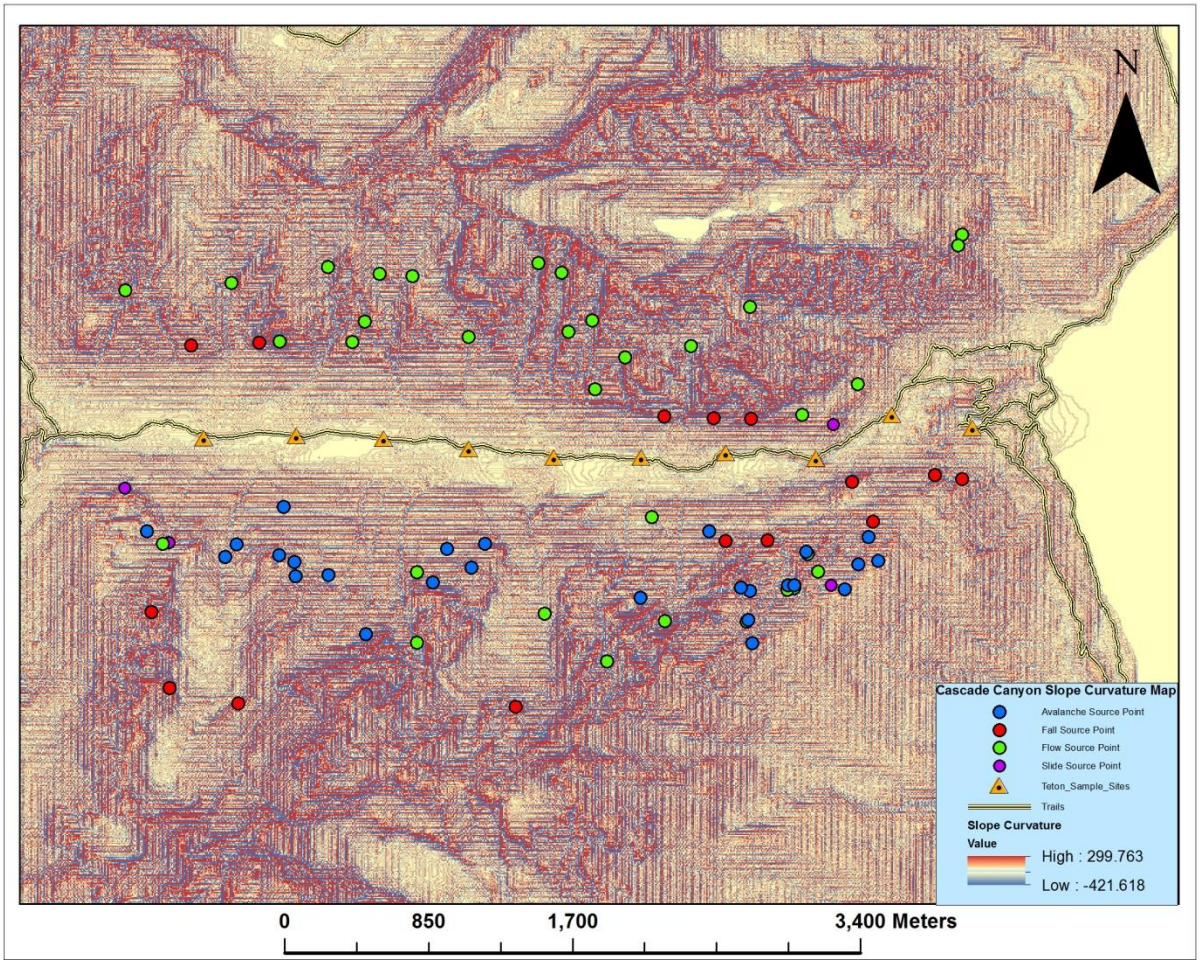

Figure 5.4: Slope curvature map with slope failure source points in Cascade Canyon, GTNP

Table 5.4: Summary statistics for slope curvature values of all source points in Cascade Canyon

	Count	Mean	Median	Minimum	Maximum	St. Dev.
Avalanches	25	2.14	0	-26.81	34.12	14.13
Falls	15	6.66	7.31	-53.62	102.36	37.00
Flows	34	-5.88	-2.44	-51.18	21.93	14.75
Slides	4	8.53	9.75	-12.19	26.81	14.77

Rock fall and rock slide slope curvature values exhibited a convex bias in Cascade Canyon, with large maximum values potentially affecting the overall distribution. Debris flows

in Cascade Canyon exhibited a concave bias, whereas avalanche source point curvatures averaged flat to slightly convex. Rock falls exhibited much more variability from the mean than avalanches, flows, and slides.

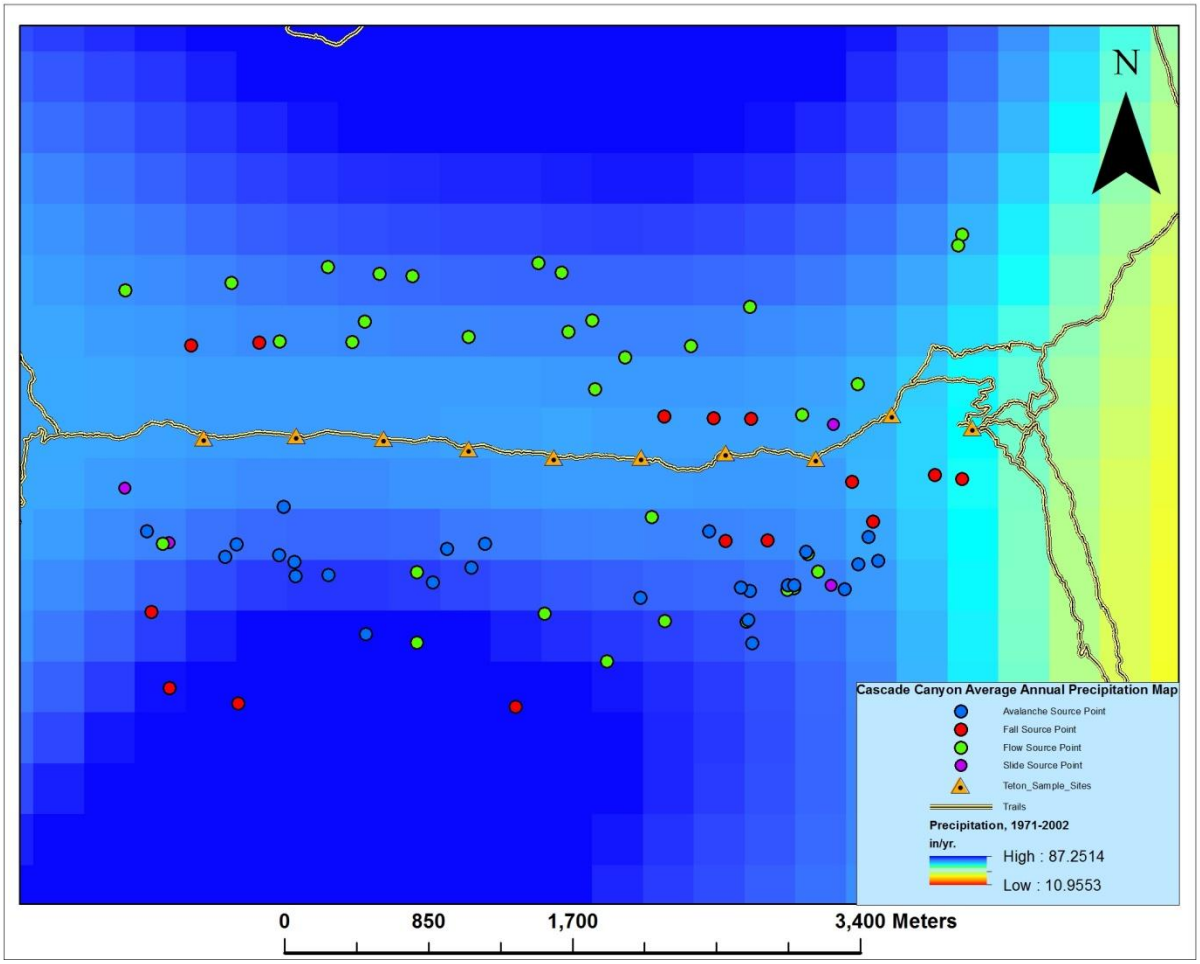

Figure 5.5: Average annual precipitation (1971-2002) map with slope failure source points in Cascade Canyon, GTNP.

Table 5.5: Average annual precipitation (in./y) summary statistics table for all source points in Cascade Canyon, GTNP

	Count	Mean	Median	Minimum	Maximum	St. Dev.
Avalanches	25	53.23	52.85	49.37	57.32	2.26
Falls	15	52.11	50.61	43.48	63.31	5.33
Flows	34	52.47	51.81	48.36	60.41	2.68
Slides	4	50.75	50.89	49.36	51.87	1.13

Rock falls exhibited the highest level of precipitation variability, the highest maximum, the lowest minimum, and the highest standard deviation. Snow avalanches averaged the highest levels of precipitation. Rock slides exhibited the lowest variability, but justifying how demonstrative this value is may inspire skepticism when considering that only four source points were sampled for rock slides in Cascade Canyon. Debris flows had the second highest variability in range and standard deviation, and locations of flow source points were located across the entire canyon area.

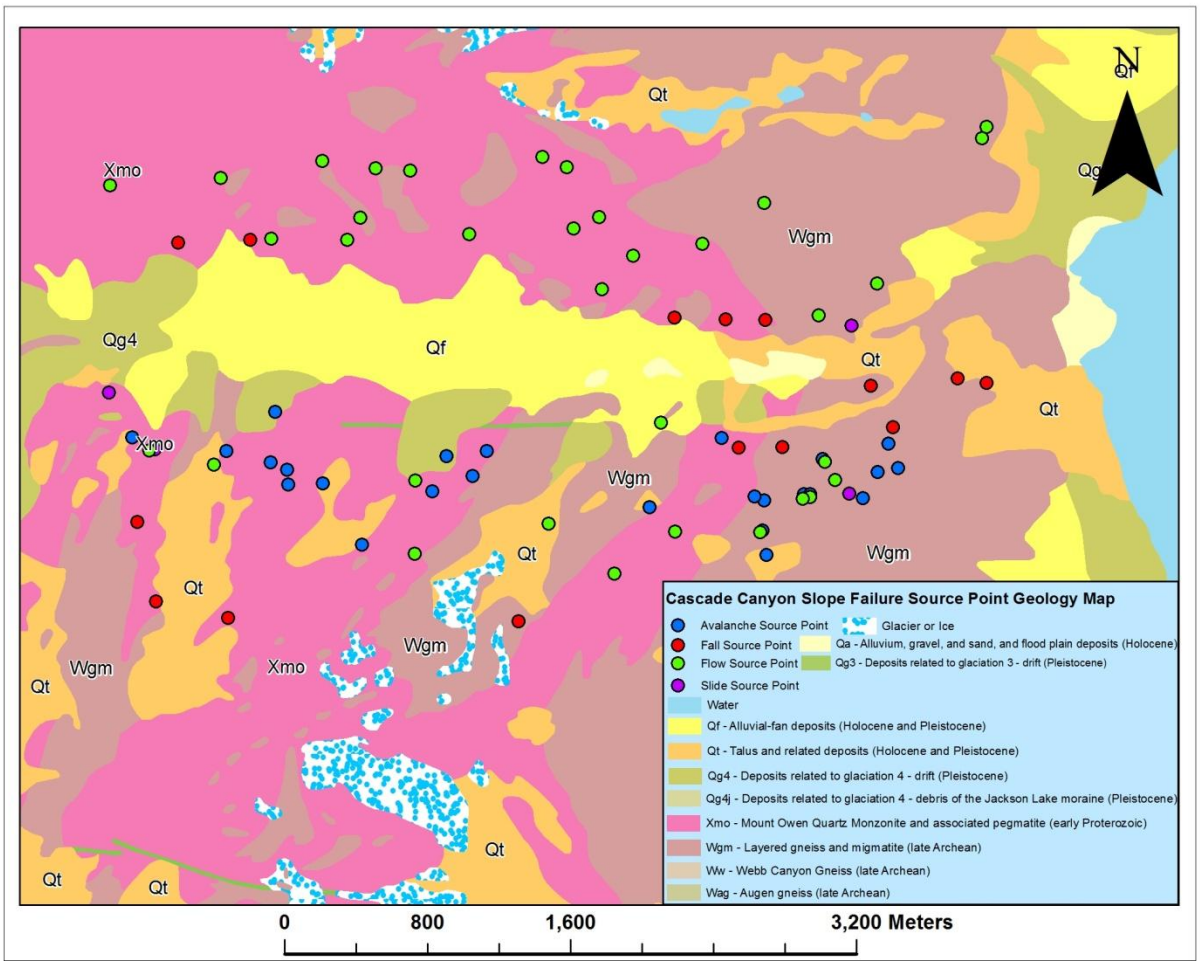

Figure 5.6: Geology map for slope failure source points in Cascade Canyon, GTNP

The upper edges of Cascade Canyon are dominated by Mount Owen Quartz Monzonite/pegmatite in the western and central thirds and layered gneiss/migmatite in the

eastern third. The bottom of the canyon is dominated by alluvial fan deposits and deposits related to glaciations. All three types of slope failure source points were either predominantly or exclusively located on layered gneiss/migmatite or Mount Owen Quartz Monzonite/pegmatite. A relatively significant number of debris flows (7) were located on combinations of the two aforementioned rock types.

Table 5.6: Rock types for slope failures in Cascade Canyon, Grand Teton National Park

Rock type	Total	Falls	Flows	Slides
All rock types	53	15	34	4
Wgm – Layered gniess and migmatite	19	6	11	2
Xmo – Mount Owen quartz monzonite and associated pegmatite	24	7	15	2
Qf – Alluvial fan deposits	1	0	1	0
Xmo Wgm – Layered Gniess/migmatite & Mount Owen quartz monzonite	9	2	7	0

5.1b Death Canyon

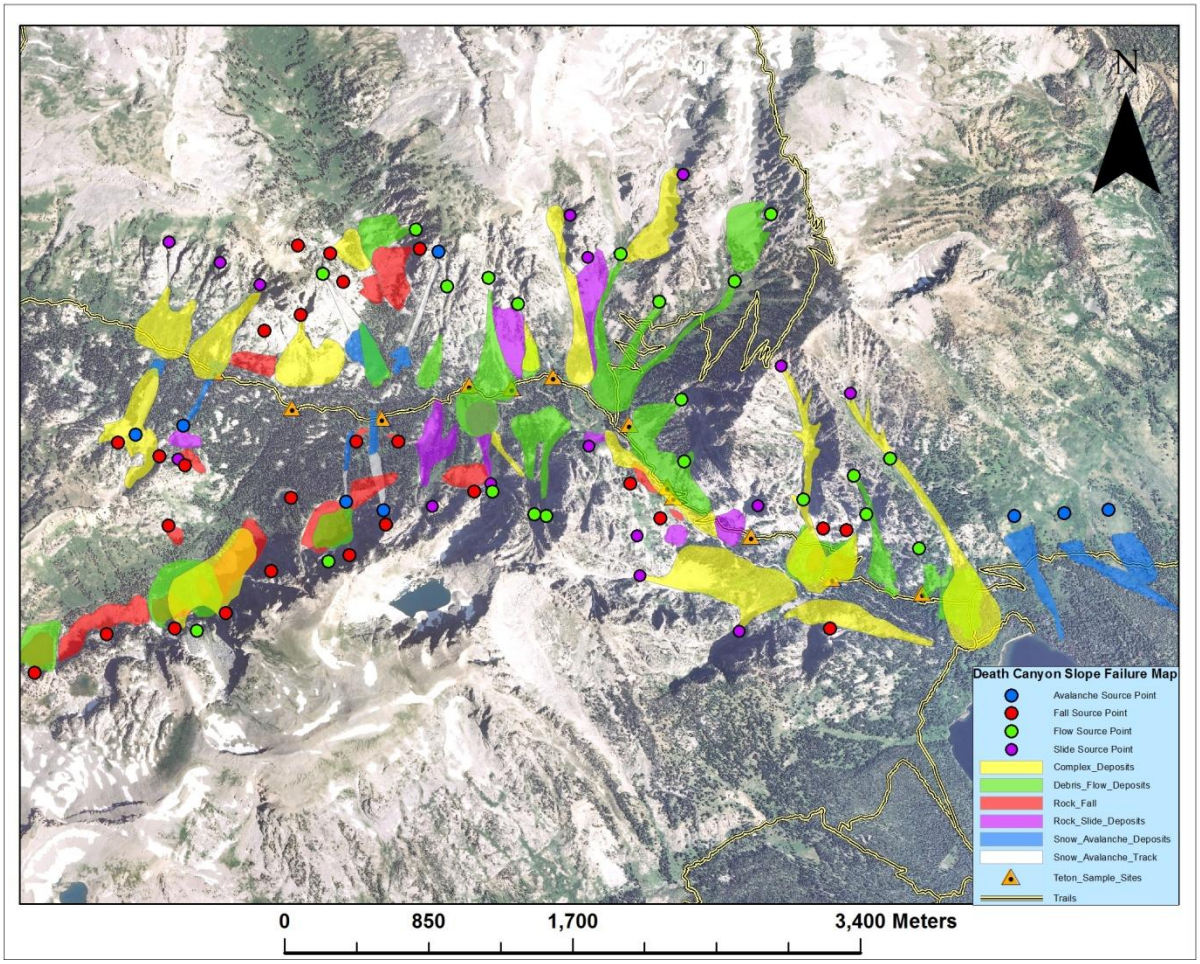

Figure 5.7: Locations of slope failure source points, tracks, and deposits superimposed over an orthorectified image of Death Canyon, GTNP

Table 5.7: Slope failure inventory for Death Canyon, GTNP

	Avalanches	Falls	Flows	Slides	Complex	Total
SF deposits	9	10	20	9	15	73
SF source points	9	26	22	16	N/A	73

Death Canyon is dominated by rock falls, debris flows, and complex deposits. The complex deposits primarily began as rock slides and rock falls. Debris flows, rock slides, and complex deposits occur often in the central section of Death Canyon where the *bend* in its shape takes place. In contrast, the western portion of the canyon is dominated by many small rock falls

mixed with snow avalanches, debris flows, and complex deposits. The lower eastern portion of Death Canyon features a predominant mix of debris flows, complex deposits, and snow avalanches.

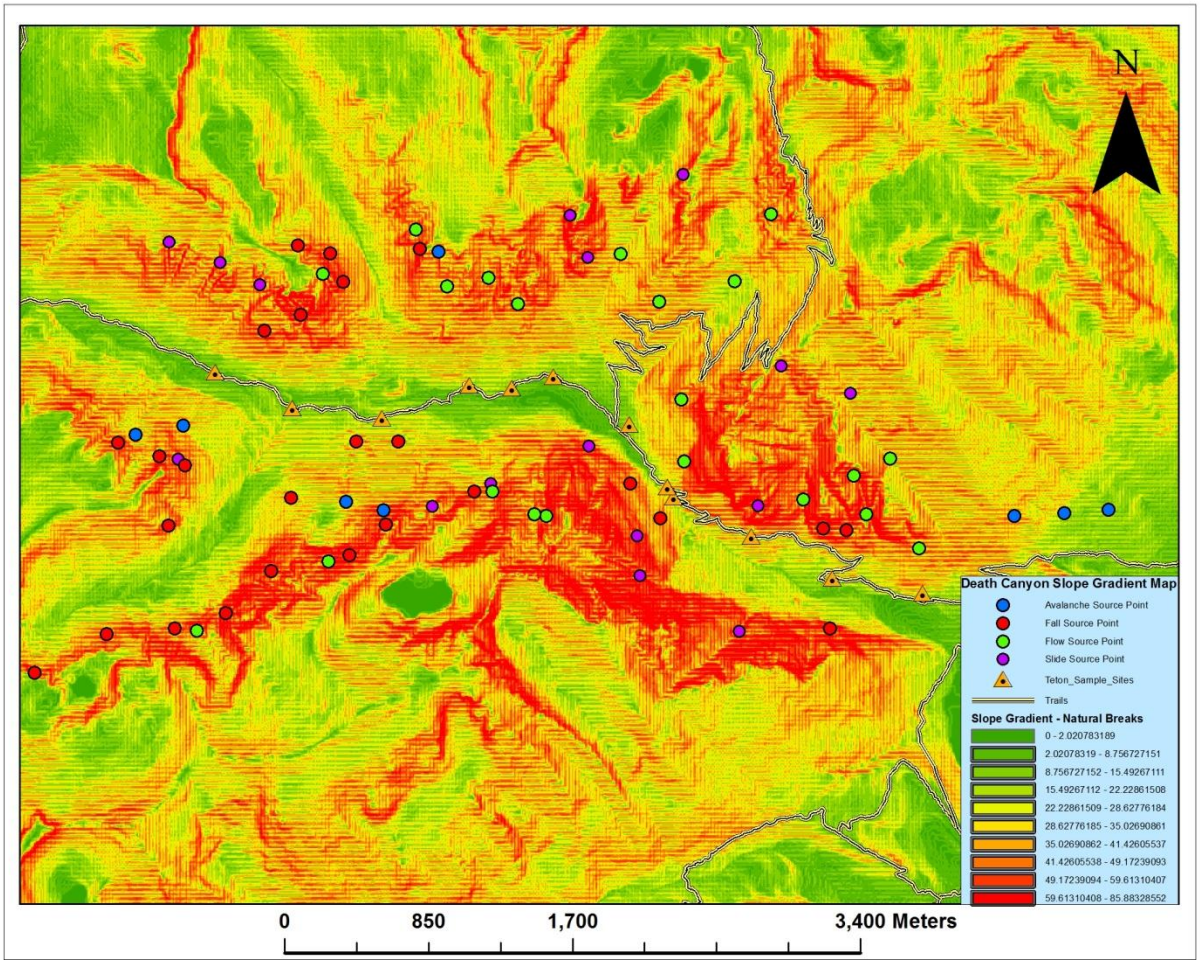

Figure 5.8: Slope gradient map with slope failure source points in Death Canyon, GTNP

Table 5.8: Summary statistics for slope gradient values for all source points in Death Canyon

	Count	Mean	Median	Minimum	Maximum	St. Dev
Avalanches	9	33.30	36.56	12.45	63.33	14.07
Falls	26	55.42	56.78	22.17	73.94	11.11
Flows	22	42.99	40.14	19.74	70.41	13.42
Slides	16	57.36	60.63	32.18	75.50	10.16

Snow avalanches displayed the lowest mean and median values for all slope failure types in Death Canyon. Debris flows also displayed relatively low slope gradient values, and rock falls

and slides displayed comparatively higher average slope gradient values in the mid to high 50s and low 60s. The range for snow avalanches, debris flows, and rock falls were highly similar at close to 51º each, whereas rock slides had a much lower range of 43.32º. Snow avalanches and debris flows showed the highest level of variability from the mean.

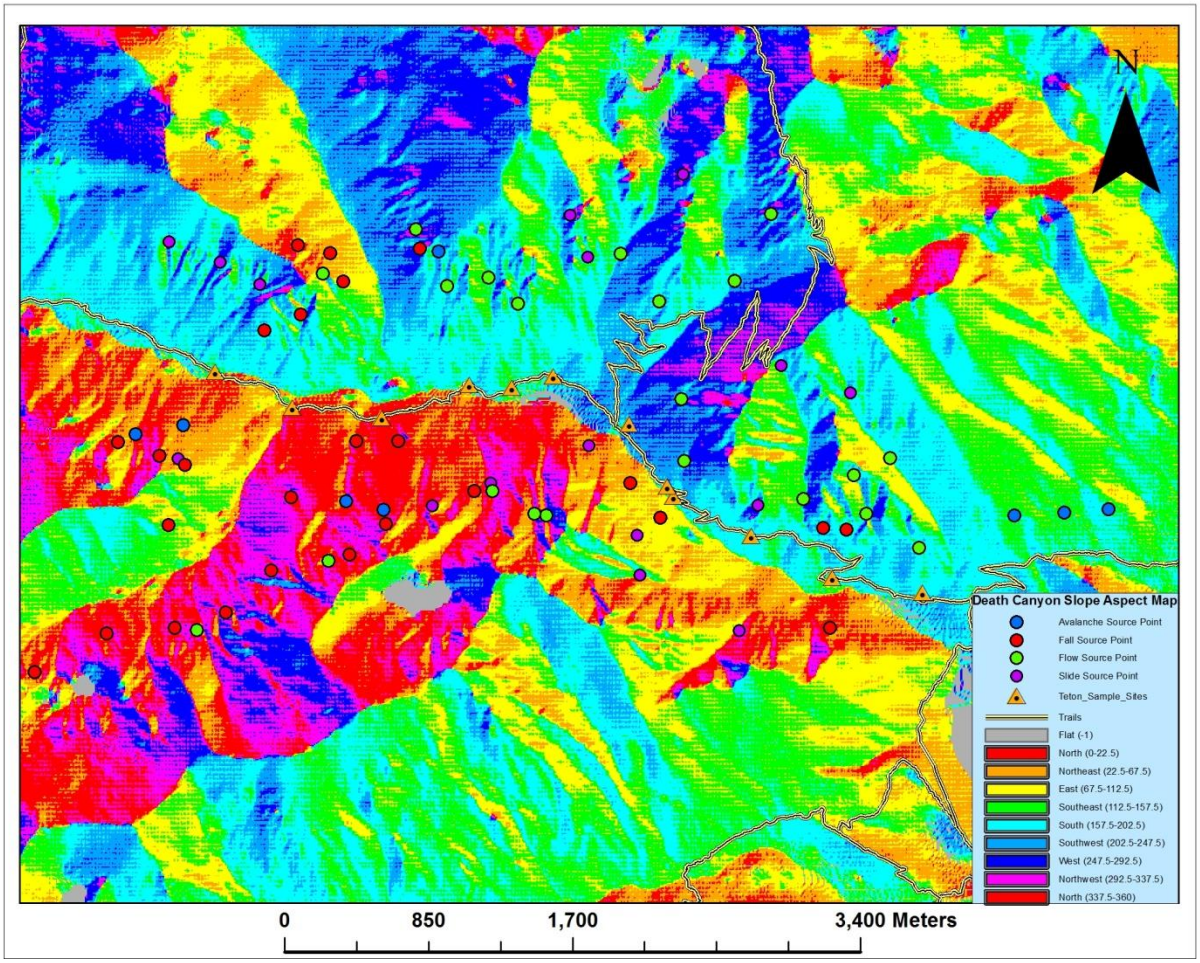

Figure 5.9: Slope aspect map with slope failure source points in Death Canyon, GTNP

Table 5.9: Slope aspect distribution table for all slope failure source points in Death Canyon

	Total	North	NE	East	SE	South	SW	West	NW
Avalanches	9	2	2	0	2	3	0	0	0
Falls	26	9	6	2	2	2	1	1	3
Flows	22	4	0	0	3	8	4	1	2
Slides	16	4	1	1	2	2	1	4	1

Slope aspect values for stand-alone snow avalanche source points displayed a northern, northeast, southern, or southeast bias. Rock falls began primarily on north-, northeast-, or northwest-facing slopes, with a small minority of six occurrences taking place on east, southeast, and southern aspects. Debris flows primarily took place on south-facing slopes with a small minority of north and northwest orientations. Rock slides did not show a noticeable slope aspect bias because orientations were distributed mostly equally with a slight emphasis on north and west values.

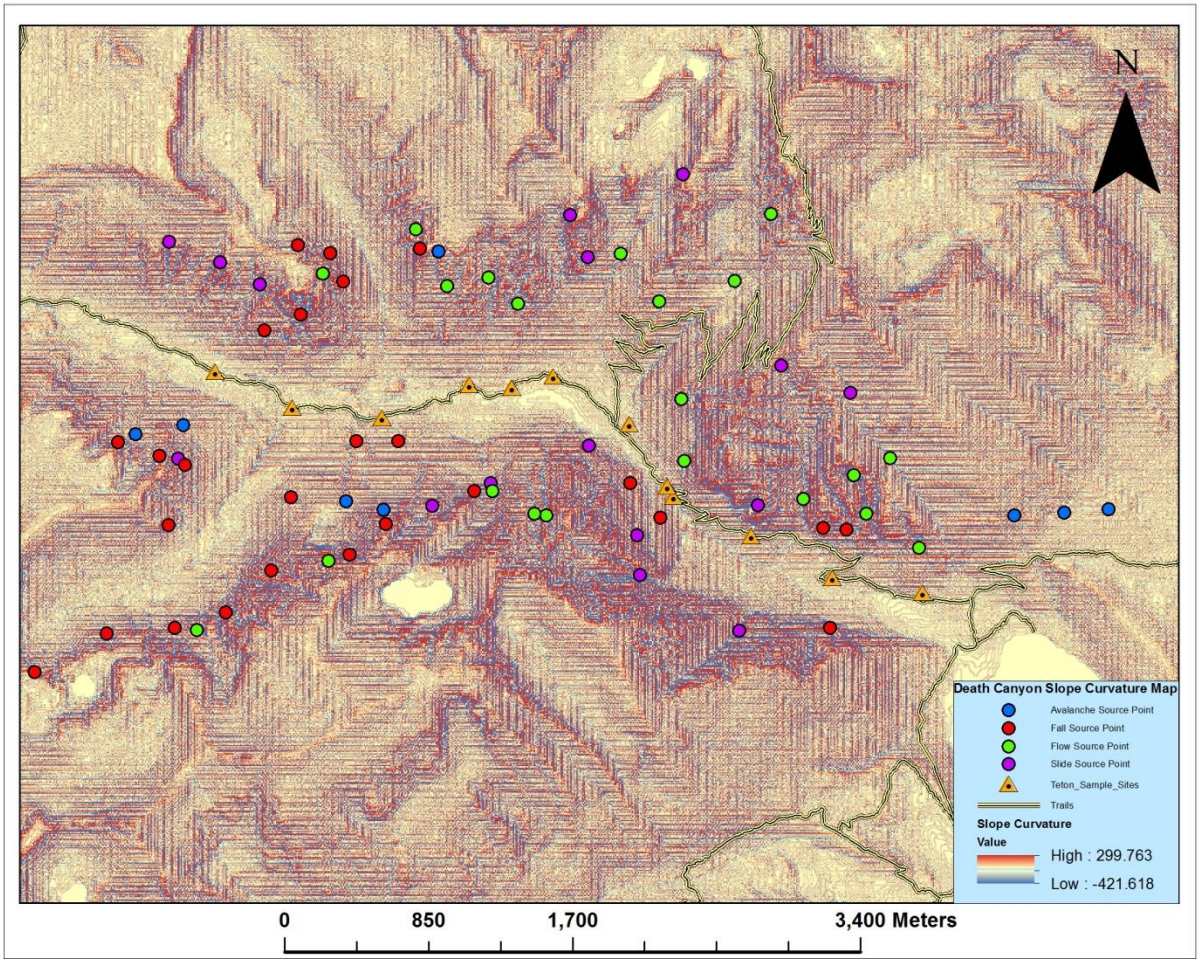

Figure 5.10: Slope curvature map with slope failure source points in Death Canyon, GTNP

Table 5.10: Summary statistics for slope curvature values of all source points in Death Canyon

	Count	Mean	Median	Minimum	Maximum	St. Dev
Avalanches	9	-9.74	-4.87	-34.12	4.87	11.88
Falls	26	2.53	0	-41.43	38.99	18.17
Flows	22	-4.65	-4.87	-56.05	24.37	17.39
Slides	16	1.98	0	-19.50	21.93	10.24

Snow avalanches and debris flows primarily occurred on concave slopes in Death Canyon, but rock falls and rock slides began on mostly flat to slightly convex slopes. Falls and flows had the highest variability values from the mean.

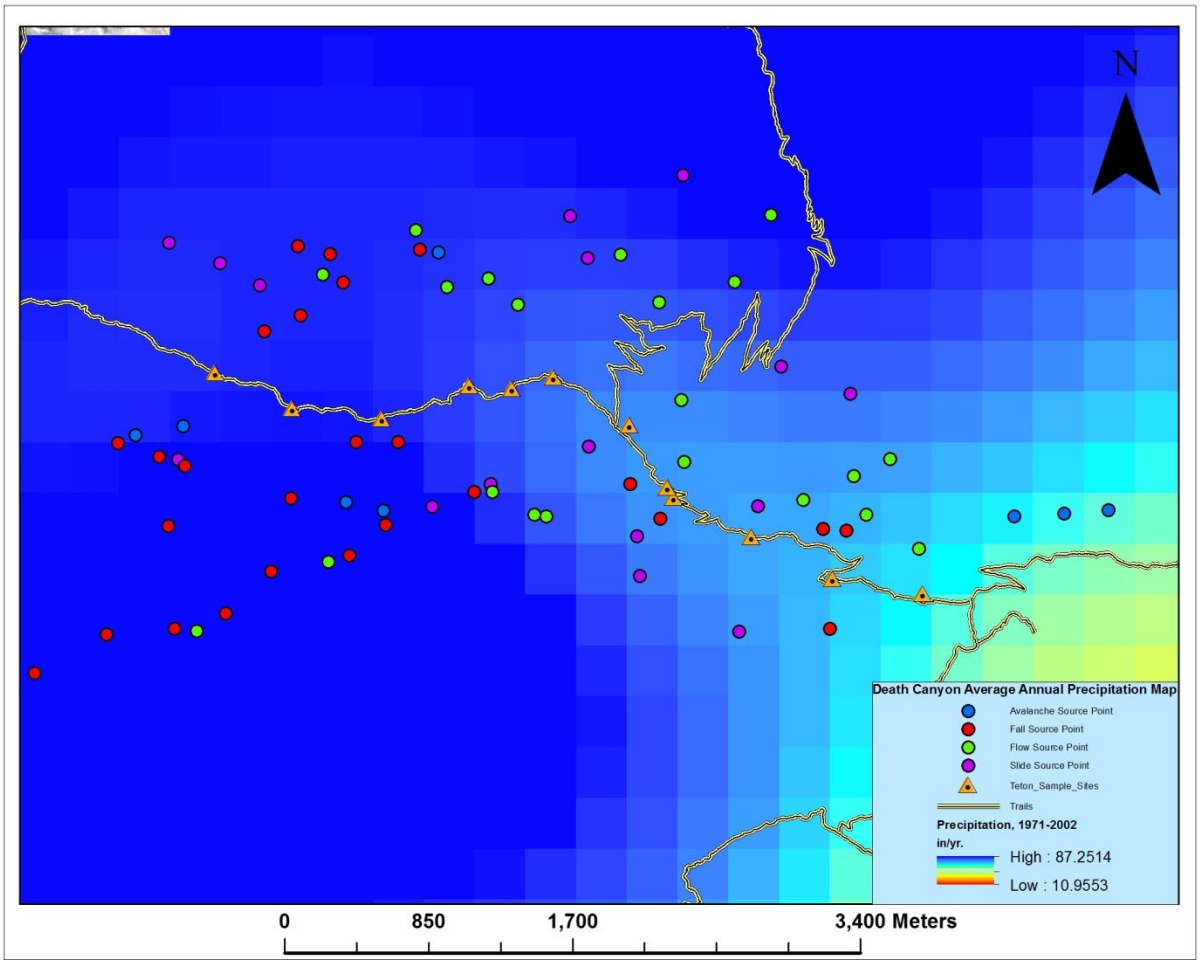

Figure 5.11: Average annual precipitation (1971-2002) map with slope failure source points in Death Canyon, GTNP.

Table 5.11: Average annual precipitation (in./y) summary statistics table for all source points in Death Canyon

	Count	Mean	Median	Minimum	Maximum	St. Dev.
Avalanches	9	53.34	58.00	41.30	62.17	8.00
Falls	26	59.20	58.72	48.21	68.64	5.95
Flows	22	55.80	55.92	45.54	68.32	5.87
Slides	16	55.34	56.15	49.44	60.98	3.75

On average, rock fall source points had the highest average annual precipitation values, followed by flows and slides; whereas snow avalanches displayed a relatively high level of difference between the mean and median. Snow avalanches also displayed the highest variability from the mean, and rock slides displayed the lowest variability value. Many of the rock falls occur in the relatively wet, western upper portion of Death Canyon, whereas snow avalanche variability can possibly be explained by the geographic distribution of the source points; avalanches occur in the relatively dry eastern portion and relatively wet western portion of the canyon. Rock slides in Death Canyon primarily occur in the central to eastern parts of Death Canyon, so the low variability in the range and standard deviation values can be attributed to a high proximity of slide points between each other.

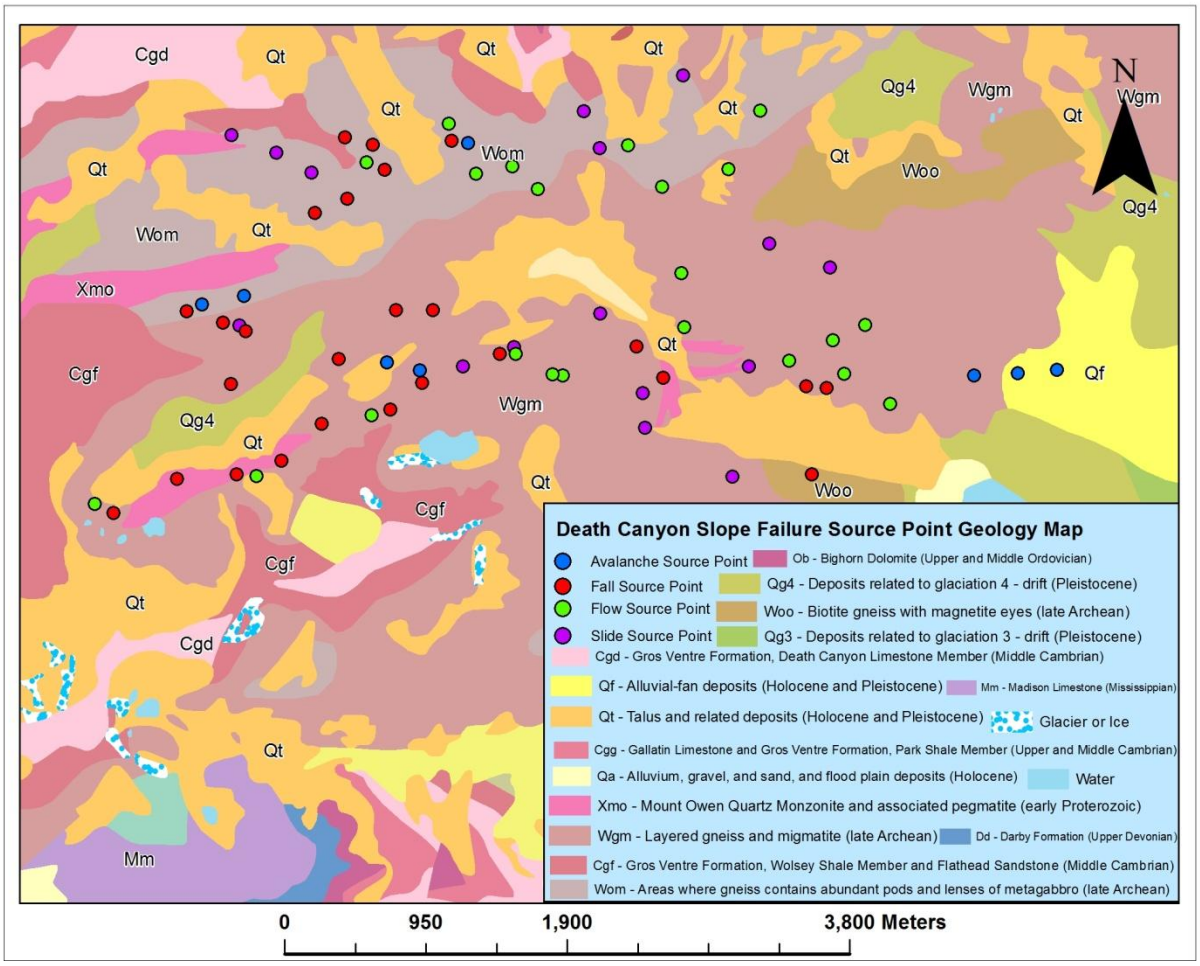

Figure 5.12: Geology map for slope failure source points in Death Canyon, GTNP

Although many different rock types occur at sites of slope failure sources in Death Canyon, layered gneiss and migmatite deposits (Wgm) and gneiss deposits with abundant pods of metagabbro (Wom) are by far the most dominant rock types present. Mount Owen Quartz Monzonite and associated pegmatite deposits (Xmo) and Xmo Wgm deposits also account for minimal numbers of rock fall source points.

Table 5.12: Rock types for slope failures in Death Canyon, Grand Teton National Park

Rock type	Total	Falls	Flows	Slides
All rock types	64	26	22	16
Cgd – Gros Ventre formation, Death Canyon limestone member	1	0	0	1
Cgf - Gros Ventre formation, Wolsey Shale member and Flathead sandstone	1	0	0	1
Wgm – Layered gniess and migmatite	33	13	12	8
Wom – Areas where gneiss contains abundant pods and lenses of metagabbro	21	7	8	6
Xmo – Mount Owen quartz monzonite and associated pegmatite	3	2	1	0
Xmo Wgm – Mount Owen quartz monzonite and associate pegmatite/layered gneiss and migmatite	2	3	0	0
Qt – Talus and other related deposits	2	0	2	0
Woo – Biotite gneiss with magnetite eyes	1	1	0	0

5.1c Garnet Canyon

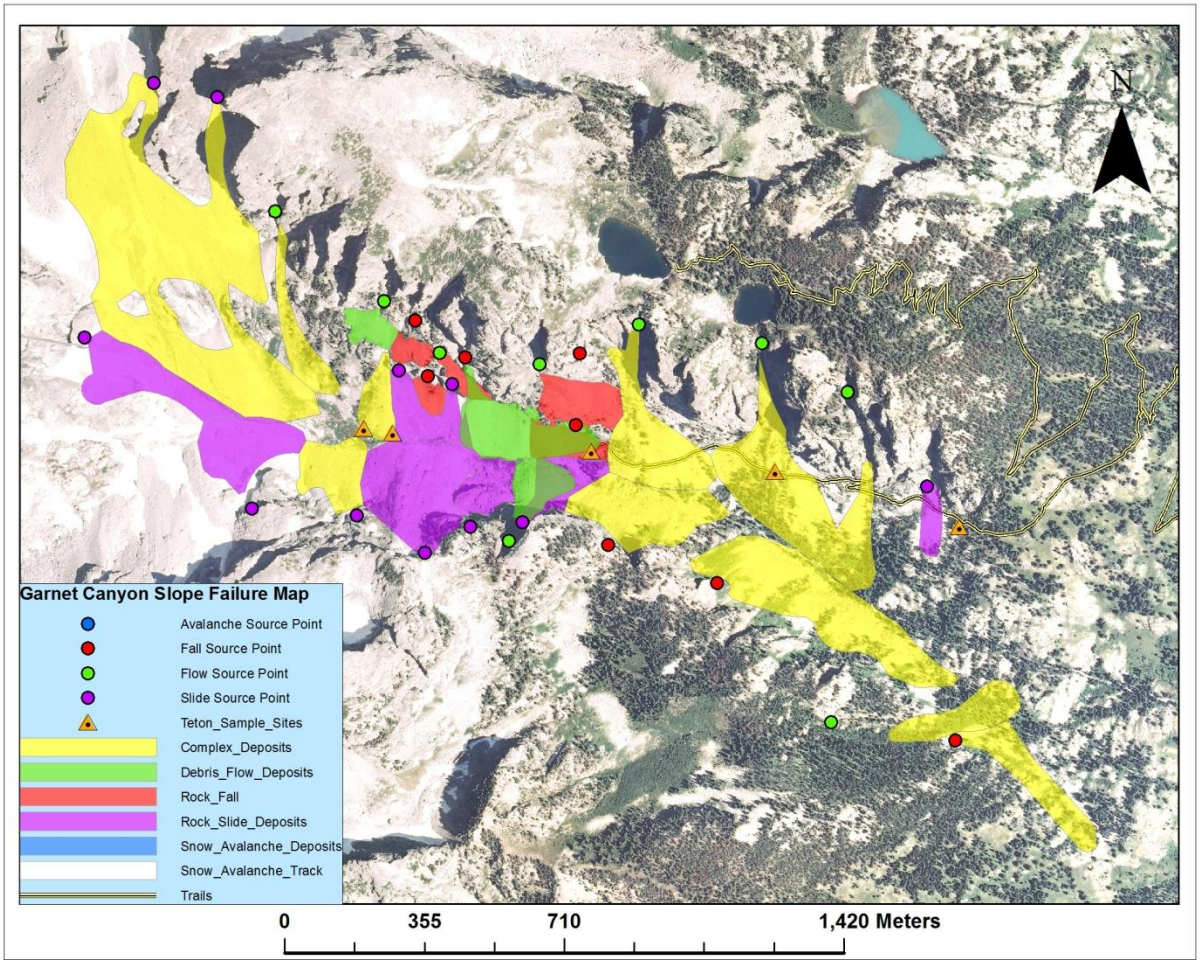

Figure 5.13: Locations of slope failure source points, tracks, and deposits superimposed over an orthorectified image of Garnet Canyon, GTNP

Table 5.13: Slope failure inventory for Garnet Canyon, GTNP

	Avalanches	Falls	Flows	Slides	Complex	Total
SF deposits	0	5	5	7	10	27
SF source points	0	8	9	11	-	28

Garnet Canyon is a steep canyon that is relatively short in length and is dominated by complex and rock slide deposits. Debris flows and rock slides also occur in significant numbers, but curiously no stand-alone snow avalanche deposits are present. Much of the terrain at the canyon bottom near the hiking trail is dominated by talus deposits, and very little low growing

vegetation is present. Although debris flow deposits are always a common risk zone for snow avalanches to occur, apparently this canyon is primarily dominated by an active regime of rock-based slope failures.

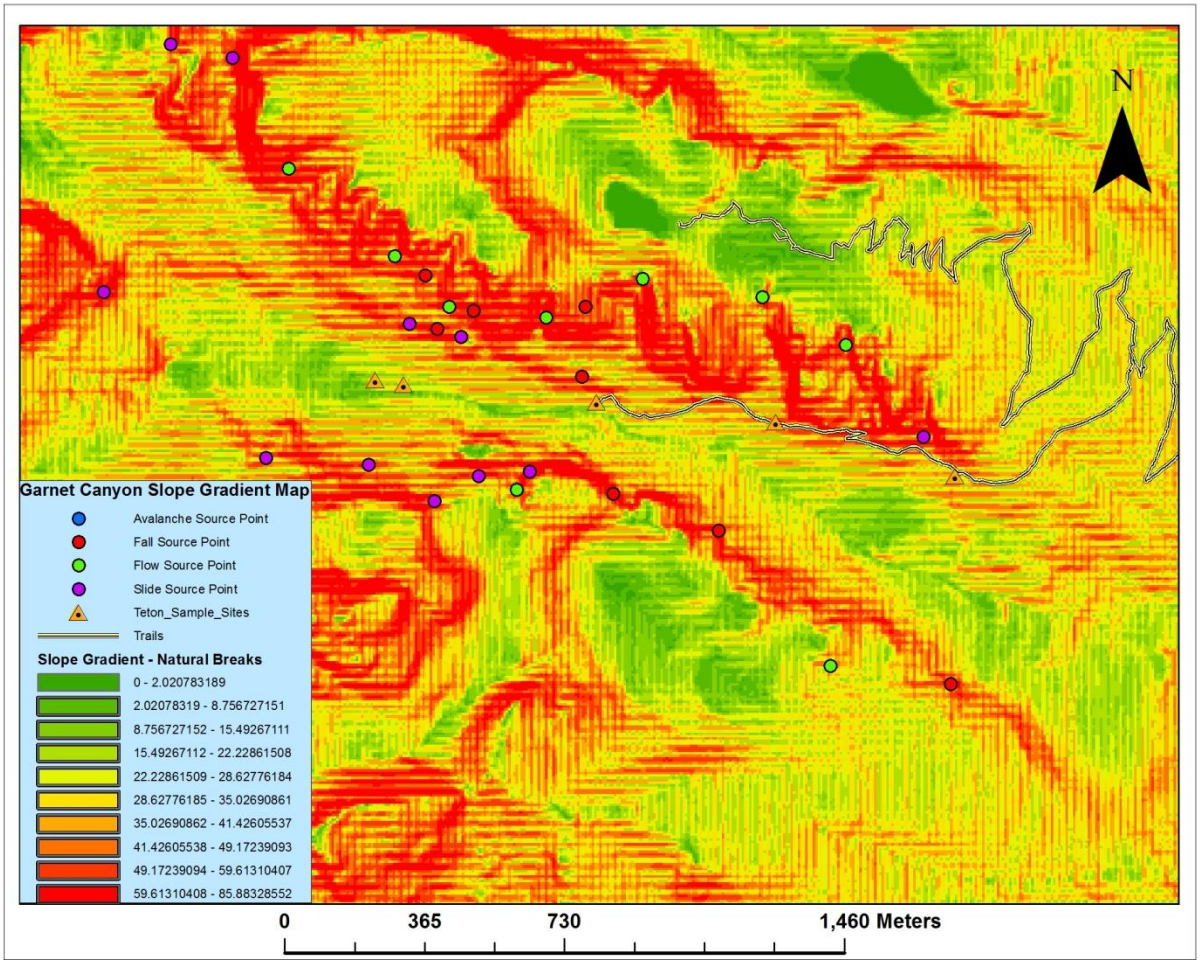

Figure 5.14: Slope gradient map with slope failure source points in Garnet Canyon, GTNP.

Table 5.14: Summary statistics for slope gradient values of all source points in Garnet Canyon

	Count	Mean	Median	Minimum	Maximum	St. Dev.
Avalanches	0	-	-	-	-	-
Falls	8	60.48	62.37	46.04	75.51	9.29
Flows	9	52.61	45.00	32.18	78.11	15.55
Slides	11	52.36	58.31	27.64	63.58	11.58

Debris flows occurred on a much higher slope gradient in Garnet Canyon than in other canyons and displayed a very high level of variability in comparison to other types of slope

failures; but they still averaged lower gradient values than falls or slides. Rock falls averaged the highest slope gradient values, and slides averaged the second highest values but displayed higher variability from the mean than rock falls.

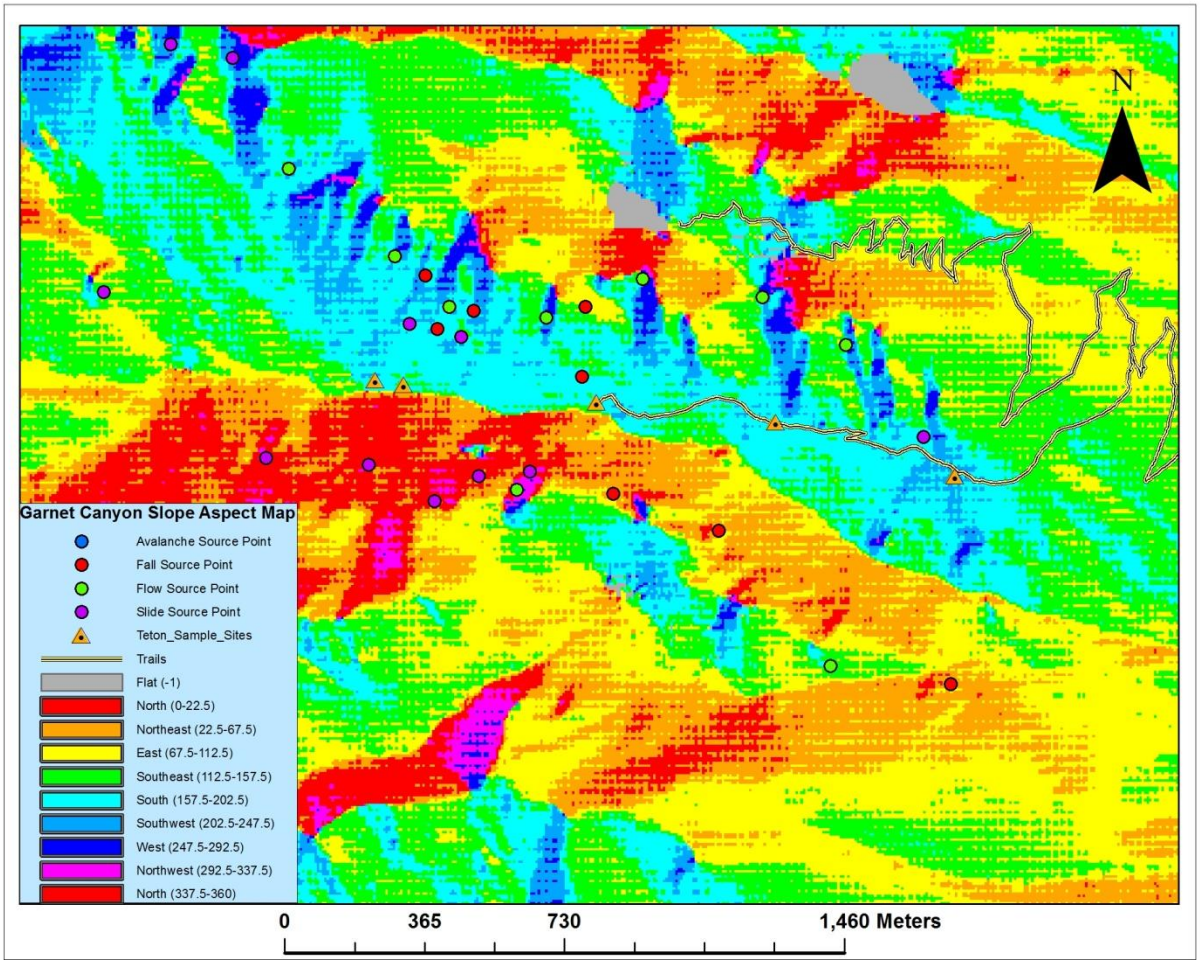

Figure 5.15: Slope aspect map with slope failure source points in Garnet Canyon, GTNP

Table 5.15: Slope aspect distribution table for all slope failure source points in Garnet Canyon

	Total	North	NE	East	SE	South	SW	West	NW
Avalanches	0	-	-	-	-	-	-	-	-
Falls	8	0	3	1	0	3	1	0	0
Flows	9	0	0	0	0	4	2	2	1
Slides	11	3	0	0	1	3	1	1	2

Rock fall aspects slightly favored northeast and southern values, whereas debris flows occurred mostly on southern, western, and southwestern slopes. Rock slides showed a very slight

bias towards northern and southern values, although the distribution of slope aspect values for slides was very even. Given the relatively low sample size of each type of slope failure source point as well as relatively even distributions, formulating any sound conclusions about whether a given type of slope failure favors a certain type of aspect or not may be difficult. However, debris flows appear not to occur very often at northern or eastern aspects.

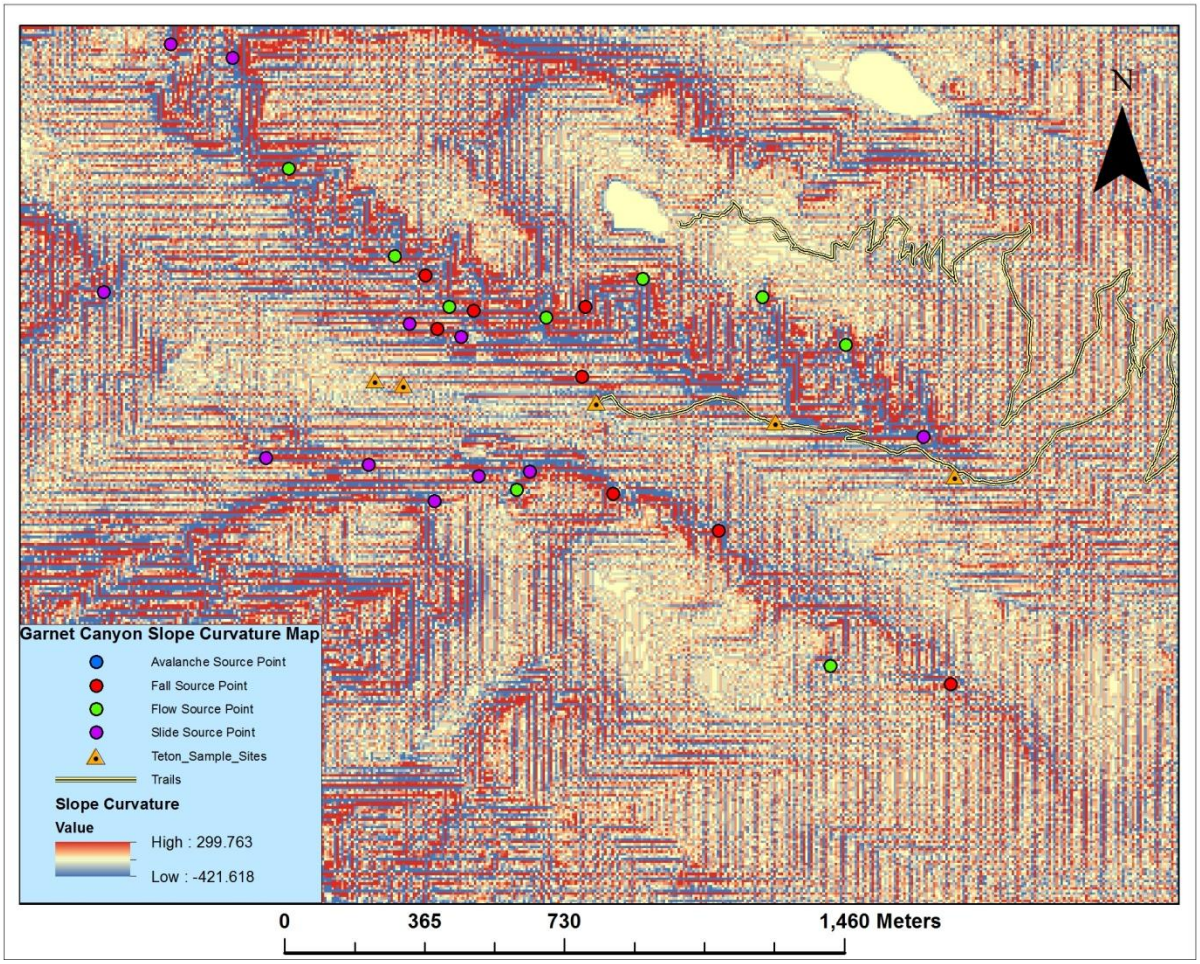

Figure 5.16: Slope curvature map with slope failure source points in Garnet Canyon, GTNP

Table 5.16: Slope curvature distribution table for all source points in Garnet Canyon

	Count	Mean	Median	Minimum	Maximum	St. Dev.
Avalanches	0	-	-	-	-	-
Falls	8	-8.53	-2.44	-68.24	26.81	26.86
Flows	9	-10.56	4.87	-63.36	12.19	28.28
Slides	11	4.21	7.31	-63.36	43.87	26.21

Rock slides demonstrated a tendency to occur on convex slopes, rock falls tended to occur on concave slopes, and debris flows showed a high level of variability to the point of being inconclusive. Each type of slope failure displayed a relatively high level of variability from the mean as well as large ranges of values. Variability of slope failure curvature statistics demonstrates the relatively extreme profile of Garnet Canyon but makes it difficult to formulate any solid conclusions about the role curvature plays in causing slope failures.

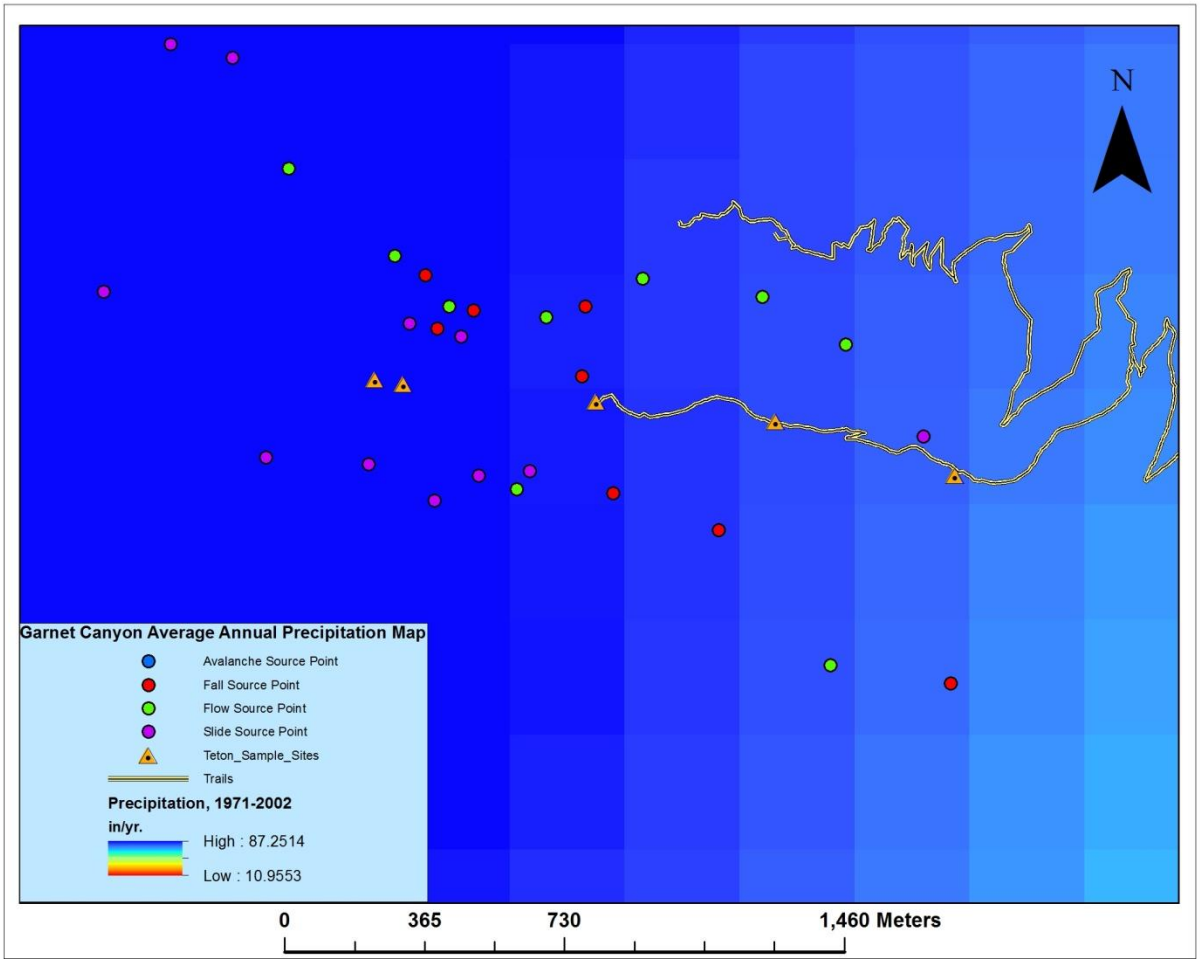

Figure 5.17: Average annual precipitation (1971-2002) map with slope failure source points in Garnet Canyon, GTNP.

Table 5.17: Average annual precipitation (in./yr.) summary statistics table for all source points in Garnet Canyon

	Count	Mean	Median	Minimum	Maximum	St. Dev.
Avalanches	0	-	-	-	-	-
Falls	8	58.38	58.68	53.35	60.02	2.08
Flows	9	58.43	58.75	55.42	61.99	2.40
Slides	11	61.60	60.12	54.08	66.85	3.64

Most of the rock slides or complex deposits beginning as rock slides occurred in the central to western portion of Garnet Canyon where precipitation is greatest, so rock slide source points displaying the highest mean and median average annual precipitation values is not surprising. Falls and flows in Garnet Canyon are mostly bunched together in the central portion of Garnet Canyon, thus displaying similar precipitation averages. All three types of slope failures displayed very low standard deviation values, suggesting a relatively uniform precipitation regime caused by spatial bunching in the short length of Garnet Canyon.

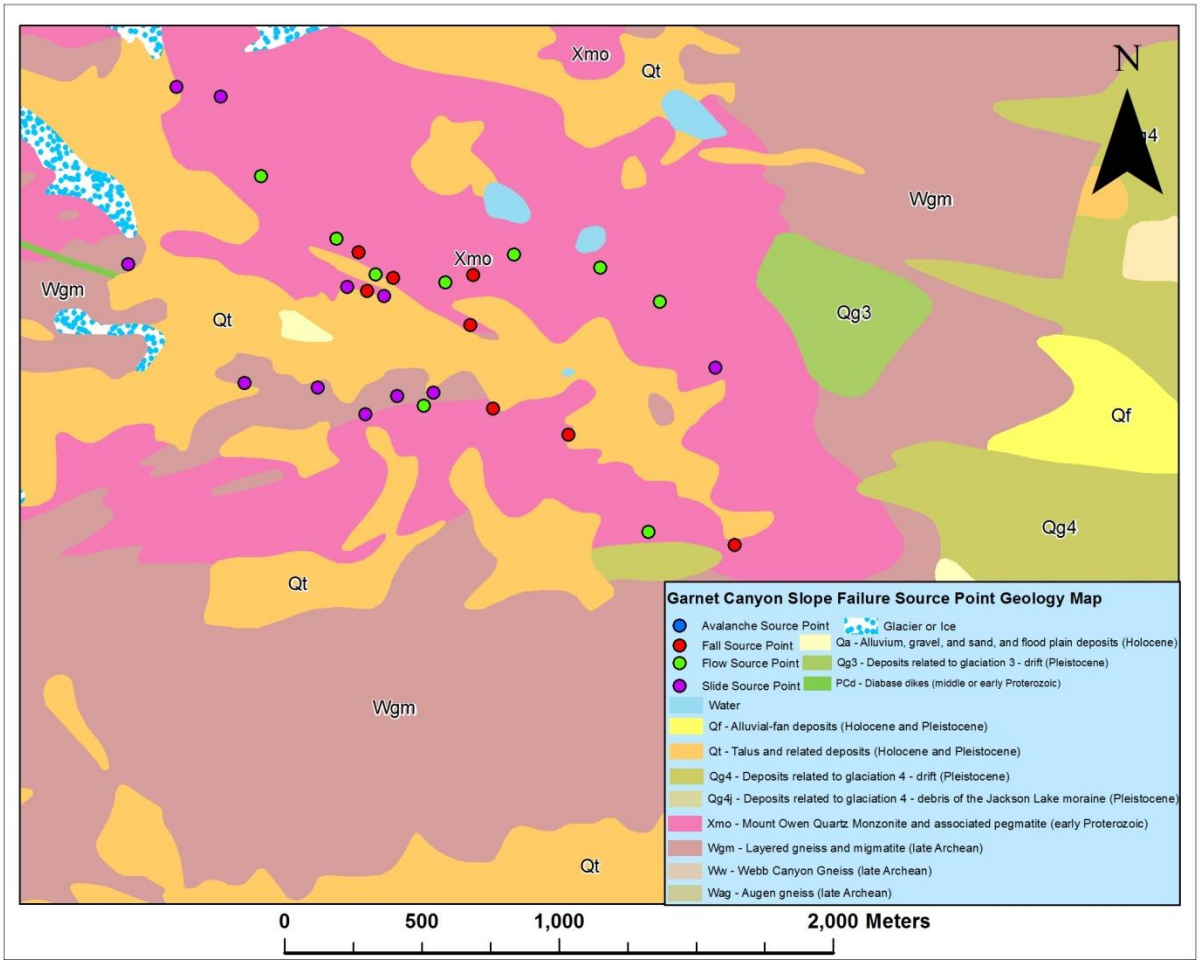

Figure 5.18: Geology map for slope failure source points in Garnet Canyon

Table 5.18: Rock types for slope failure source points in Garnet Canyon, GTNP

Rock Type	Total	Falls	Flows	Slides
All Rock Types	28	8	9	11
Wgm – Layered Gneiss and migmatite	5	0	0	5
Xmo – Mount Owen quartz monzonite and associated pegmatite	19	7	8	4
Xmo Wgm – Mount Owen quartz monzonite and associated pegmatite/layered gneiss and migmatite	2	1	0	1
Qt – Talus and other related deposits	2	0	1	1

5.1d Granite Canyon

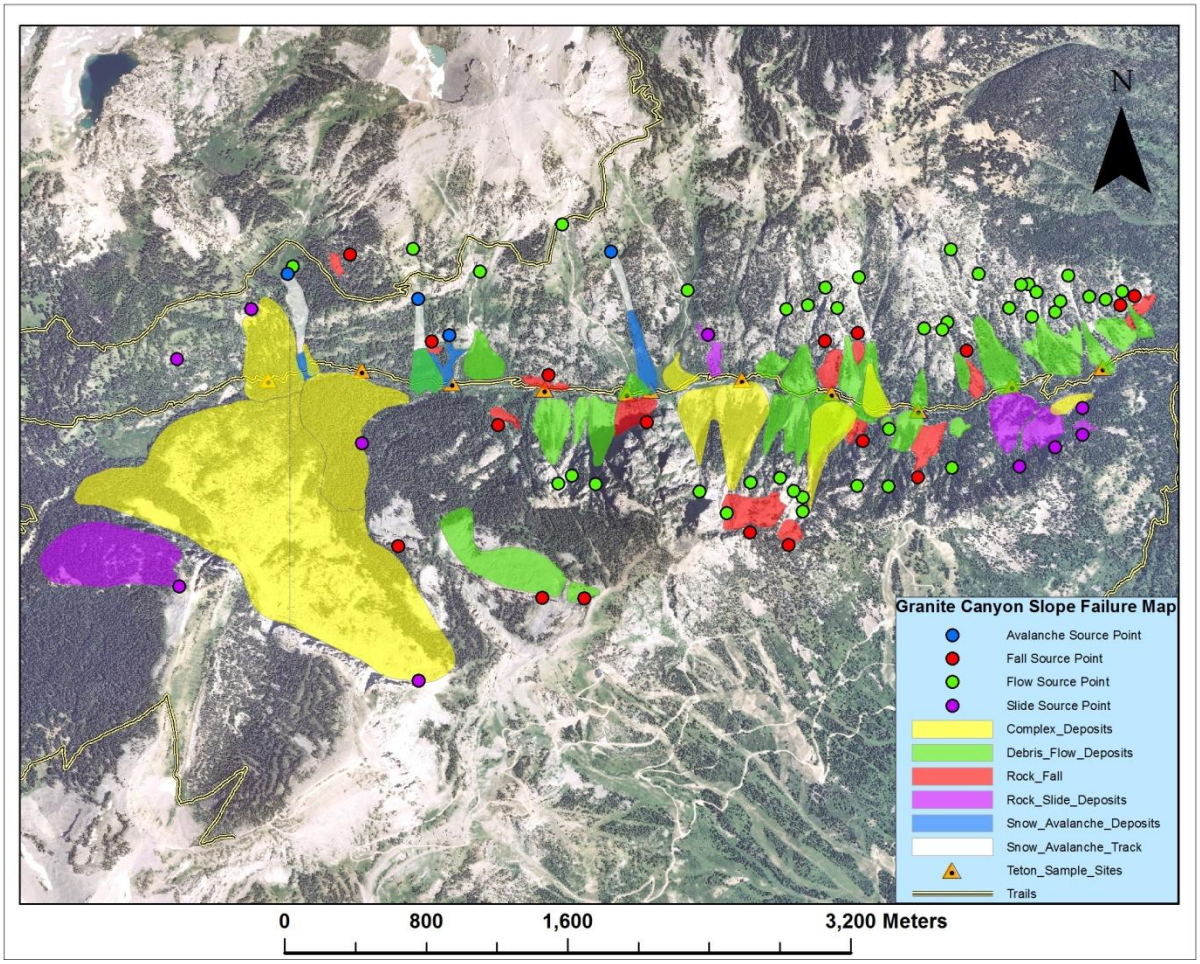

Figure 5.19: Locations of slope failure source points, tracks, and deposits superimposed over an orthorectified image of Granite Canyon, GTNP.

Table 5.19: Slope failure inventory for Granite Canyon, GTNP

	Avalanches	Falls	Flows	Slides	Complex	Total
SF deposits	4	14	28	5	11	62
SF source points	4	17	40	10	-	71

Granite Canyon is dominated by debris flows first and foremost, with significant quantities of rock falls and complex deposits. Few stand-alone rock slides and avalanches exist, although almost half of the complex slope failures in Granite Canyon began as rock slides.

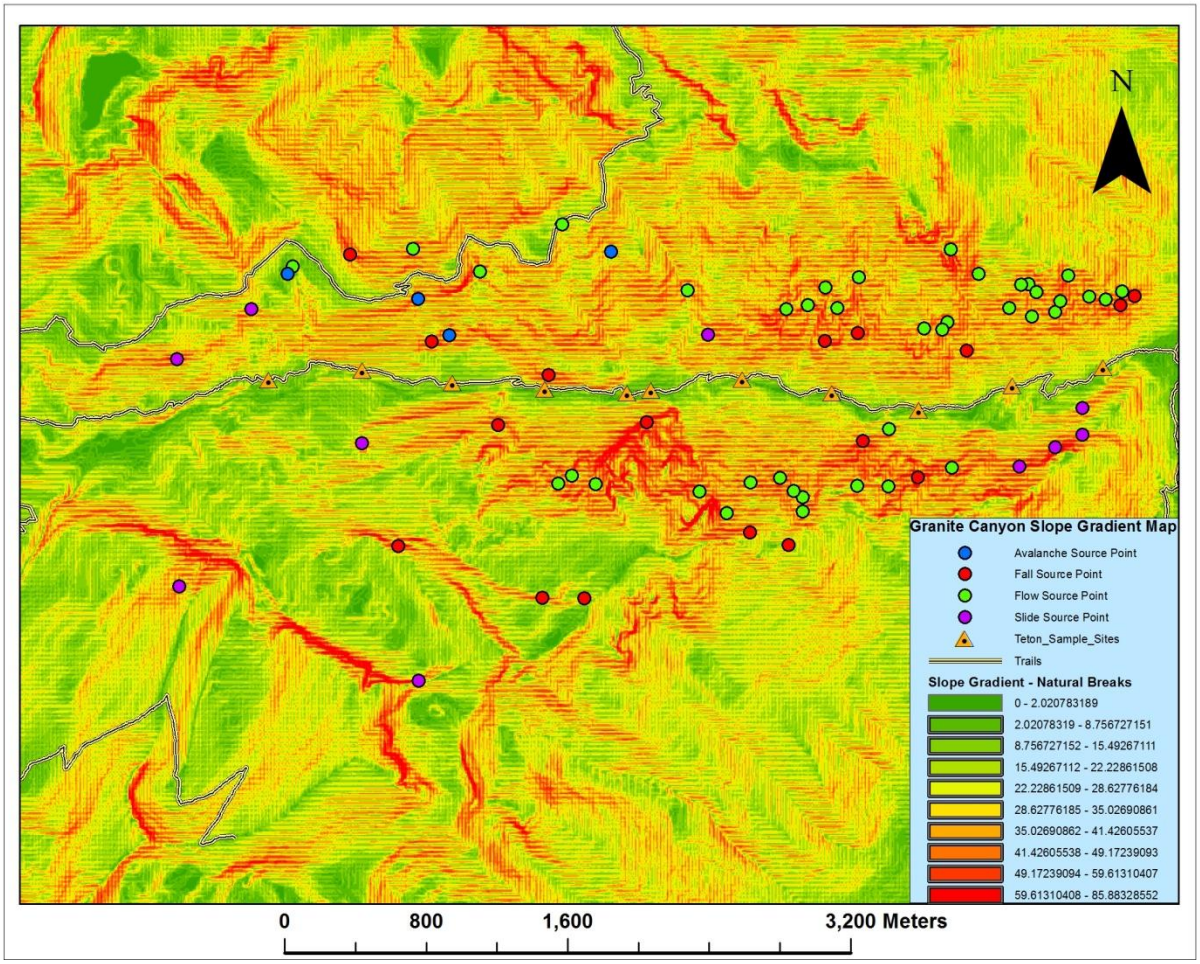

Figure 5.20: Slope gradient map with slope failure source points in Granite Canyon, GTNP.

Table 5.20: Summary statistics for slope gradient values of all source points in Granite Canyon

	Count	Mean	Median	Minimum	Maximum	St. Dev.
Avalanches	4	32.65	33.76	13.18	49.89	13.22
Falls	17	47.36	44.18	13.35	78.71	14.45
Flows	40	38.69	38.25	9.90	59.95	11.28
Slides	10	51.97	52.74	40.61	63.13	7.26

Slope gradient values for avalanches and debris flows averaged near 33º and 38º, respectively; whereas rock falls and rock slides averaged much higher near 45-46º and 52º, respectively. These averages follow the pattern seen in the previous three canyons: snow avalanches and debris flows tend to occur at lower slope gradients than their fall and slide counterparts. Avalanches and falls had the highest variability from the mean, although the low

sample size of snow avalanche source points should be factored in as a potential source of skepticism. Rock falls occurred on a very wide variety of slopes, from shallow, gentle slopes near the bottom of the canyon to incredibly high gradients in areas of considerable steepness.

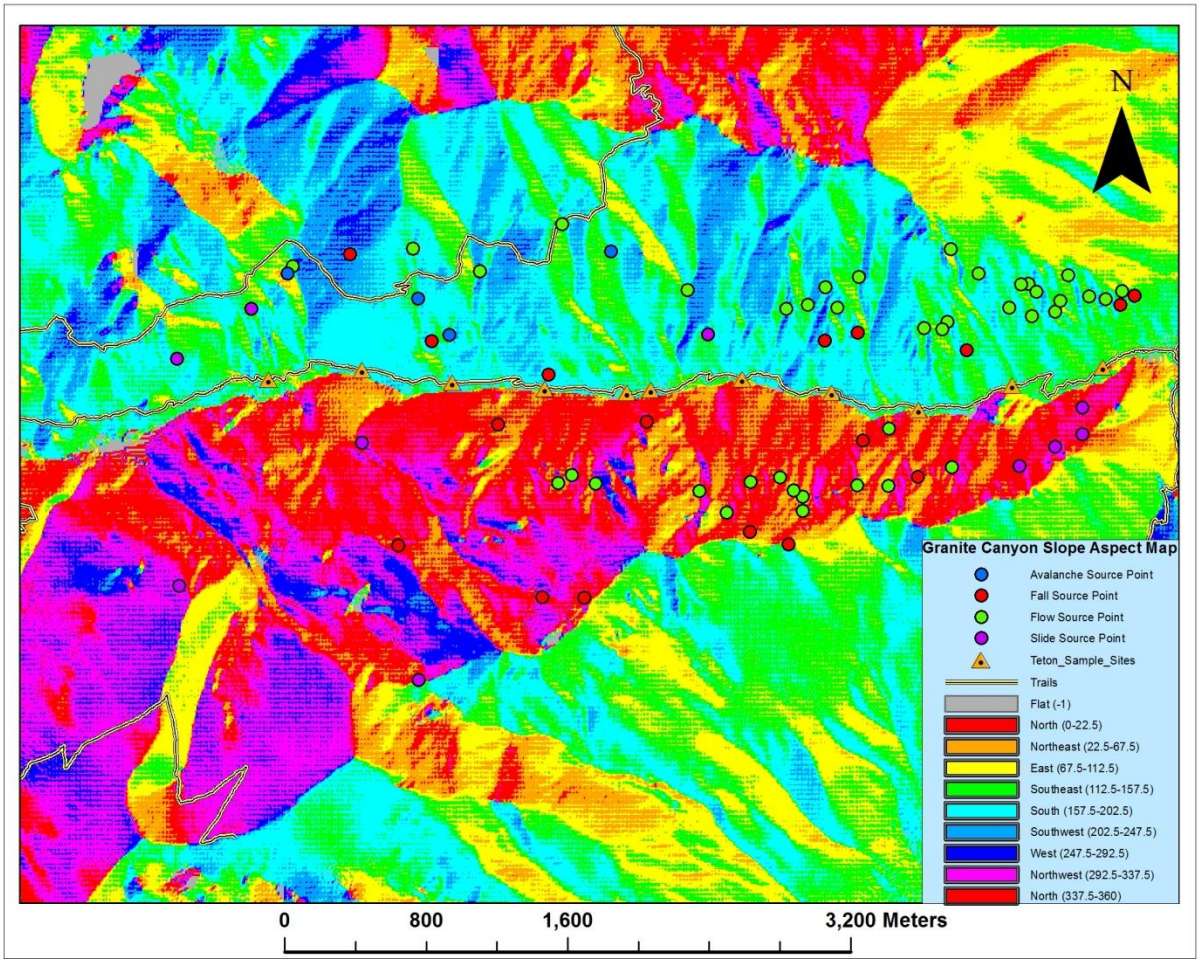

Figure 5.21: Slope aspect map with slope failure source points in Granite Canyon, GTNP

Table 5.21: Slope aspect distribution table for all slope failure source points in Granite Canyon

	Total	North	NE	East	SE	South	SW	West	NW
Avalanches	4	0	0	1	1	2	0	0	0
Falls	17	6	2	0	2	6	0	1	0
Flows	40	6	6	2	18	5	2	0	1
Slides	10	5	0	0	1	2	0	1	1

Slope aspect distributions for snow avalanches in Granite Canyon were inconclusive, primarily because of a low sample size. Rock falls occurred most commonly and evenly on northern and southern slopes with small amounts of northeast and southeast orientations present. Debris flows displayed a clear tendency to occur most frequently on southeast- or southern-facing slopes, although significant numbers of flows also occurred on northern and northeast aspects. Rock slides occurred mostly on north-facing slopes with a lesser tendency toward southern slopes.

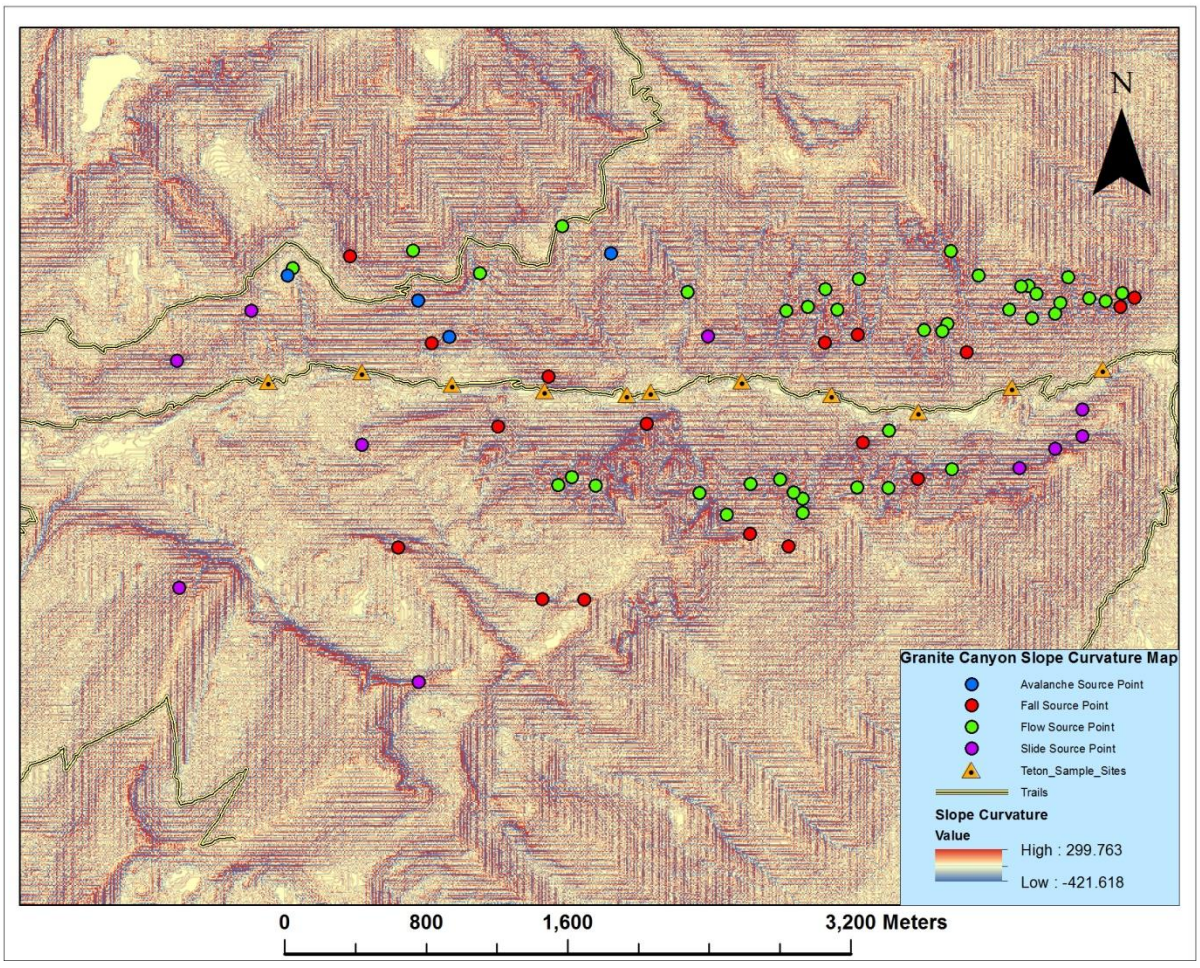

Figure 5.22: Slope curvature map with slope failure source points in Granite Canyon, GTNP

Table 5.22: Summary statistics for slope gradient values of all source points in Granite Canyon

	Count	Mean	Median	Minimum	Maximum	St. Dev.
Avalanches	4	1.83	-1.22	-4.87	14.62	7.59
Falls	17	-1.29	-7.31	-26.81	85.30	25.93
Flows	40	-2.92	1.22	-43.87	21.93	14.51
Slides	10	-5.12	-7.31	-29.25	14.62	11.96

Snow avalanches and debris flows had differing mean and median values, suggesting that the average curvature for each type is close to flat. Rock falls showed a slight bias toward occurring on concave slopes, albeit with major differences between mean and median values and a high variability from the mean. Rock slides primarily occurred on concave slopes and displayed a relatively low variability from the mean.

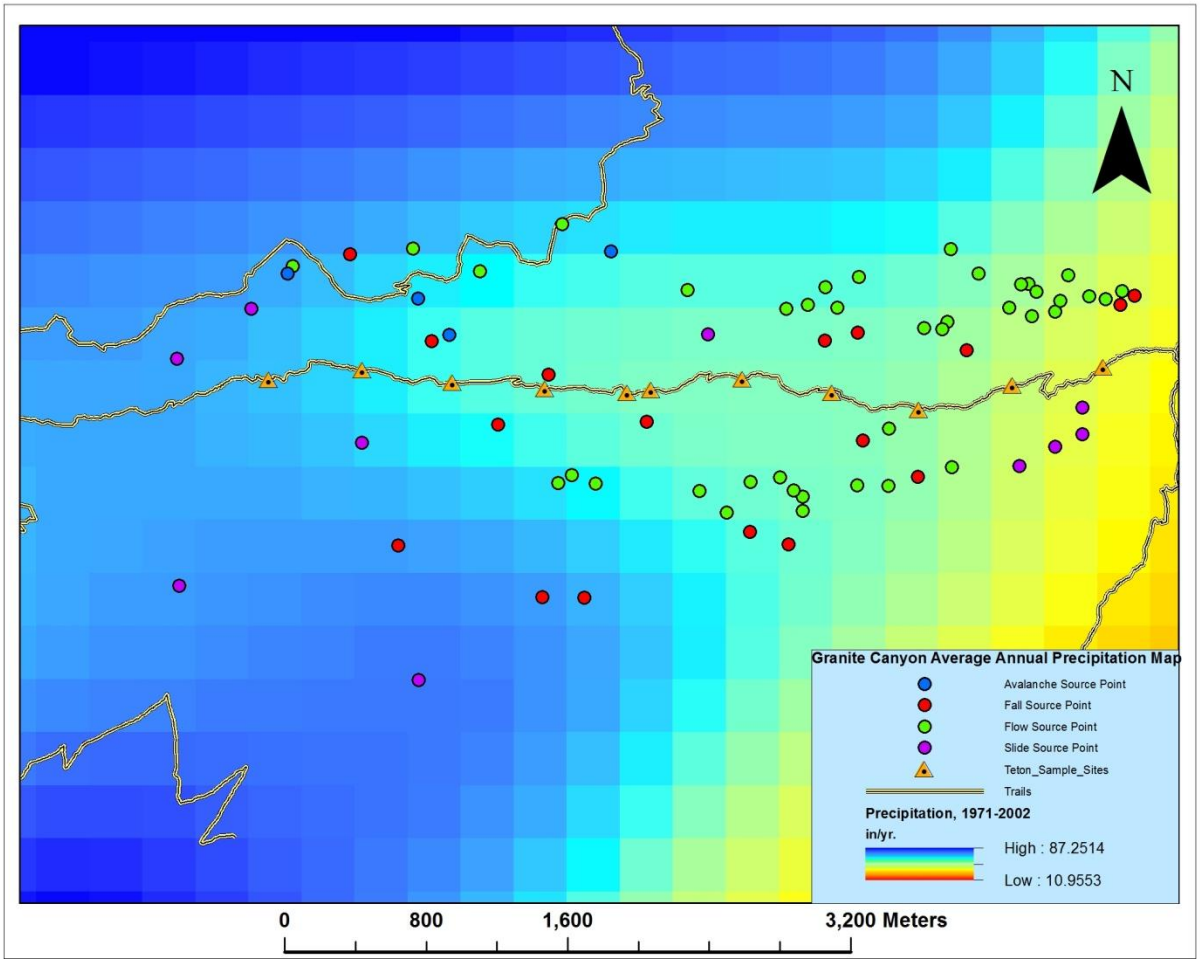

Figure 5.23: Average annual precipitation (1971-2002) map with slope failure source points in Granite Canyon, GTNP.

Table 5.23: Average annual precipitation (in./y) summary statistics table for all source points in Granite Canyon

	Count	Mean	Median	Minimum	Maximum	St. Dev.
Avalanches	4	45.55	45.23	42.81	48.90	2.19
Falls	17	41.59	40.65	31.82	50.07	5.41
Flows	40	39.45	39.91	31.82	48.90	4.01
Slides	10	41.28	43.10	30.84	52.57	8.47

Debris flows in Granite Canyon occurred under drier conditions than its avalanche, fall, and slide counterparts. Many of these flows occurred in the relatively dry eastern third of Granite Canyon, whereas falls and slides were more equally distributed over the full canyon area. All four snow avalanche source points were located in the center to western parts of Granite Canyon. Rock slides displayed the highest variability from the mean as well as the starkest spatial differences among its source points; four occurred on the extreme eastern edge of the canyon and five were located in the wetter western portion of the canyon.

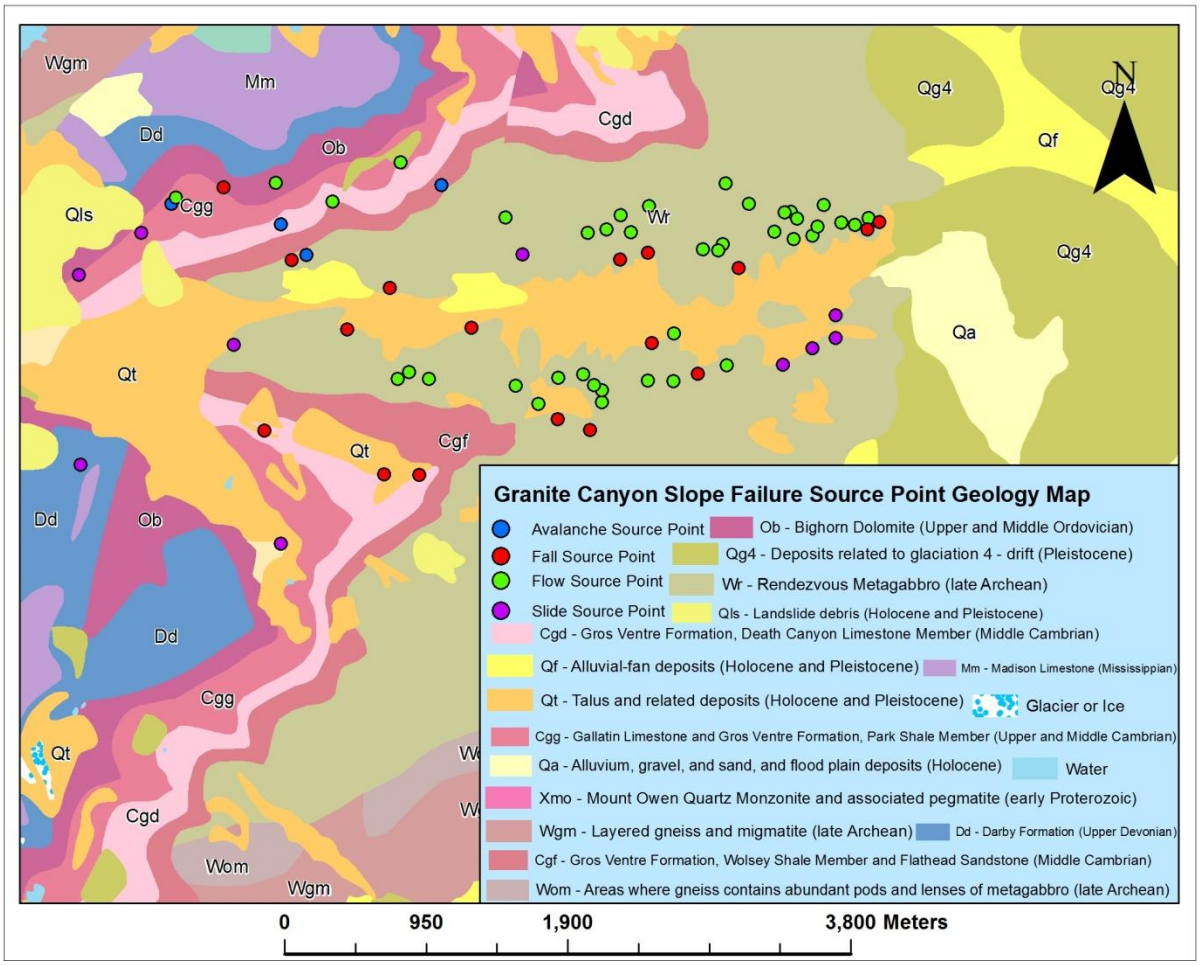

Figure 5.24: Geology map for slope failure source points in Granite Canyon, GTNP

Lower elevations of Granite Canyon are dominated by deposits of rendezvous metagabbro (Wr) and then quaternary talus (Qt). Higher elevations of Granite Canyon, especially on its northwest edge, consist of layered deposits of the Gros Ventre Formation with Wolsey Shale Member/Flathead Sandstone, Park Shale Member, and Death Canyon Limestone Member as well as Bighorn Dolomite and Darby Formation. Deposits of Wr accounted for 50% or more of the rock type for each category of slope failure source point in Granite Canyon. Rock falls and debris flows were especially located on Wr deposits at rates of 70.6% and 85%, respectively. Quaternary talus and related deposits (Qt) accounted for the next most dominant rock type, and

Gallatin Limestone & Gros Ventre Formation deposits accounted for 20% of rock slide source point rock types in Granite Canyon.

Table 5.24: Rock types for slope failure source points in Granite Canyon, GTNP

Rock Type	Total	Falls	Flows	Slides
All Rock Types	67	17	40	10
Cgd – Gros Ventre formation, Death Canyon limestone member	2	1	1	0
Cgg – Gallatin limestone and Gros Ventre formation, Park Shale member	3	0	1	2
Dd – Darby formation	1	0	0	1
Ob – Bighorn Dolomite	2	1	1	0
Qg4 – Deposits related to glaciation	1	0	1	0
Wr – Rendezvous metagabbro	51	12	34	5
Qt – Talus and related deposits	6	3	2	1
Qs – Swamp deposits	1	0	0	1

5.1e Paintbrush Canyon

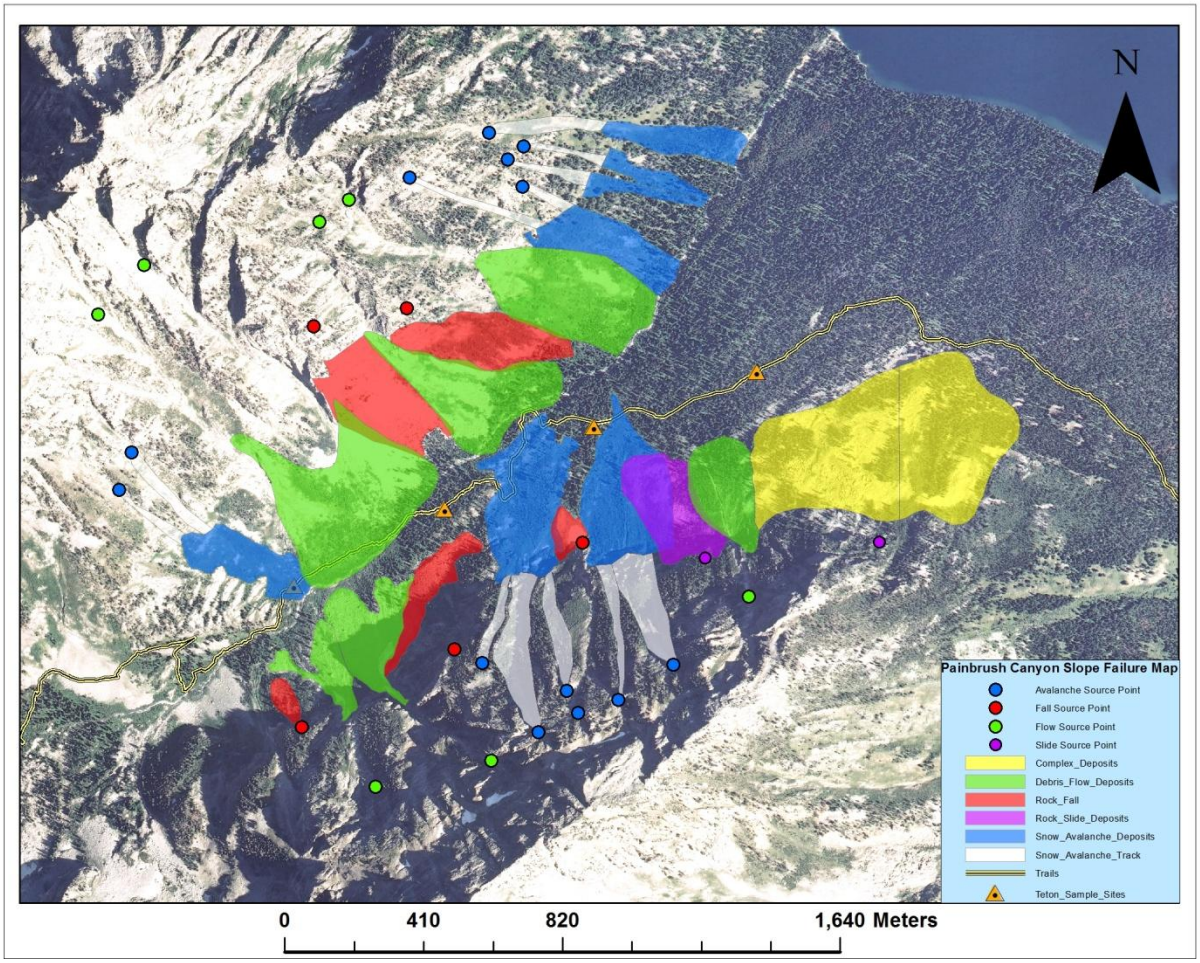

Figure 5.25: Locations of slope failure source points, tracks, and deposits superimposed over an orthorectified image of Paintbrush Canyon, GTNP.

Table 5.25: Slope failure inventory for Paintbrush Canyon, GTNP

	Avalanches	Falls	Flows	Slides	Complex	Total
SF deposits	7	5	6	1	2	21
SF source points	14	5	7	2	-	28

Paintbrush is a relatively small canyon where snow avalanches, debris flows, and rock falls are all very active; whereas rock slides and complex deposits are much less frequent. Many of these snow avalanches are relatively large deposits with potentially multiple contributing *tracks* that combine into one another. The short length of the canyon negatively impacts the total

number of slope failures that are present, but Figure 5.25 conveys that much of the canyon bottom is still marked by myriad slope failure deposits.

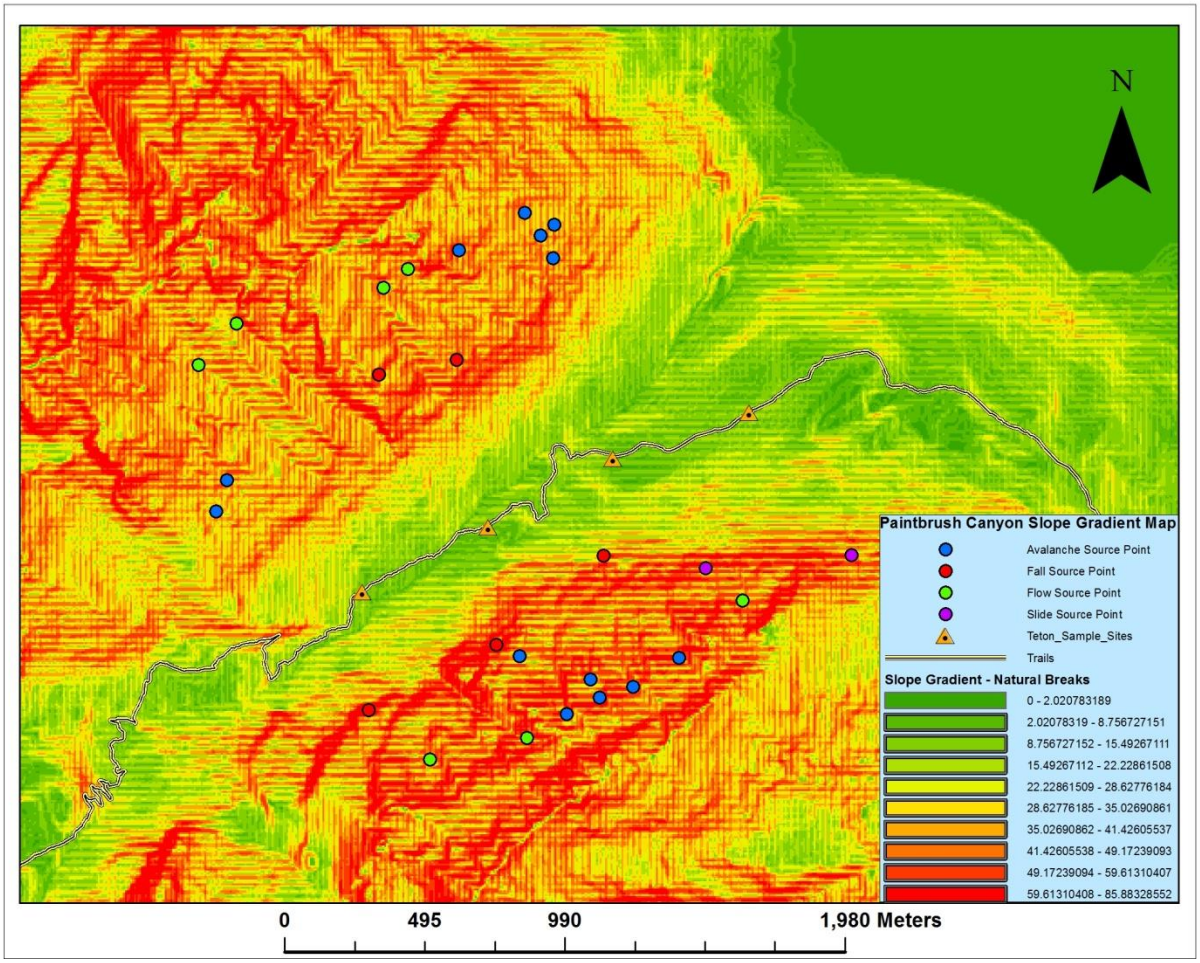

Figure 5.26: Slope gradient map with slope failure source points in Paintbrush Canyon, GTNP

Table 5.26: Summary statistics for slope gradient values of all source points in Paintbrush Canyon

	Count	Mean	Median	Minimum	Maximum	St. Dev.
Avalanches	14	50.50	49.90	33.56	65.68	9.88
Falls	5	49.90	51.83	32.40	59.18	9.48
Flows	7	44.26	44.57	32.89	61.57	9.73
Slides	2	43.60	43.60	35.46	51.75	8.15

Snow avalanches bucked trends seen in other canyons by occurring at higher gradients in Paintbrush Canyon than in any of the other four canyons, with a gradient average near 50º for

avalanches surpassing slide and flow gradient values. Variability from the mean was relatively low for each type of slope failure.

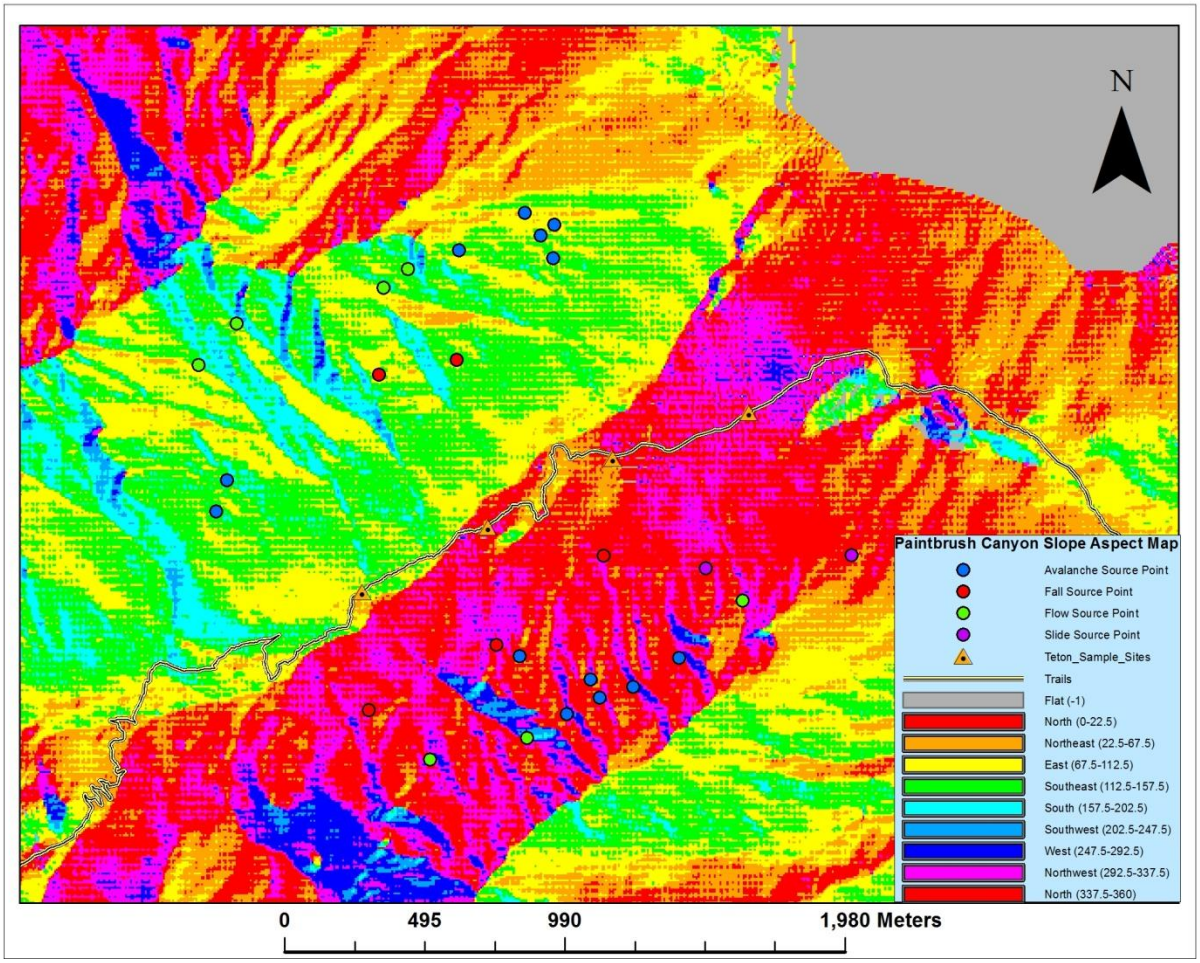

Figure 5.27: Slope aspect map with slope failure source points in Paintbrush Canyon, GTNP

Table 5.27: Slope aspect distribution table for all slope failure source points in Paintbrush Canyon

	Total	North	NE	East	SE	South	SW	West	NW
Avalanches	14	5	0	2	5	0	0	0	2
Falls	5	1	0	1	1	0	0	0	2
Flows	7	2	0	1	3	0	1	0	0
Slides	2	2	0	0	0	0	0	0	0

Snow avalanches occurred most commonly on northern- and southeastern-facing slopes, with two events occurring on northwest-facing slopes and two more occurring on east-facing

slopes. Rock falls were evenly distributed between northern, eastern, and southeastern aspects and slightly favoring a northwest aspect. Debris flows were situated on southeastern, northern, eastern, and southwestern aspects, with southeastern aspects being slightly favored over the other aspect values. Both rock slide instances occurred on north-facing slopes.

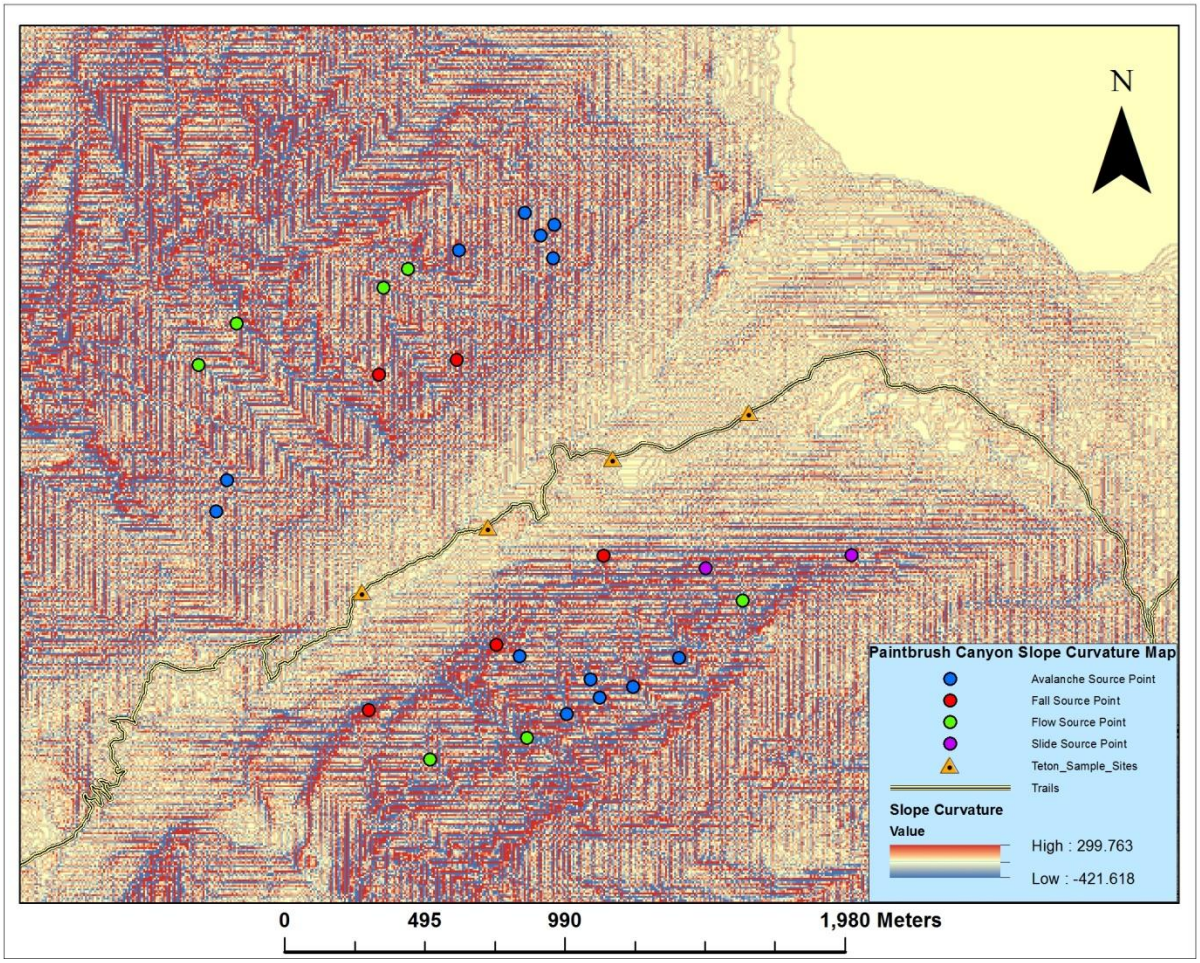

Figure 5.28: Slope curvature map with slope failure source points in Paintbrush Canyon, GTNP

Table 5.28: Summary statistics for slope curvature values of all source points in Paintbrush Canyon

	Count	Mean	Median	Minimum	Maximum	St. Dev.
Avalanches	14	-6.96	-8.53	-29.25	24.37	13.38
Falls	5	-6.82	-7.31	-51.18	34.12	27.20
Flows	7	-10.44	-4.87	-60.93	14.62	23.69
Slides	2	0	0	-4.87	4.87	4.87

Avalanches, falls, and flows all showed average concave curvature values; whereas both rock slide source points averaged each other out. Rock falls and debris flows had relatively high deviations from the mean and very low minimum (concave) values.

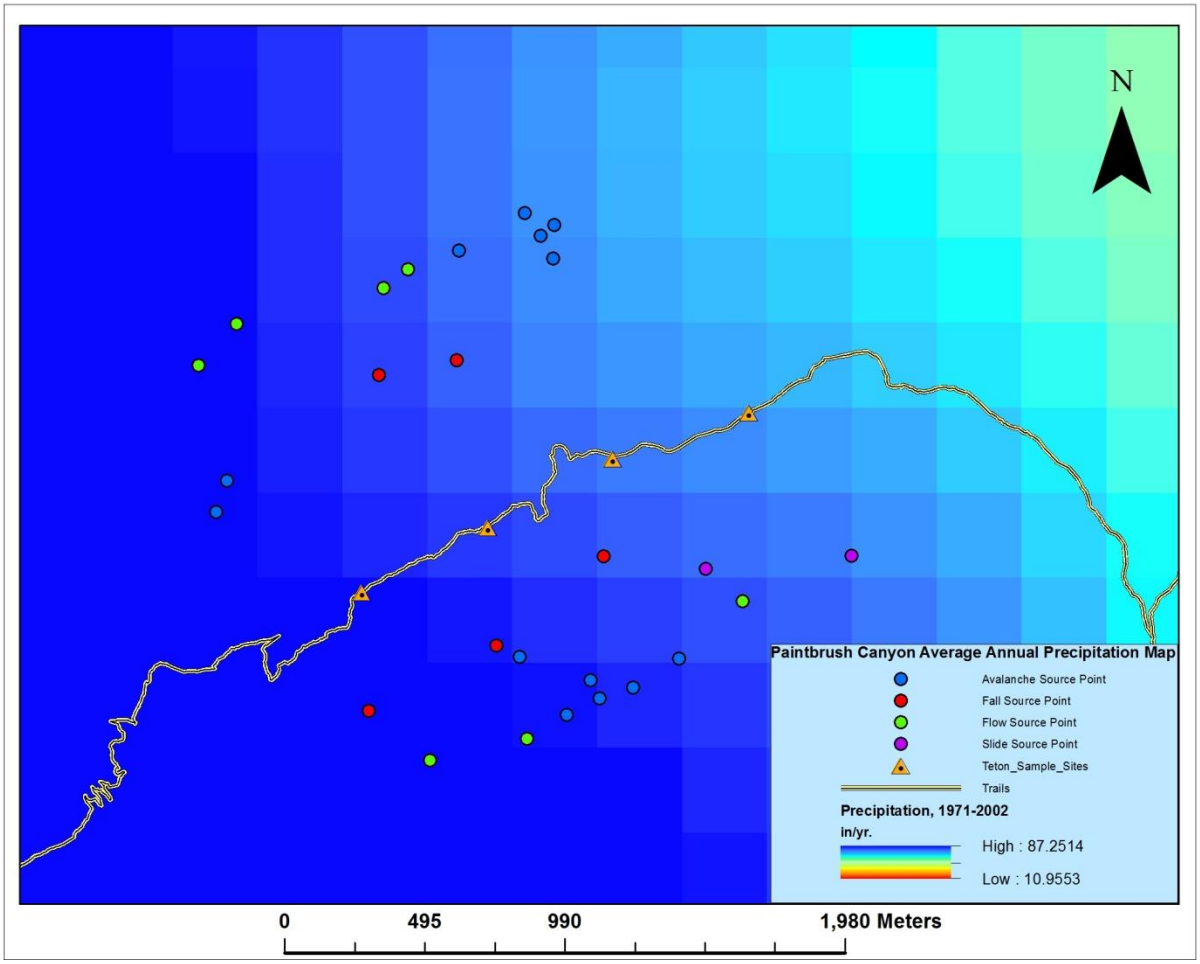

Figure 5.29: Average annual precipitation (1971-2002) map with slope failure source points in Paintbrush Canyon, Grand Teton National Park.

Table 5.29: Average annual precipitation (in./y) summary statistics table for all source points in Paintbrush Canyon

	Count	Mean	Median	Minimum	Maximum	St. Dev.
Avalanches	14	56.13	58.10	50.50	60.93	3.88
Falls	5	56.78	56.27	54.10	60.25	2.44
Flows	7	57.99	59.39	55.39	60.81	2.12
Slides	2	52.66	52.66	52.12	53.21	0.55

Paintbrush Canyon's precipitation pattern shifts from relatively dry in the northeast to relatively wet in the southwest, and each type of slope failure's precipitation statistics are dependent on their spatial locations in reference to this pattern. Debris flow source points received the highest average levels of precipitation out of the four slope failure categories, and most of them are in the southwest portion of the canyon. Snow avalanche source points had the second highest average level of annual precipitation and the highest level of variation, which lines up with the high level of spatial variation of avalanche source points with a slight tendency toward the southwest part of Paintbrush Canyon. Rock fall source points had a similar statistical and spatial distribution to snow avalanches, whereas both rock slide source points were located in the drier northeast portion of the canyon.

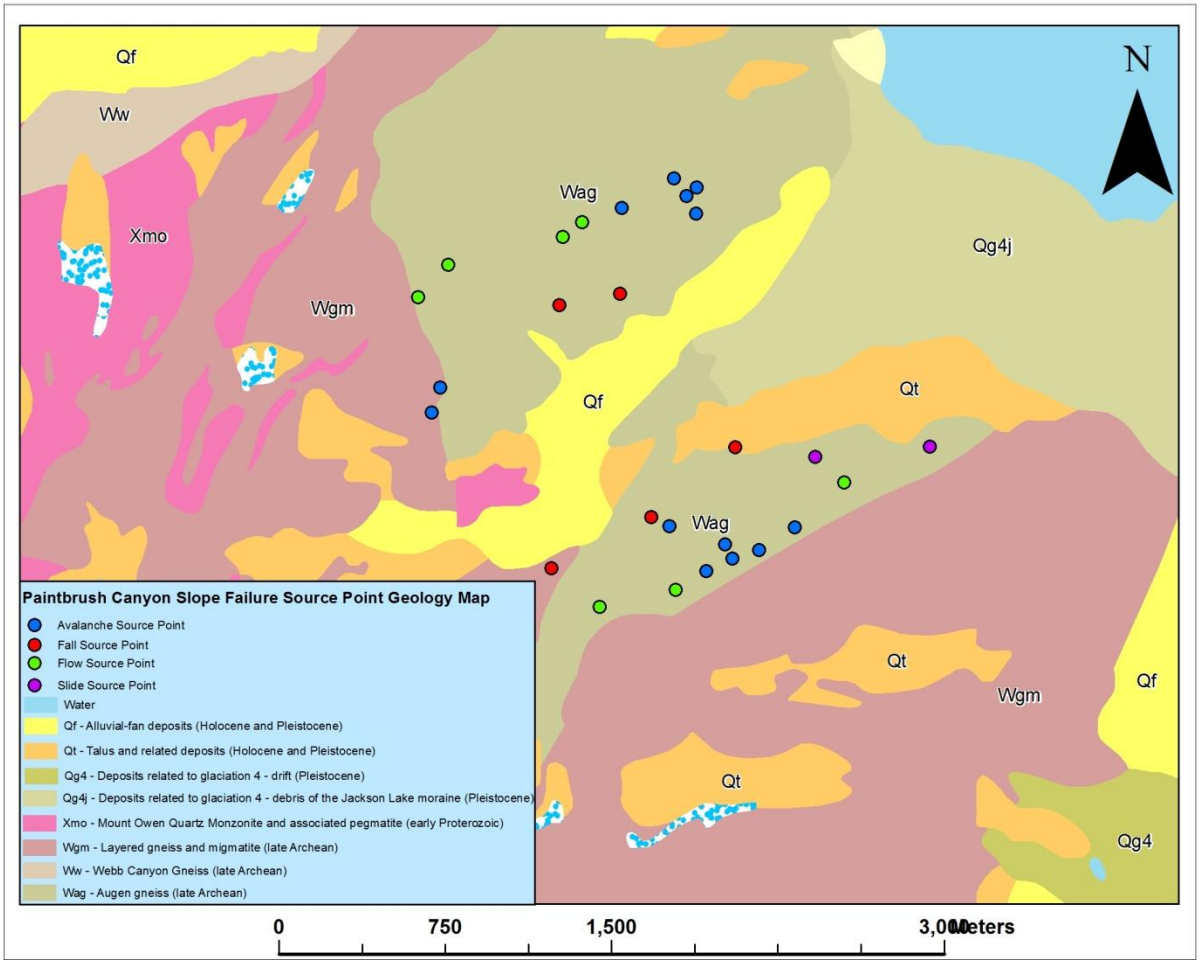

Figure 5.30: Geology map for slope failure source points in Paintbrush Canyon, GTNP

Table 5.30: Rock types for slope failure source points in Paintbrush Canyon, GTNP

Rock type	Total	Falls	Flows	Slides
All rock types	14	5	7	2
Wag – Augen gneiss	13	4	7	2
Wgm – Layered gneiss and migmatite	1	1	0	0

Three primary regimes of rock types are present in Paintbrush Canyon: glaciations deposits in the east to northeast part of the canyon, layered gneiss and migmatite deposits in the southeast and west portions of the canyon, and Augen gneiss deposits in the central and north central portions of the canyon. Smaller but significantly sized deposits of quaternary talus and

alluvial fan material are present in the lower elevations of Paintbrush Canyon. A vast majority of slope failure source points are located in the central to northern portion of the canyon where Augen gneiss (Wag) deposits are present. A lone exception is one rock fall deposit located on a Wgm deposit in the southwest part of the canyon.

5.1f Discussion

Cascade Canyon's relatively gentle profile and length accounted for a high number of slope failures, but especially snow avalanches and debris flows with relatively low average slope gradients at source areas. Avalanches, falls, and slides tended toward a north-facing slope aspect, although debris flows showed a southern aspect bias. Avalanches, falls, and slides also shared a slight to pronounced bias toward convex slope curvatures, whereas debris flow source areas mostly occurred on concave slopes.

Death Canyon had very low slope gradient averages for snow avalanche and debris flow source points, though rock falls and rock slides occurred on relatively steep slopes in comparison to all other canyons aside from Garnet. Rock falls occurred in Death Canyon on north- and northeast-facing slopes, and debris flows continued to occur on south- to southeast-facing slopes. However, snow avalanche and rock slide source point aspects were more evenly distributed than in other canyons. Snow avalanche source points showed a strong bias toward concave slopes in Death Canyon as well as debris flows. Falls and slides showed a flat to convex bias in contrast to avalanches and flows.

Garnet Canyon's steep profile elevated the average slope gradient values for fall, flow, and slide source points (no avalanches were present); but debris flows continued to lag behind slides and especially rock falls in slope gradient averages. Rock fall slope aspect values were more evenly distributed over different orientations, rock slides continued to be relatively evenly

distributed with slight preferences to north and south values, and debris flows were located on mostly south-facing slopes as was the case in Cascade and Death Canyons. Rock slide source points showed a strong preference for convex slope curvatures in Garnet Canyon, whereas debris flow source points varied wildly between mean and median values, and rock falls averaged a concave slope curvature. The high level of variability in the data in Garnet Canyon suggests that these curvature data may be somewhat inconclusive.

Granite Canyon's relatively gentle profile saw some of the lowest slope gradient averages for avalanches, falls, and flows (and potentially slides), although Paintbrush's lack of sample size of rock slide source points may render its low slope gradient average irrelevant. As has been common in the previous three canyons, snow avalanches and debris flows had lower slope gradient averages than falls and slides. Falls and slides showed a clear bias toward north-facing aspects, and flows continued to be most common on south- and southeast-facing slopes. However, snow avalanche source points favored primarily south-facing slopes, although the sample size of four was low and may not be representative of avalanches in GTNP as a whole. Avalanches and debris flows displayed a slope curvature average of close to flat, whereas falls and slides showed a considerable concave bias.

Paintbrush Canyon generated slope data that at times defied patterns seen in the other four canyons. Snow avalanche source points were curiously located at slope gradients higher than flows or slides and just below rock falls. Rock slide source points occurred at a relatively low slope gradient average of ~ 43º, but the low number of slide or complex slide deposits in Paintbrush Canyon means that it may not be representative of slope gradient data for slides as a whole. Snow avalanches occurred on north-facing and southeast-facing slopes equally, whereas flows continued their SSE-facing bias, albeit with a low sample size of seven. Aspect data for

falls and slides were equally distributed and/or inconclusive. Avalanches, falls, and flows all showed a strong bias toward concave slopes.

Precipitation gradients in each canyon varied based on the shape of each canyon; for example, if a canyon has a west-east orientation, average annual precipitation would increase from east to west, a southwest-northeast orientation would see precipitation increase from northeast to southwest, and so on. Precipitation averages in individual canyons were contingent on the geographic distribution of each category of source point, and determining any discernible patterns that would suggest that one category of slope failure most commonly occurs in a certain precipitation regime or another was difficult. Chi-square analysis was needed to glean any statistical strength to these patterns.

5.2 Summary Statistics - All Canyons Combined

In addition to canyon-wide statistical analysis displayed in section 5.1, histograms and spatial statistics for slope gradient, aspect, curvature, and estimated annual average precipitation were generated for each category of slope failure source point. The histograms display the frequency distribution for the range of values of each statistic, and accompanying tables display point count, average, minimum, maximum, standard deviation, and median values for each statistic.

5.2a Snow Avalanches

Slope Gradient

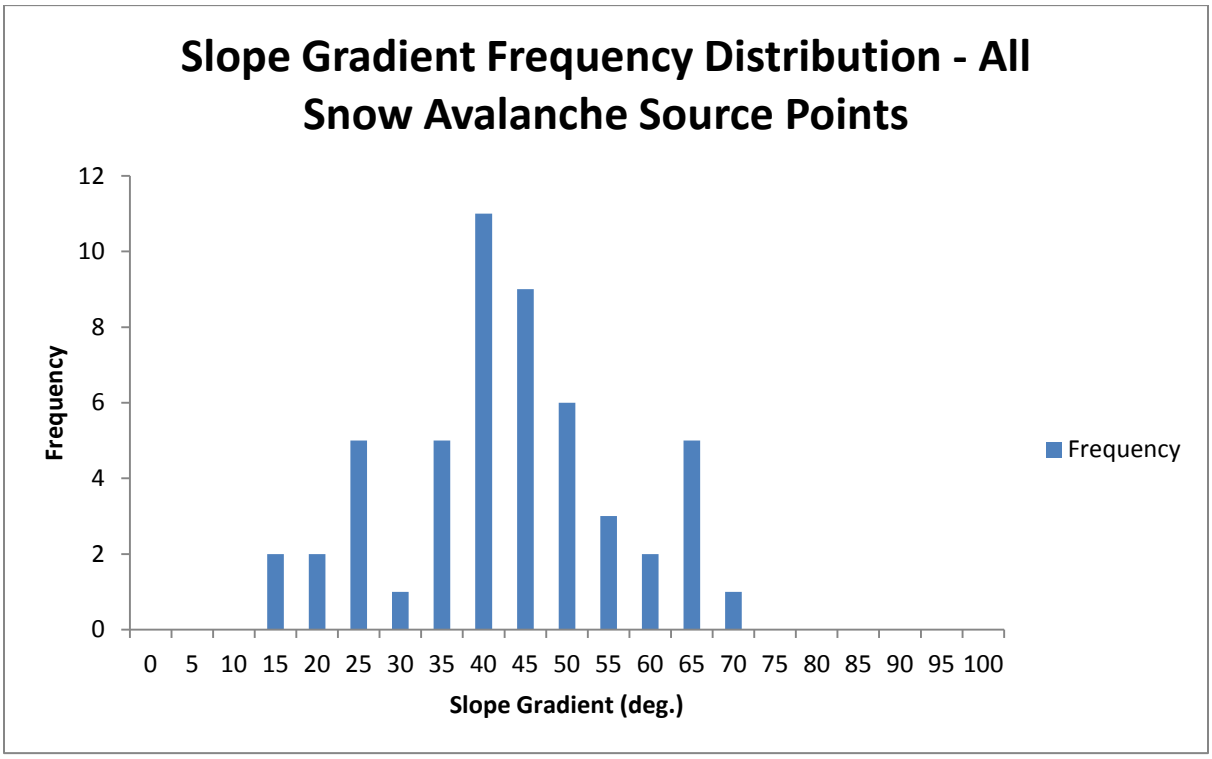

Figure 5.31: Histogram of the slope gradient frequency distribution of all snow avalanche source points in GTNP.

Table 5.31: Summary statistics of slope gradient for all snow avalanche source points in GTNP

Point count	Minimum value	Maximum value	Mean	Median	Standard deviation
52	12.45	65.58	39.87	39.7	13.43

Slope gradient values for all snow avalanche source points in Grand Teton National Park showed a relatively normal distribution with the majority of gradient values falling between 31 and 54º. Mean and median values were closely tied together at 39.86º and 39.34º, respectively.

Slope Aspect

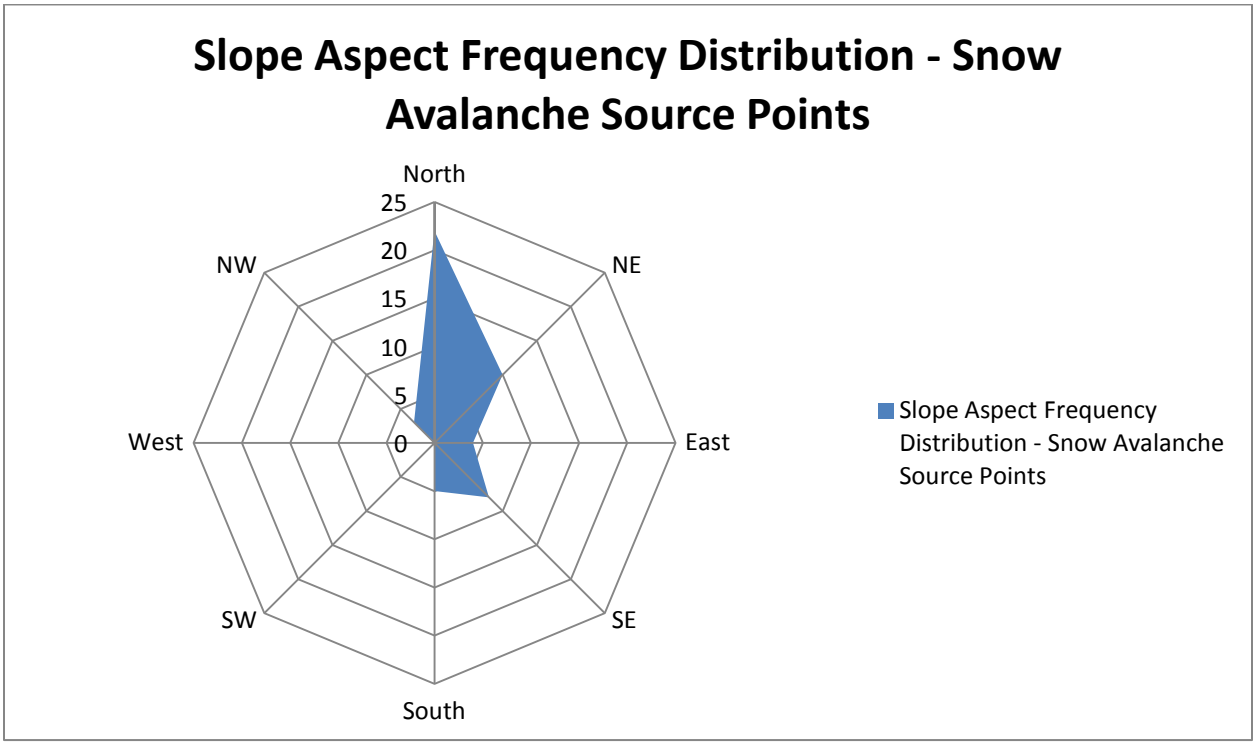

Figure 5.32: "Radar" chart of the distributions of avalanche source point orientations.

Table 5.32: Frequency table for aspect orientations for all snow avalanche source points

	Total	North	NE	East	SE	South	SW	West	NW
Avalanche source points	52	22	10	4	8	5	0	0	3

Table 5.33: Summary statistics of slope aspects for all snow avalanche source points in GTNP

Point count	Mean	Median	Standard deviation
52	132.56	91.19	128.52

The distribution of slope aspect values as displayed in Tables 5.32 and 5.33 show a strong bias toward north, northeast, and southeast orientations, with fewer values bearing a southern and northwest orientation. Slopes with west and southwest orientations did not generate any observed snow avalanches in Grand Teton National Park. Mean and median values for slope

aspect were highly separated. The mean value was a southeast orientation of 131.56º, and the median value was an eastern orientation of 91.19º.

Slope Curvature

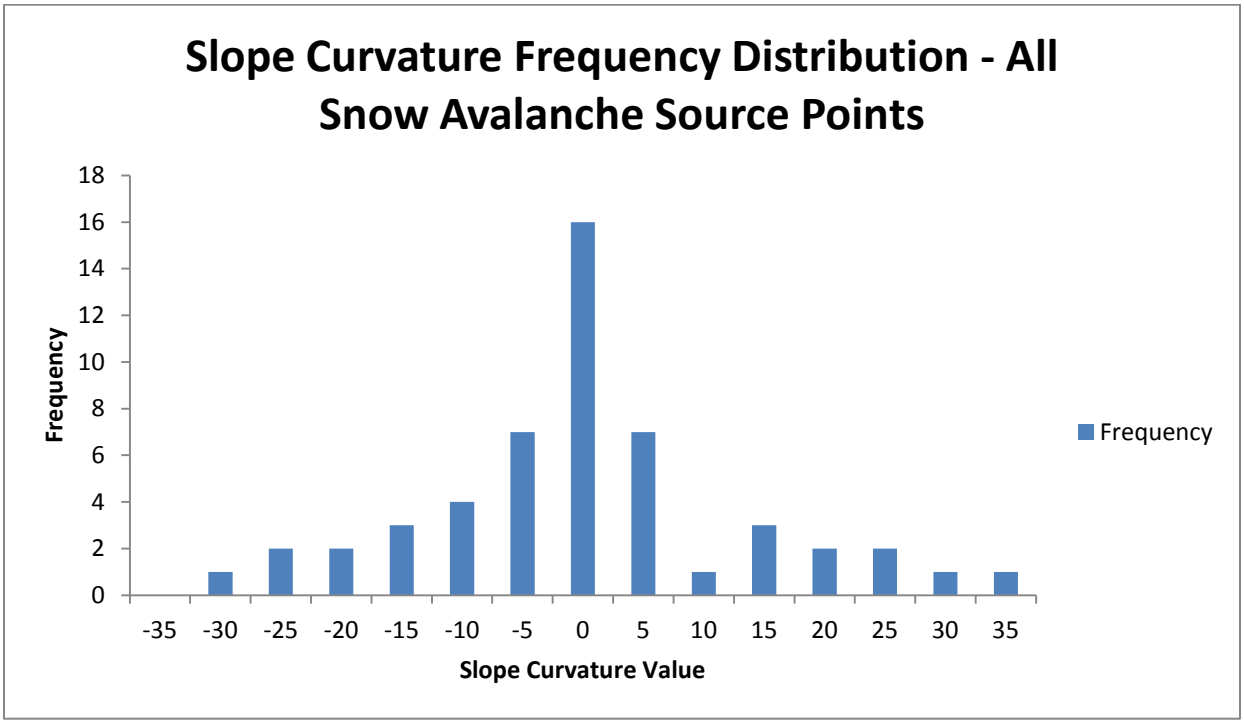

Figure 5.33: Histogram of the slope curvature frequency distribution of all snow avalanche source points in GTNP.

Table 5.34: Summary statistics of slope curvatures for all avalanche source points in GTNP

Point count	Minimum value	Maximum value	Mean	Median	Standard deviation
52	-34.12	34.12	-2.39	-2.44	14.26

Snow avalanche source points displayed a very slight tendency toward being located on concave slopes. The distribution of curvature values for avalanche sources is close to normal with a major spike in frequency between -4.99 and 0, and the standard deviation from the mean is relatively low at 14.26.

Average Annual Precipitation

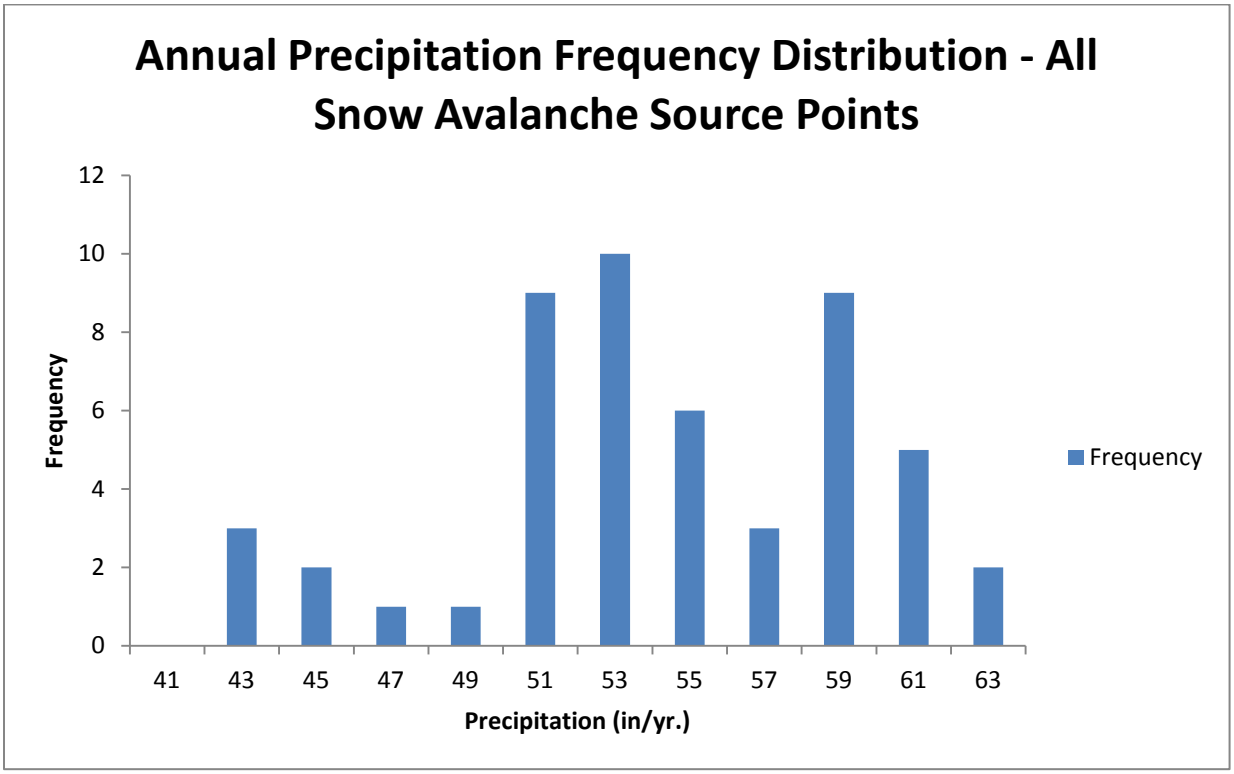

Figure 5.34: Histogram of the average annual precipitation (in./y) frequency distribution of all snow avalanche source points in GTNP.

Table 5.35: Summary statistics for average annual precipitation values (in./yr.) for all snow avalanche source points in GTNP

Point count	Minimum value	Maximum value	Mean	Median	Standard deviation
51	41.30	62.17	53.44	52.85	5.03

Snow avalanche source points in the study area averaged close to 53 inches of precipitation a year with values ranging between ~ 41 and ~ 62 in./y. The distribution of the histogram in Figure 5.29 was relatively inconclusive, and an observable skewness is not present.

5.2b Debris Flows

Slope Gradient

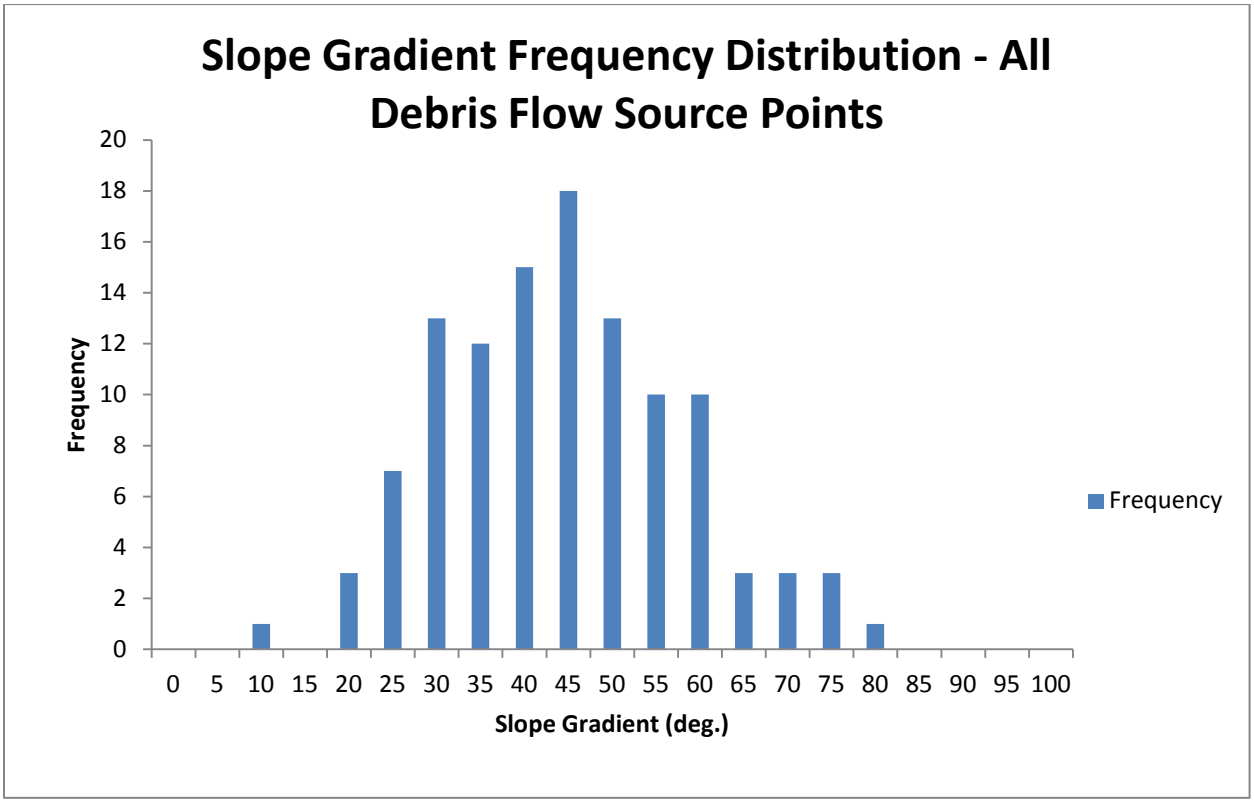

Figure 5.35: Histogram of the slope gradient frequency distribution of all debris flow source points in GTNP.

Table 5.36: Summary Statistics of slope gradient for all debris flow source points in GTNP

Point count	Minimum value	Maximum value	Mean	Median	Standard deviation
112	9.90	78.11	41.99	42.47	13.63

Slope gradient averages for debris flow source points were slightly higher than their snow avalanche counterparts at around 42º, but variances from the mean for avalanches and flows were almost identical. The histogram in Figure 5.30 shows a normal distribution and suggests that through all five canyons, debris flows are most likely to occur at gradients between 26 and 50º.

Slope Aspect

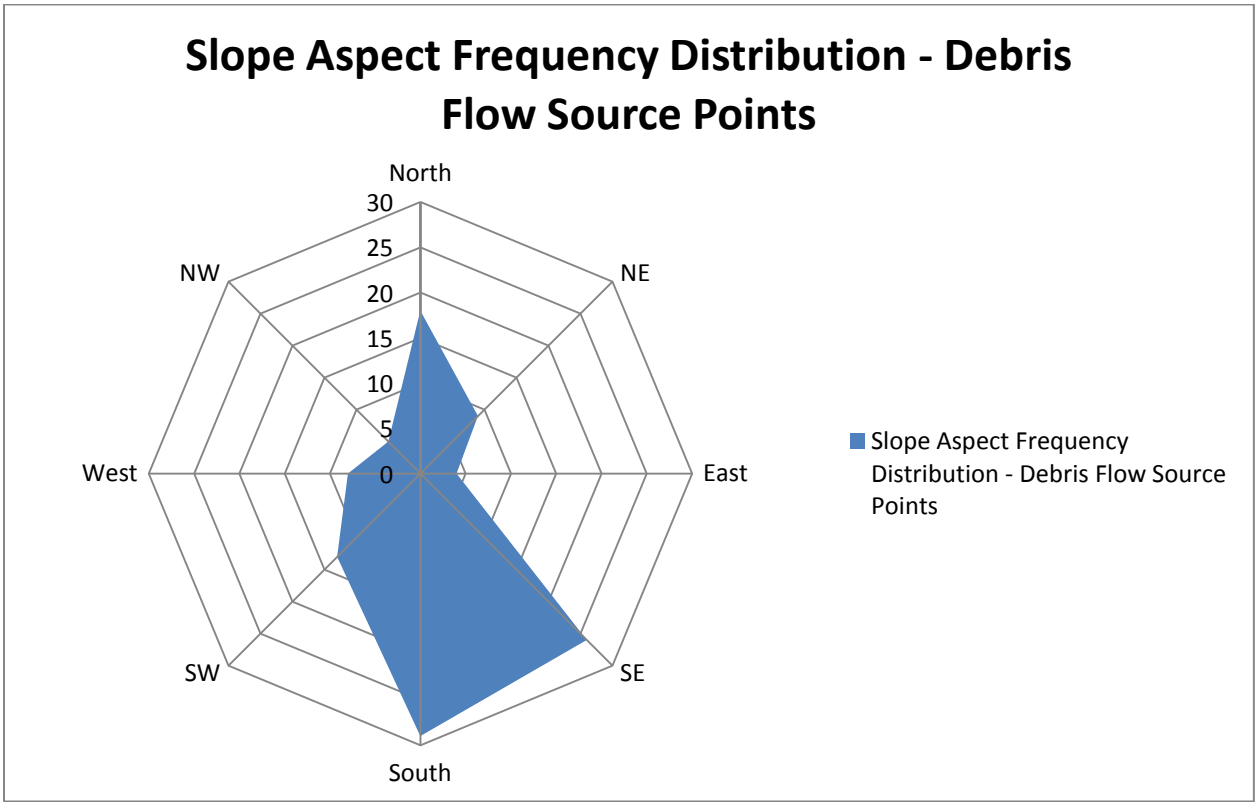

Figure 5.36: "Radar" chart of the distributions of debris flow source point orientations.

Table 5.37: Summary statistics of slope aspects for all debris flow source points in GTNP

Point count	Mean	Median	Standard deviation
112	162.47	163.89	92.79

Table 5.38: Frequency table for aspect orientations for all debris flow source points in GTNP

	Total	North	NE	East	SE	South	SW	West	NW
Debris flow source points	112	18	9	4	26	29	13	8	5

Debris flow source points showed a noted bias toward occurring on south-, southeast-, and southwest-facing slopes, although 28.5% of debris flows occurred on north-, northeast-, or northwest-facing slopes. These results depart from the aspect data of snow avalanches, which

tended to favor north- and northeast-facing slopes. Although canyon shape is a major control of slope aspect values for each type of slope failure, four of the five canyons (Cascade, Death, Granite, and Garnet) had similar distributions where south- and southeast-facing aspects were dominant for debris flows. Paintbrush Canyon, however, had a more even distribution of flow aspect values and contained a relatively high number of southeast-facing snow avalanche paths.

Slope Curvature

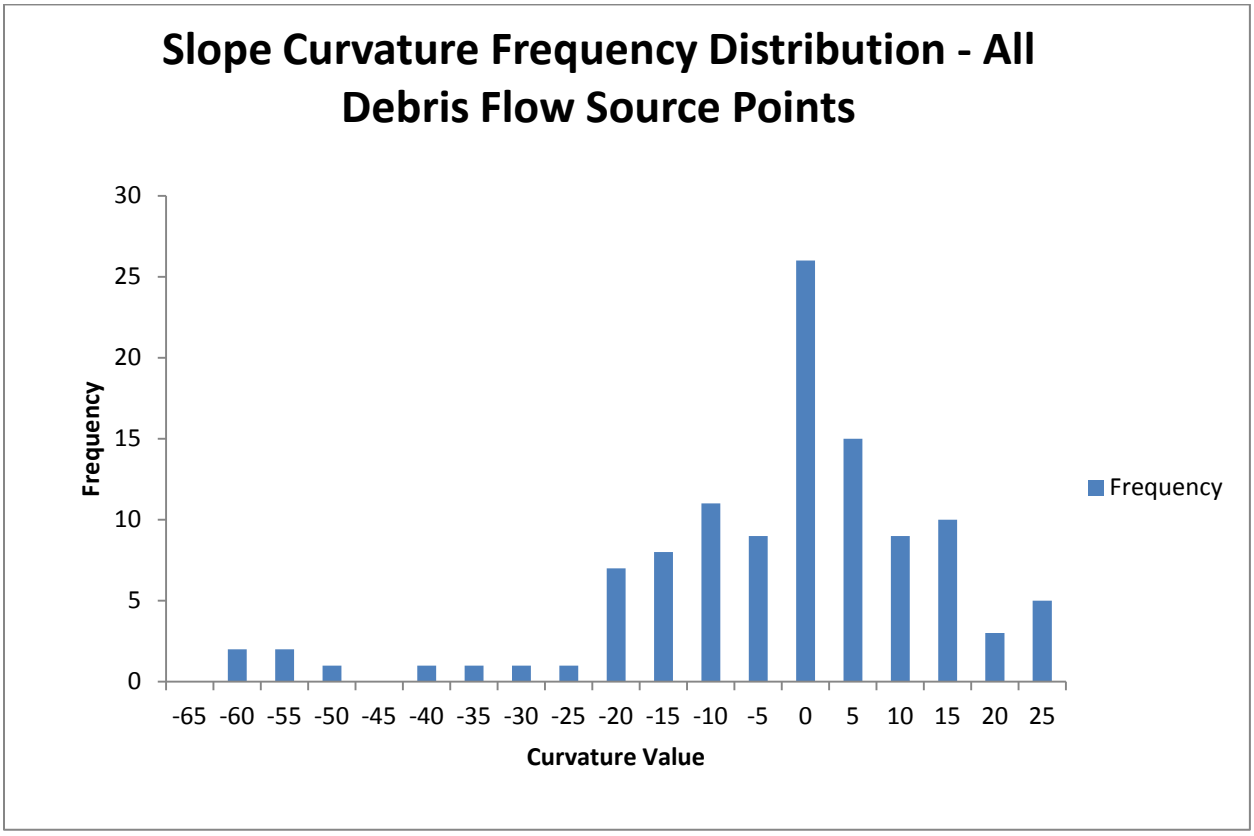

Figure 5.37: Histogram of the slope curvature frequency distribution of all debris flow source points in GTNP.

Table 5.39: Summary statistics of slope curvatures for all debris flow source points in GTNP

Point count	Minimum value	Maximum value	Mean	Median	Standard deviation
112	-63.36	24.37	-5.24	-2.44	17.57

Debris flow source point averages showed a tendency toward being located on concave slopes. However, a notable negative skewness of the histogram in Figure 5.37 suggests that a number of large concave values may act as outliers on the full data set. If these outliers are removed from the data set, one can surmise that the mean and median values of debris flow source points would move closer to a flat value of 0.

Average Annual Precipitation

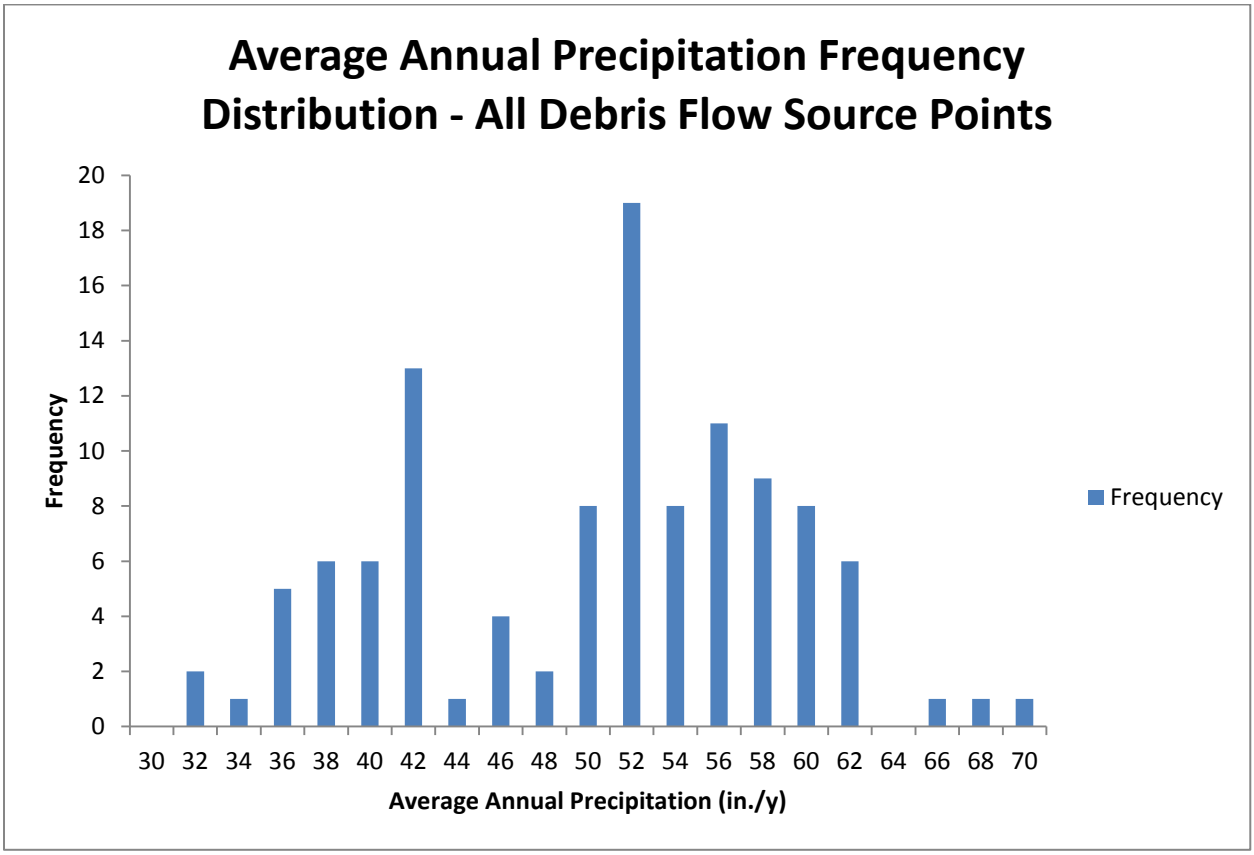

Figure 5.38: Histogram of the average annual precipitation frequency distribution of all debris flow source points in GTNP.

Table 5.40: Summary statistics of average annual precipitation values (in./y) for all debris flow source points in GTNP

Point count	Minimum value	Maximum value	Mean	Median	Standard deviation
112	31.82	68.32	49.30	51.19	8.58

Average annual precipitation values for debris flow source points tallied around 50 in./y, around three in./y less than snow avalanches. However, the range and standard deviation of precipitation data for debris flows was higher than snow avalanches, suggesting a higher variability for precipitation conditions in which debris flows are likely to occur.

Geology

Table 5.41: Distributions of rock types of debris flow source points in GTNP

Rock type	Number	Relative percentage	Canyon(s) present (#)
All rock types	112	100%	-
Wr – Rendezvous metagabbro	34	30.36%	Granite (34)
Xmo – Mount Owen quartz monzonite and associated pegmatite	23	20.54%	Cascade (15), Garnet (8)
Wgm – Layered gneiss and migmatite	23	20.54%	Cascade (11), Death (12)
Wom – Areas where gneiss contains abundant pods and lenses of metagabbro	8	7.14%	Death (8)
Xmo Wgm – Mount Owen quartz monzonite and associated pegmatite/layered gneiss and migmatite	7	6.25%	Cascade (7)
Wag – Augen gneiss	7	6.25%	Paintbrush (7)
Qt – Talus and other related deposits	5	4.46%	Death (2), Granite (2), Garnet (1)
Qg4 – Deposits related to glaciations 4 – drift	1	0.89%	Granite (1)
Cgd – Gros Ventre formation, Death Canyon limestone member	1	0.89%	Granite (1)
Cgg – Gallatin limestone and Gros Ventre formation, Park Shale member	1	0.89%	Granite (1)
Ob – Bighorn Dolomite	1	0.89%	Granite (1)
Qf – Alluvial fan deposits	1	0.89%	Cascade (1)

A preliminary examination of Table 5.41 conveys three dominant rock types where debris flows occur in the study area: Rendezvous metagabbro (Wr), Mount Owen quartz monzonite and associated pegmatite (Xmo), and layered gneiss and migmatite. However, the geomorphic implications of these results may be more indicative of local geologic distributions than debris flow source points occurring more commonly on a specific rock type or types over the whole study area. For example, Rendezvous metagabbro and Augen gneiss (Wag) deposits only corresponded with debris flow source points in Granite and Paintbrush canyons, respectively, yet they also comprised the only rock types on which debris flows source points were located in those two canyons. Only one rock type—quaternary talus deposits (Qt)—intersected a debris flow source point in three canyons or more, and the total number of source points that occurred in these three canyon comprised less than 5% of all debris flow source points in all five canyons. Therefore the most likely—although preliminary—conclusion from these data is that debris flows are most likely to occur on whatever rock type is the most dominant in the canyon in which the failure is located rather than one or multiple rock types having the highest susceptibility to debris flows throughout the entire study area.

5.2c Rock Falls

Slope Gradient

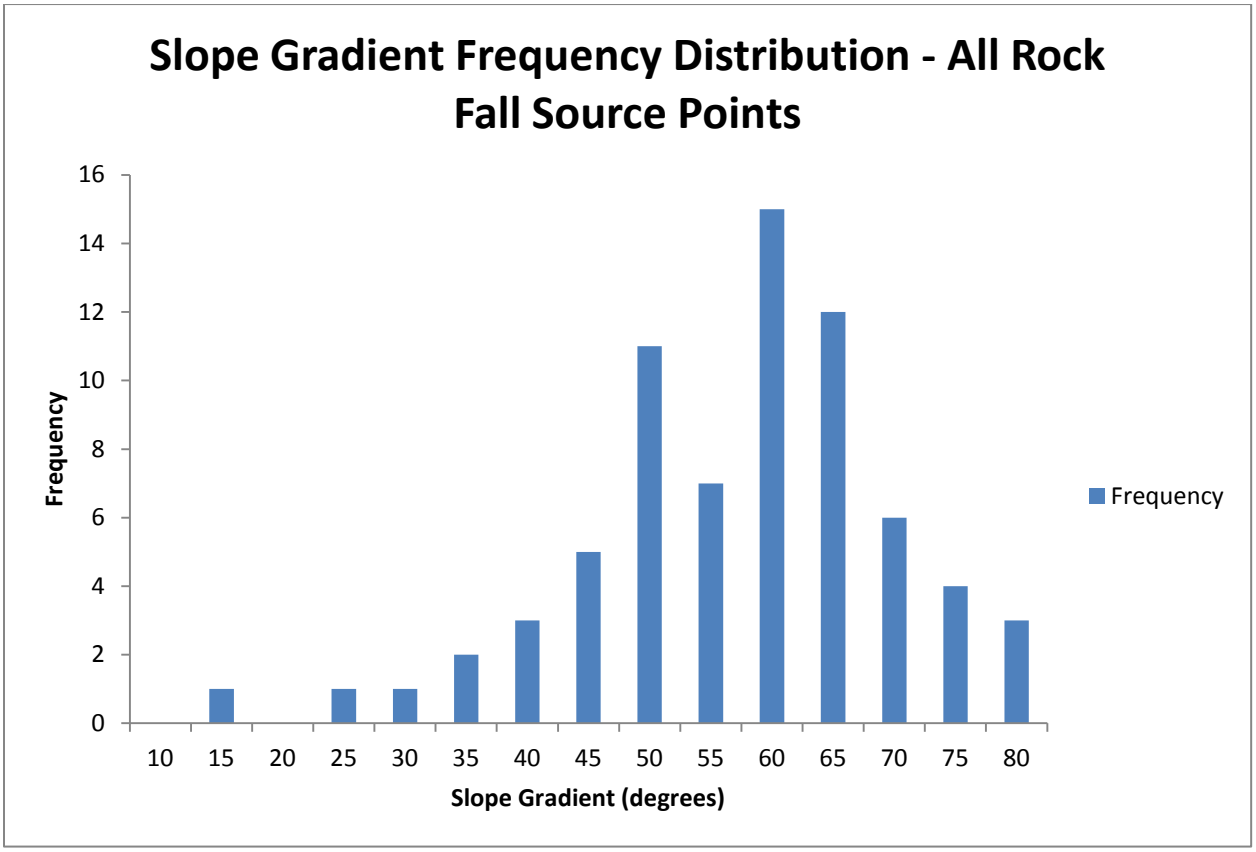

Figure 5.39: Histogram of the slope gradient frequency distribution of all rock fall source points in GTNP.

Table 5.42: Summary statistics of slope gradient for all rock fall source points in GTNP

Point count	Minimum value	Maximum value	Mean	Median	Standard deviation
71	13.35	76.71	54.57	56.67	12.70

Unsurprisingly, rock fall source points were located at higher slope gradients than either snow avalanches or debris flows, averaging around 55.5º. Variance from the mean was lower for rock falls than its flow and avalanche counter parts, although the range of values for rock falls was smaller than that of debris flows. A negative skewness of the histogram in Figure 5.34 is present with a slight outlier on the low end of slope gradient values at 13.35.

Slope Aspect

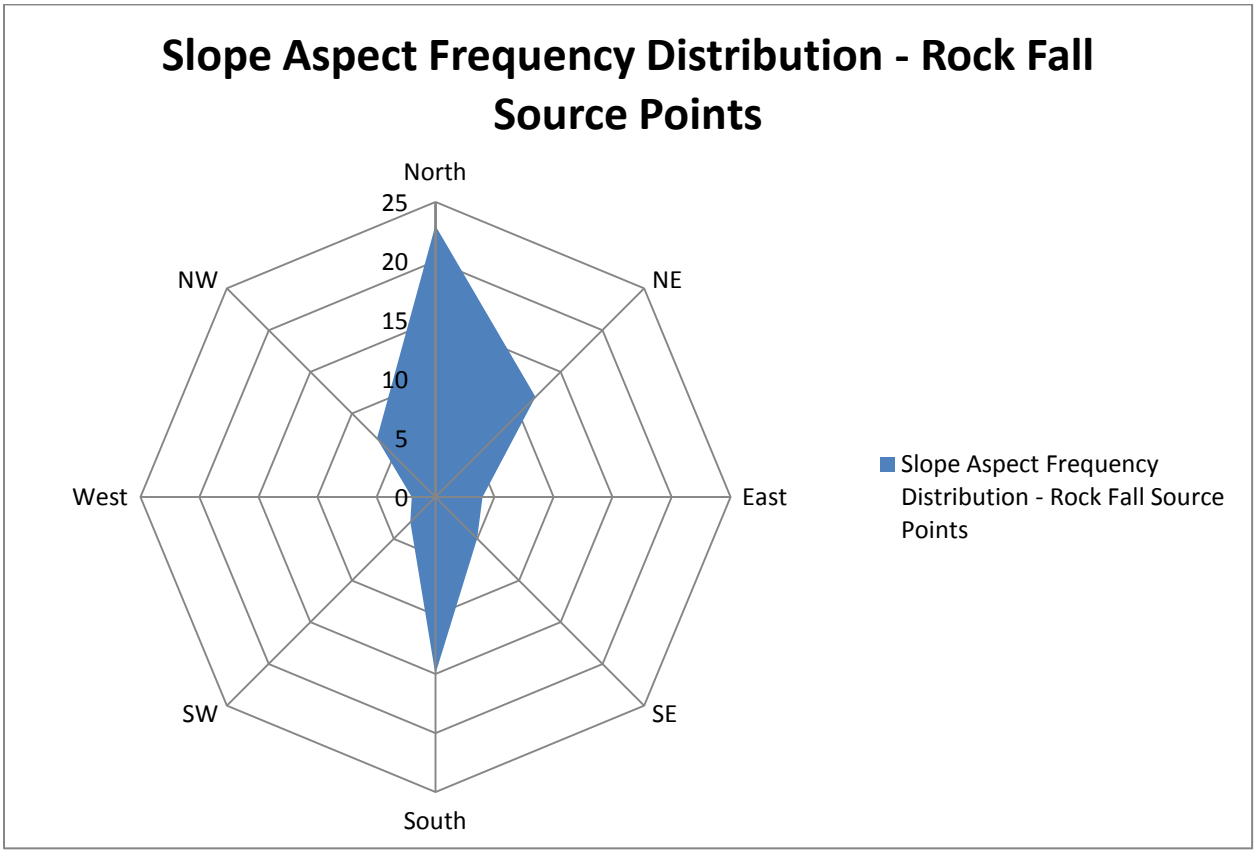

Figure 5.40: "Radar" chart of the distributions of rock fall source point orientations.

Table 5.43: Summary statistics of slope aspect values for all rock fall source points in GTNP

Point count	Mean	Median	Standard deviation
71	182.79	176.88	124.78

Table 5.44: Frequency table for aspect orientations for all rock fall source points

	Total	North	NE	East	SE	South	SW	West	NW
Rock fall source points	71	23	12	4	5	15	3	2	7

Rock fall source point aspect values showed a clear bias for north- and northeast-facing slopes, although 21% of rock falls also took place on south-facing slopes. A relatively high level

of variability exists in these data, and the distribution of aspect values was relatively even outside of north-facing aspects. Freeze-thaw shattering playing a prominent weathering role on north-facing slopes has been well documented (Butler, 1983, 1990; Matsuoka *et al.*, 1998) and may play an active role in causing rock falls in Grand Teton National Park as well.

Slope Curvature

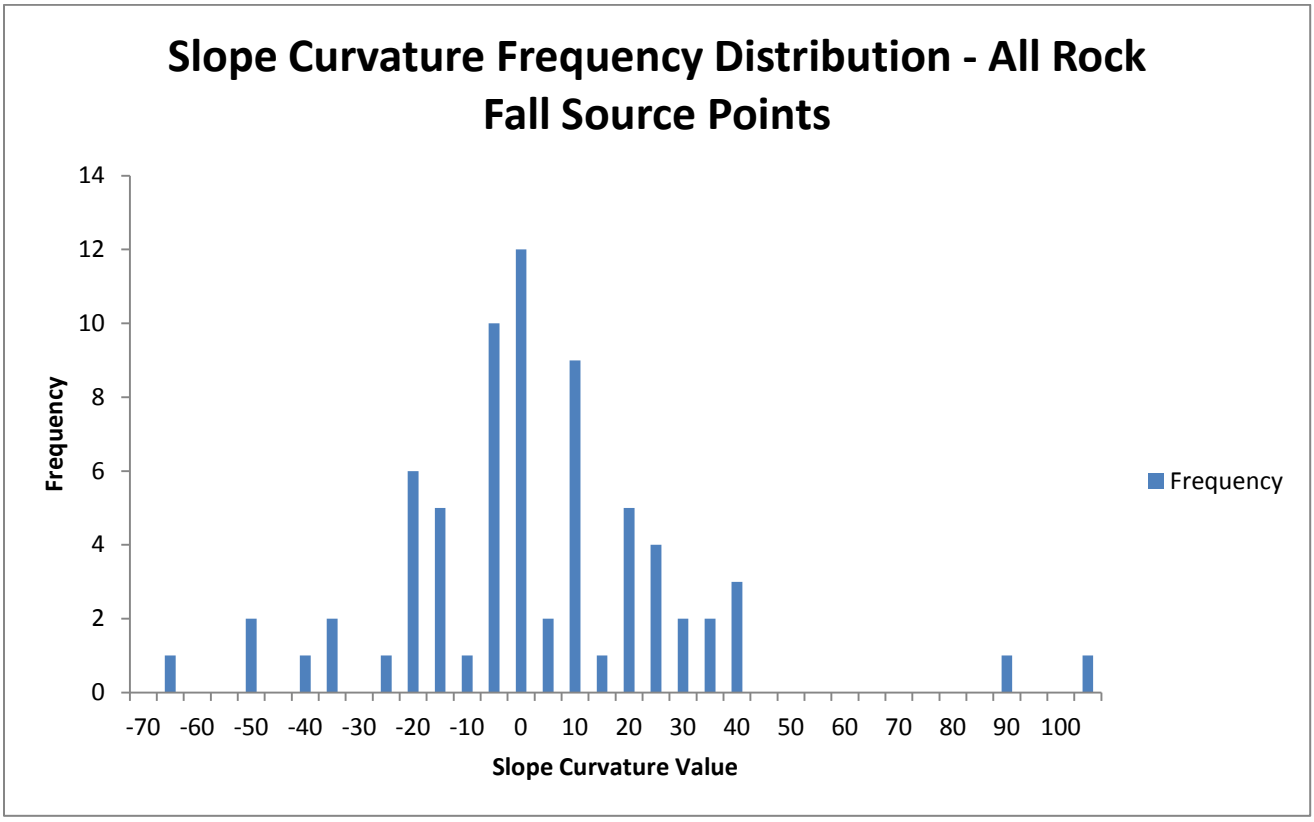

Figure 5.41: Histogram of the slope curvature frequency distribution of all snow avalanche source points in GTNP.

Table 5.45: Summary statistics of slope curvatures for all debris flow source points in GTNP

Point count	Minimum value	Maximum value	Mean	Median	Standard deviation
71	-68.24	102.36	0.58	0	27.17

Rock fall source points averaged a close to flat curvature value, but a high range and standard deviation suggest high variability in the data, as seen in Figure 5.36. A very slight

positive skew exists for the histogram in Figure 5.36, with pronounced convex outliers affecting the overall distribution.

Average Annual Precipitation

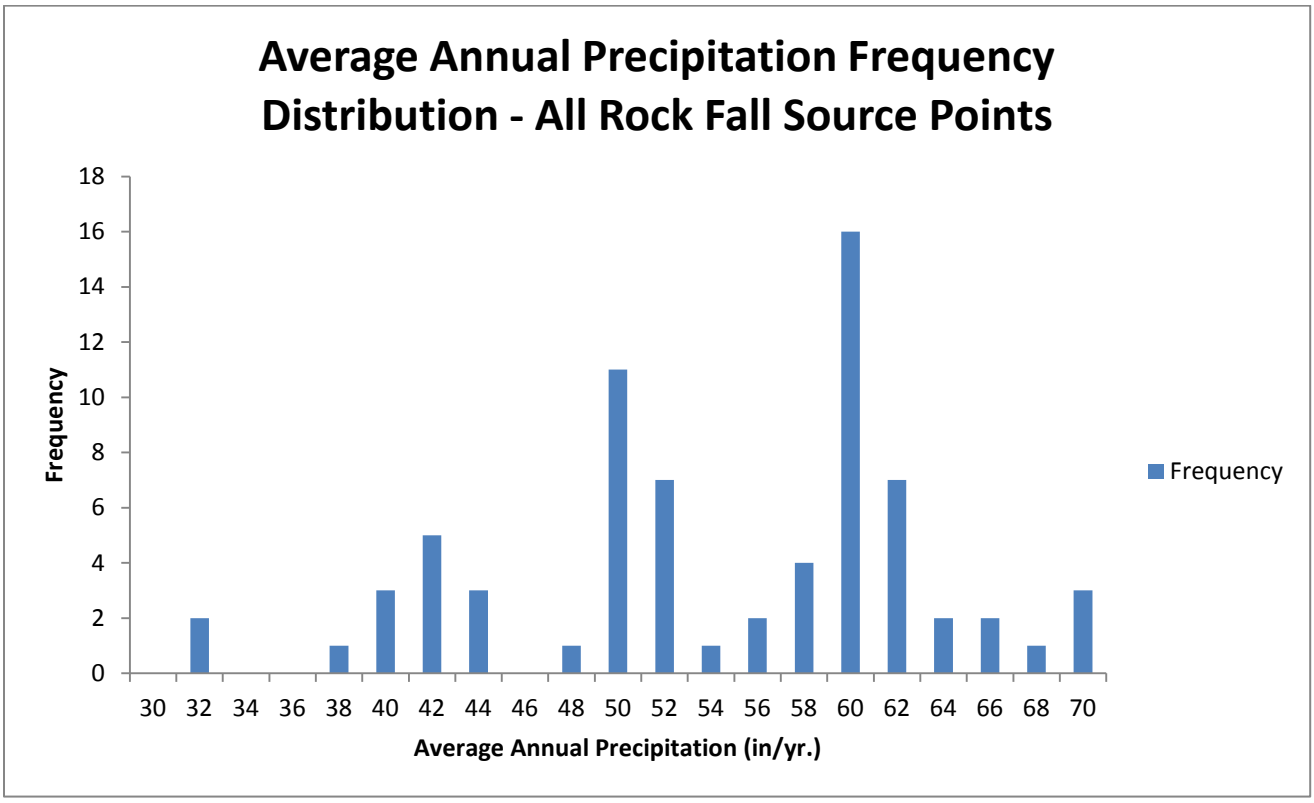

Figure 5.42: Histogram of the slope curvature frequency distribution of all rock fall source points in GTNP.

Table 5.46: Summary statistics of average annual precipitation values (in./y) for all rock fall source points in GTNP

Point count	Minimum value	Maximum alue	Mean	Median	Standard deviation
71	31.82	68.64	53.22	54.34	8.81

Rock fall annual precipitation values for source points saw an average of close to 54 in./y, slightly higher than snow avalanches and 4 in./y more than debris flows. Data variability was relatively high for rock falls like their flow counterparts, with a range of close to 37 in./y and a standard deviation of 8.81.

Geology

Table 5.47: Distributions of rock types of rock fall source points in GTNP

Rock type	Number	Relative percentage	Canyon(s) present (#)
All Rock Types	71	100%	-
Wgm – Layered gneiss and migmatite	20	28.17%	Cascade (6), Death (13), Paintbrush (1)
Xmo – Mount Owen quartz monzonite and associated pegmatite	16	22.54%	Cascade (7), Death (2), Garnet (7)
Wr – Rendezvous metagabbro	12	16.90%	Granite (12)
Wom - Areas where gneiss contains abundant pods and lenses of metagabbro	7	9.86%	Death (7)
Xmo Wgm – Mount Owen quartz monzonite and associated pegmatite/layered gneiss and migmatite	6	8.45%	Cascade (2), Death (3), Garnet (1)
Wag – Augen gneiss	4	5.63%	Paintbrush (4)
Qt – Talus and related deposits	3	4.23%	Granite (3)
Ob – Bighorn Dolomite	1	1.41%	Granite (1)
Cgd – Gros Ventre formation, Death Canyon limestone member	1	1.41%	Granite (1)
Woo – Biotite gneiss with magnetite eyes	1	1.41%	Death (1)

Three dominant rock types are present at rock fall source points, and, as was the case with debris flows, they are Wgm, Xmo, and Wr. As was also the case with debris flow source points, Wgm and Xmo deposits are common in Death and Garnet Canyons, respectively, and both are common in Cascade Canyon. Significant minorities of Wom, Xmo Wgm, and Wag deposits are also present. Deposits of Wr accounted for most rock fall source points in Granite Canyon, and Augen gneiss deposits accounted for all but one rock fall source point in Paintbrush

Canyon. These results make formulating a conclusion that departs from that of debris flows—that source points are most likely to occur on the most dominant local rock type than a specific rock type or types over the whole study area—difficult.

5.2d Rock Slides

Slope Gradient

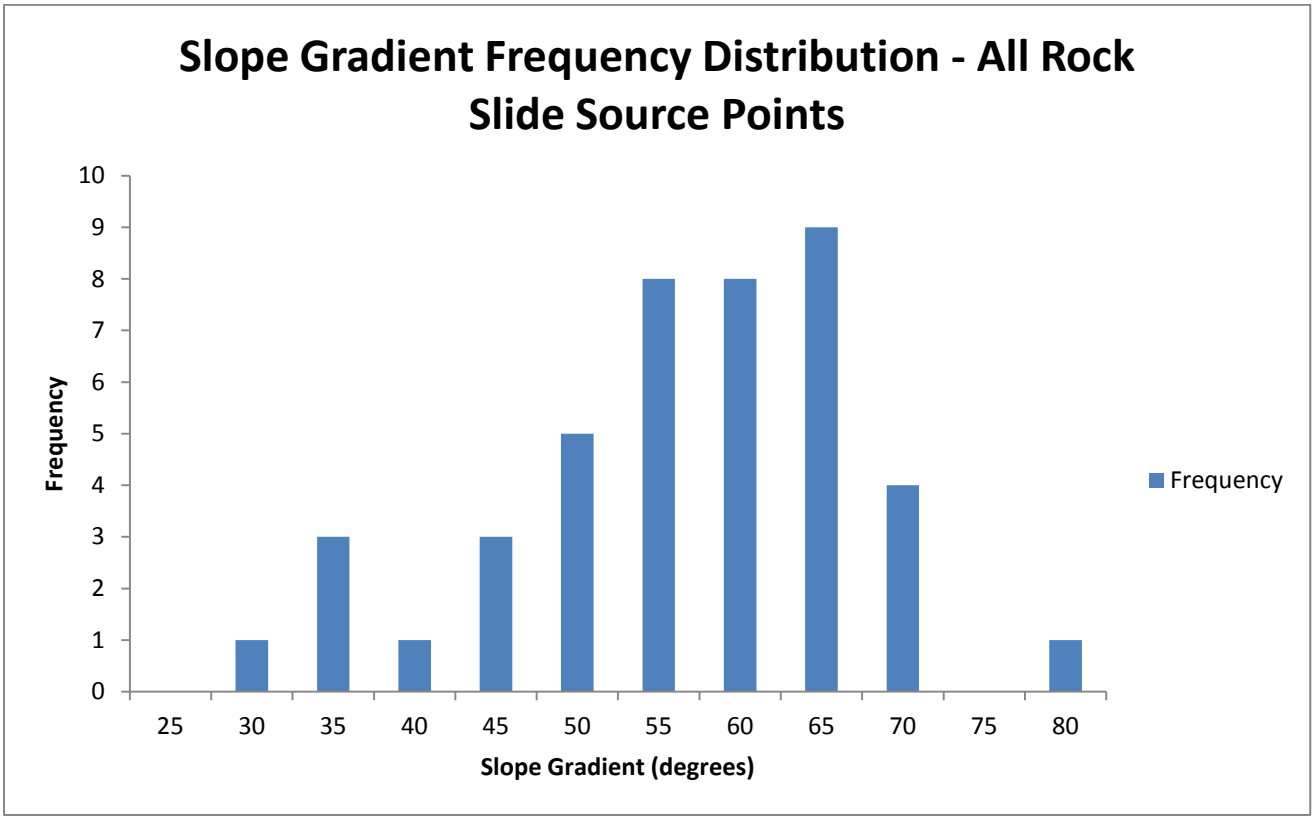

Figure 5.43: Histogram of the slope gradient frequency distribution of all rock slide source points in GTNP.

Table 5.48: Summary statistics of slope gradient for all debris flow source points in GTNP

Point count	Minimum value	Maximum value	Mean	Median	Standard deviation
43	27.64	75.50	53.92	55.64	10.99

Average slope gradient values for rock slide source points were near a relatively high 54º and data variability was low with the lowest range of values and standard deviation out of the

four categories of slope failures. Figure 5.43 displays a slight negative skew with the data, but few noticeable outliers exist.

Slope Aspect

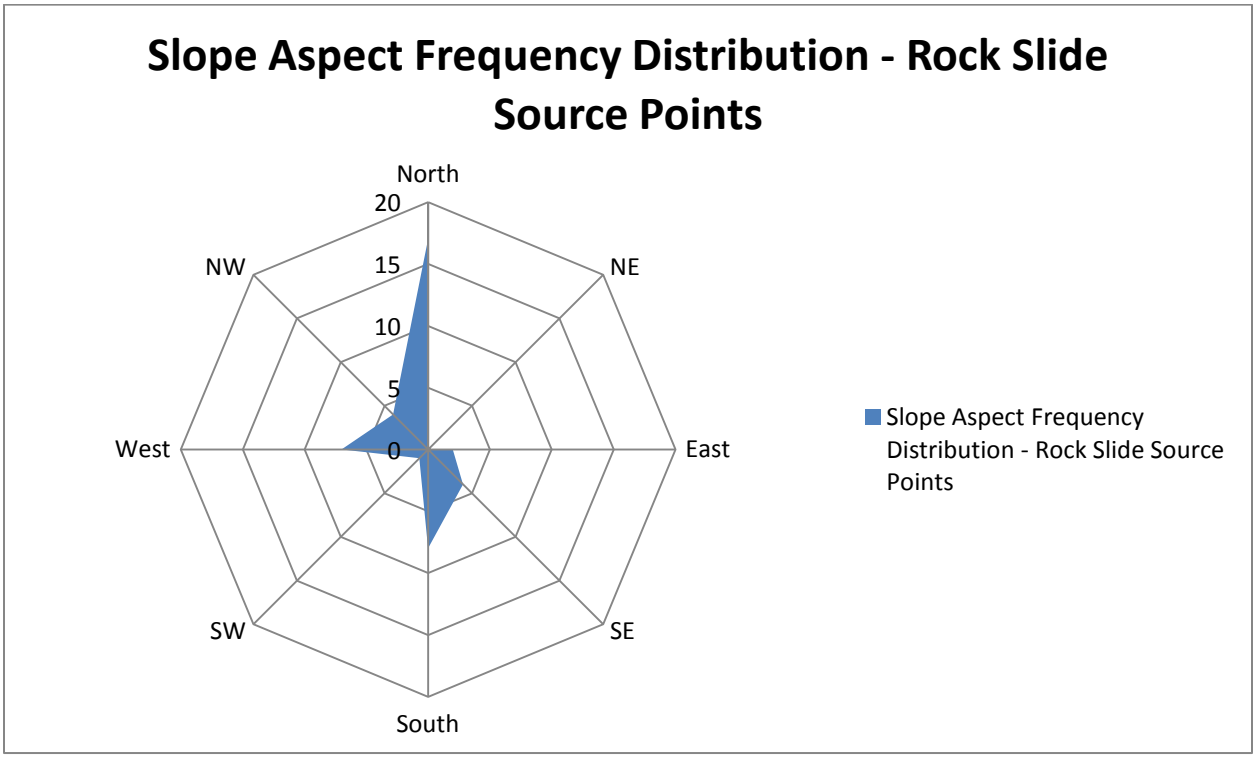

Figure 5.44: "Radar" chart of the distributions of rock fall source point orientations.

Table 5.49: Summary statistics for aspect orientations for all rock fall source points.

Point count	Mean	Median	Standard deviation
43	210.37	242.90	122.29

Table 5.50: Frequency table for aspect orientations of all rock slide source points.

	Total	North	NE	East	SE	South	SW	West	NW
Rock slide source points	43	17	0	2	4	8	1	7	4

Rock slide source points showed a decided bias toward north-facing slopes, although south-facing and west-facing slopes experienced close to an equal number of events at 8 and 7,

respectively. The role of freeze-thaw shattering in causing alpine slope instability (Matsuoka et al., 1998) on north-facing slopes may be reflected in these aspect results for rock slides.

Slope Curvature

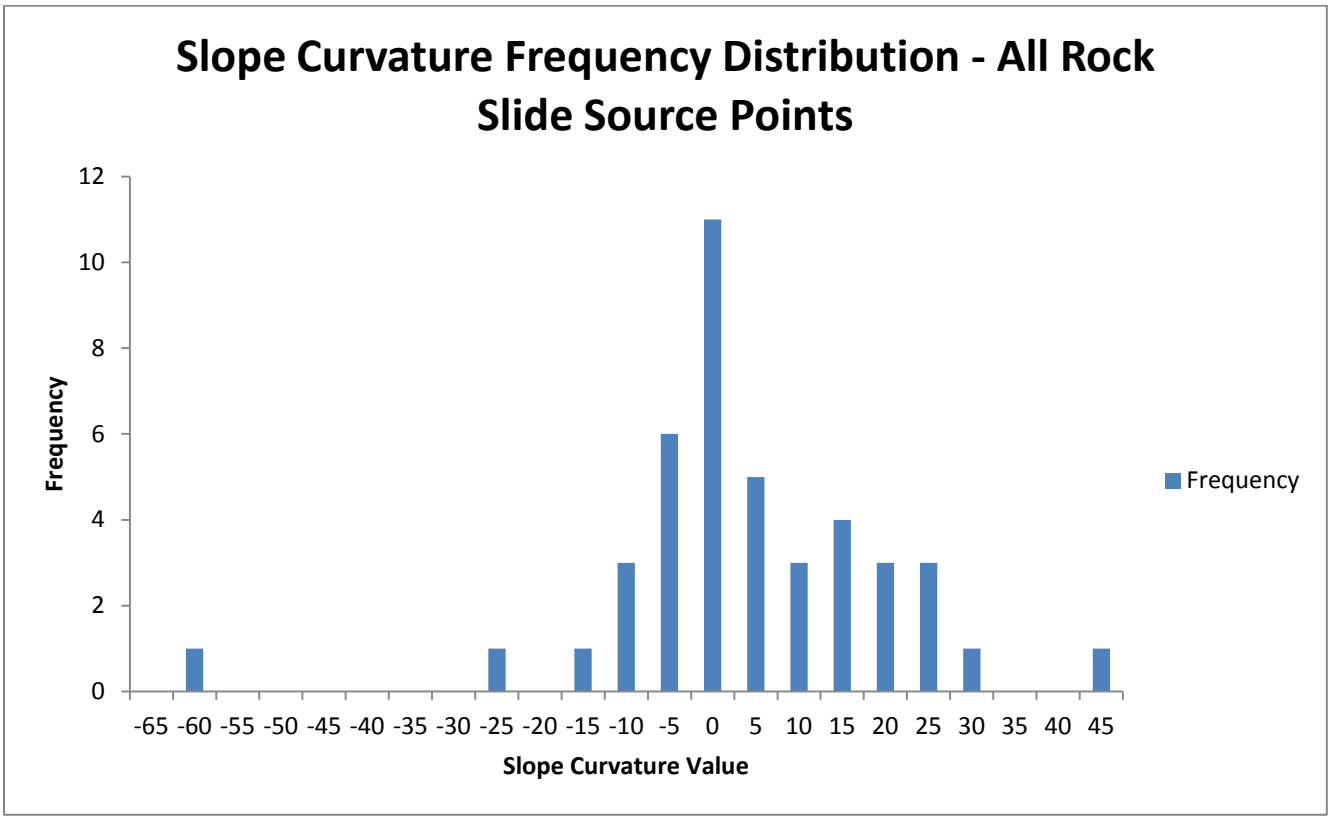

Figure 5.45: Histogram of the slope curvature frequency distribution of all rock slide source points in GTNP.

Table 5.51: Summary statistics of slope curvatures for all rock slide source points in GTNP

Point count	Minimum value	Maximum value	Mean	Median	Standard deviation
43	-63.36	43.87	1.42	0	17.12

Slope curvature values for rock slide source points showed a flat to slightly convex bias. The data for curvatures of rock slide sources showed a relatively high level of variability comparable to debris flows, although the range of values for slides was higher. The histogram in

Figure 5.45 shows a somewhat negative skew of the slide source point data, although the minimum concave value of -63.36 serves as a significant outlier.

Average Annual Precipitation

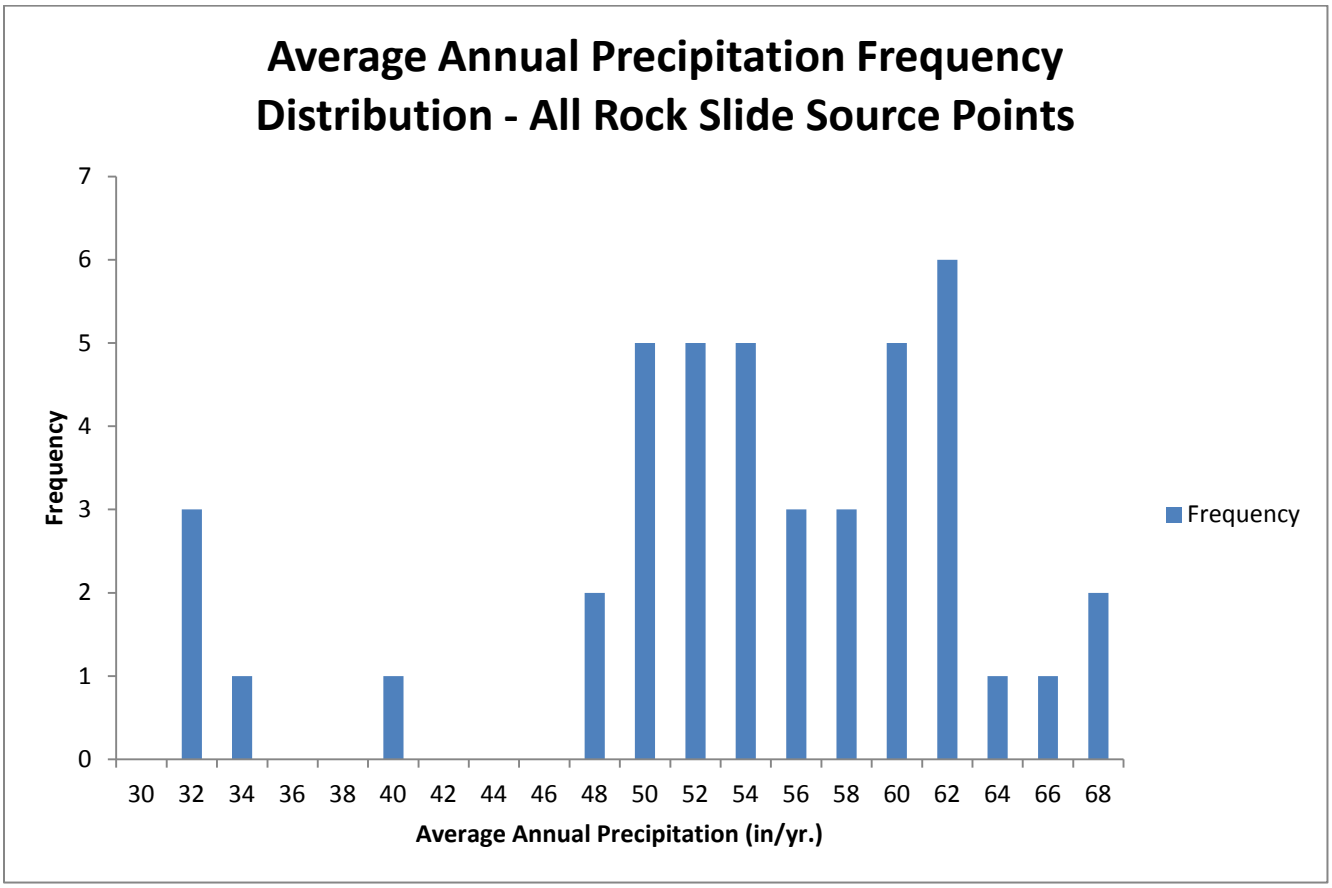

Figure 5.46: Histogram of the average annual precipitation frequency distribution of all rock slide source points in GTNP.

Table 5.52: Summary statistics of average annual precipitation values (in./yr.) for all rock slide source points in GTNP.

Point Count	Minimum Value	Maximum Value	Mean	Median	Standard Deviation
43	30.84	66.85	53.12	53.21	8.98

Rock slide source point values for average annual precipitation showed an average of 53 in/y, a relatively high standard deviation of 8.98, and a lack of discernible distribution in Figure 5.46.

Table 5.53: Distributions of rock types of rock slide source points in GTNP

Rock type	Number	Relative percentage	Canyons present
All rock types	43	100%	-
Wgm – layered gneiss and migmatite	15	34.88%	Cascade (2), Death (8), Garnet (5)
Xmo – Mount Owen quartz monzonite and associated pegmatite	6	13.95%	Cascade (2), Garnet (4)
Wom – Areas where gneiss contains abundant pods and lenses of metagabbro	6	13.95%	Death (6)
Wr – Rendezvous metagabbro	5	11.63%	Granite (5)
Cgg – Gallatin limestone and Park Shale member	2	4.65%	Granite (2)
Wag – Augen gneiss	2	4.65%	Paintbrush (2)
Qt – Talus and other related deposits	2	4.65%	Garnet (1), Granite (1)
Cgf – Gros Ventre formation, Wolsey Shale member and Flathead sandstone	1	2.33%	Death (1)
Qs – Swamp Deposits	1	2.33%	Granite (1)
Xmo Wgm – Mount Owen quartz monzonite and associated pegmatite/layered gneiss and migmatite	1	2.33%	Garnet (1)
Dd – Darby formation	1	2.33%	Granite (1)
Cgd – Gros Ventre formation, Death Canyon limestone member	1	2.33%	Death (1)

Deposits of Wgm were by far the most common rock type where rock slide source points were present, especially in Death Canyon as in the case of debris flows and rock slides. Death Canyon also has a large deposit of gneiss with pods and lenses of metagabbro, hence the high number of rock slide source points intersecting Wom deposits in that canyon. However, rock slide source points intersecting Wgm deposits was a more common occurrence in Garnet Canyon

than Cascade Canyon, unlike debris flows or rock falls. Rock slide source points intersecting Xmo deposits were relatively common in Garnet Canyon given the small sample size and a smaller minority of slide source points intersecting Xmo deposits in Cascade Canyon was present as well. Deposits of rendezvous metagabbro accounted for half of all rock slide source point intersections in Granite Canyon, by far the highest number for a rock type there. Augen gneiss deposits accounted for all rock slide source points in Paintbrush Canyon as was the case with debris flow source points and almost all rock fall source points.

5.2e Snow Avalanche Deposit Slope Data

Table 5.54: Slope gradient data for snow avalanche polygon deposits in GTNP.

SF Type	Count	Mean	Median	Standard deviation	Minimum	Maximum
Snow avalanche	38	53.46	57.8	15.56	8.92	81.66

The mean and median slope gradient of a snow avalanche in the study area is much higher with values in the mid 50s when compared to the mean and median values of snow avalanche source points (~ 40º). The standard deviation value for snow avalanche deposits is slightly higher (15.56) than snow avalanche source points (13.43), conveying a slightly higher variance from the mean for deposit data, and the range of values for snow avalanche deposits was much higher (72.74) than the range for snow avalanche source points (53.13).

5.2f Discussion and Comparisons with Section 5.1

Snow avalanche source points occurred on relatively low slope gradients, averaging close to 40º. This average was likely affected by the relatively high slope gradient values for the 14 points occurring in Paintbrush Canyon: The gradient averages of Cascade, Death, and Granite were closer to 35º than 40º, and Paintbrush's gradient average was closer to 50º. North- to northeast-facing slopes were the most common slope aspect values for snow avalanche points,

although 8 of the 51 points sampled occurred on south-facing slopes. However, this distribution was highly affected by Cascade Canyon's source points, as 15 points occurred on north-facing slopes and 8 on northeast-facing slopes. Death and Granite Canyons had much more even distributions of aspects, and Paintbrush Canyon had equal distribution between north-facing and southeast-facing points. Slope curvature values for avalanches displayed a minor convex tendency in a normally distributed data set. Death, Granite, and Paintbrush Canyons exhibited a noticeable concave bias, whereas Cascade source points tended to be flat to convex.

Debris flow source points averaged a slightly higher slope gradient average than their avalanche counterparts at approximately 42º. Cascade, Death, and Paintbrush Canyons had slope gradient averages close to 42º, although unsurprisingly Garnet Canyon's debris flow slope gradient average was much higher and Granite Canyon's average was lower in the high 30s. Unlike snow avalanches, flow source points showed a pronounced south to southeast tendency in slope aspect values. All five canyons followed this tendency, although Paintbrush Canyon's aspect distribution was relatively even. Debris flow source points showed a concave tendency; and Cascade, Death, and Paintbrush Canyons followed this tendency. Curiously, Garnet and Granite Canyons had differing mean and median values for slope curvature, as the means were concave values and the medians were convex values. The gap between the mean and median values for Garnet Canyon was particularly pronounced, and curvature values for that canyon exhibited very high variance from the mean.

Rock falls had the highest average slope gradient values of the four slope failure categories at ~ 55º. Rock falls in Cascade and Garnet canyons averaged closer to 60º slopes at source points, and Granite Canyon unsurprisingly had a lower canyon average of ~ 45-46º. Slope aspect values showed a north-northeast tendency, although a significant south-facing component

was present as well. Cascade, Death, Garnet, and Granite Canyons were dominated by north and northeast-facing aspects, although Granite Canyon had an equal number of south-facing source points as north-facing source points. Paintbrush Canyon was evenly distributed with a very small sample size. On average, rock fall source points occurred on flat to slightly convex slopes, but variation in the whole data set was high as range and standard deviation values were elevated. Moreover, slope curvature averages between individual canyons varied considerably. Garnet, Granite, and Paintbrush Canyons all averaged considerably concave values for rock fall source points, Death Canyon averaged flat to slightly convex values, and Cascade Canyon's average was considerably convex. Cascade, Death, and Granite Canyons contain the vast majority of rock fall source points. The variation across data sets and canyons suggests that the role slope curvature plays in rock fall occurrence rates is inconclusive.

Slope gradient averages for rock slides were the second highest of the four slope failure categories at ~ 54-55º. Slides in Death Canyon had a slightly higher average than the total average, and Paintbrush's slope gradient average for rock slides was considerably lower, although a sample size of two source points may not be enough to call that data representative of any pattern. Rock slide source point aspect values displayed a tendency toward being located on north-facing slopes throughout the study area, as aspects between 337.5 and 22.5º were either the most common or tied for the most common aspect category in each individual canyon. Curvature averages for all rock slides leaned flat to slightly convex, although considerable variability existed between the five canyons. Granite Canyon showed a concave tendency, whereas Garnet and Cascade Canyons showed convex tendencies. Death Canyon (which had the largest slide sample size of 16) and Paintbrush Canyon (with the smallest sample size of 2) tended closest toward the mean. Despite the variance in patterns between canyons, the variance from the mean

for all rock slide curvature data was considerably lower than rock falls and about analogous with debris flows.

Histograms for average annual precipitation data for all four slope failure source point types were highly variable and did not show any noticeable distribution or pattern. Further chi-square analysis was needed to evaluate the statistical validity of these data. Results for rock type distributions in each canyon appeared to have a similar local bias; debris flow, rock fall, and rock slide source points all displayed a bias more dependent on the dominant rock type in the specific canyon they were located than a bias toward one or multiple rock types over the whole study area regardless of how spatially dominant said rock type(s) would be.

Marston et al. (2011) performed a similar set of analyses with data from slope failure polygons. Their analyses of histograms and X^2 testing showed that rock falls occurred at the greatest frequency where slope aspect is between 300º and 60º and slope gradient lies in the range of 56-62º, and the combination of these two variables provides "a significant explanation at $p < 0.0001$ for the distribution of rock falls in the study area" (Marston et al., 2011; p. 8). Marston et al. (2011) also determined that rock slides occur at the greatest frequency where slope gradient is greater than 49º. They also determined that debris flows occur at the greatest frequency on slope aspects that are south-facing between 140 and 220º, RMS is greater than 60, and slope gradient lies between 28º and 54º. Chi-square analysis for debris flows in Marston, Weihs, and Butler (2011) showed that a combination of the aforementioned aspect, RMS, and gradient variables provides "a significant explanation at $p < 0.0001$ for the distribution of flows" (Marston, Weihs, and Butler, 2011; p. 9). Snow avalanches occurred most commonly on north-facing aspects between 320º and 40º and gradients between 32 and 48º, and chi-square analysis showed that the combination of those two variables provides a "significant explanation at p <

0.0001 for the distribution of snow avalanches" (Marston et al., 2011; p. 9). All of the patterns gleaned from the updated data set in this study appear to be close or identical to those found in Marston et al., (2011).

In summary, pronounced patterns can be gleaned from the descriptive statistics for slope failure source points. Snow avalanches tend to occur most often on slopes that face north and northeast, are close to 40º in gradient, and are slightly concave. Debris flows also have shown a pattern of starting on relatively gentle, concave slopes near 42º in gradient, but differ considerably in slope aspect in being located on south- and southeast-facing slopes. Although snow avalanches can occur at any time in a debris flow path during the winter, apparently stand-alone avalanche paths show a considerably different pattern in which types of aspect favor their occurrence rates. Rock falls and rock slides consistently occur at steeper slope gradient than their counterparts at around 55º. Rock falls occurred most commonly on north-, northeast-, and south-facing slopes; whereas rock slides also favored north-facing slopes but had a significant number of south- and west-facing aspects as well. As previously mentioned, the role of freeze-thaw shattering in causing slope instability on north-facing slopes may be a reflection of these aspect data. Slope curvature values for slides and falls had a flat to convex lean, although high variability between canyons and data sets for these data and a non-normal distribution of curvature data for rock falls call into question the relevance of slope curvature values in the occurrence rates of these two categories of slope failures. Further chi-square analysis was conducted to test the statistical validity of these patterns.

5.3 Chi-Square Analysis

5.3a Chi-square testing for geomorphic characteristics of slope failure types

Patterns and trends observed from the descriptive statistics in sections 5.1 and 5.2 were tested further via chi-square analysis. The first set of geomorphic data tested was for the four slope failure types. The most common geomorphic data for each type of characteristic is listed in Table 5.55 for comparison against patterns noted in Section 5.1. These data were then tested for chi-square analysis. The p-value results for these chi-square tests are listed in Table 5.56.

Table 5.55: Most common or dominant value for slope failure types and their geomorphic characteristics

SF Type	**Geomorphic Category**						
	Slope Gradient (deg.)	Slope Aspect	Slope Curvature	Precip (in./y)	Rock Type	Trimline Position	Distance from fault (m)
Avalanches	36-40.9	N	Concave	50-54.9	-	Above	3001-4000
Falls	56-60.9	S	Concave	55.59.9	Xmo	Above	2001-3000
Flows	41-45.9	N	Concave	50-54.9	Wr	Above	1001-2000
Slides	61-65.9	N	Concave	50-54.9	Wgm	Above	3001-4000

Table 5.56: Chi-square p-value testing results for slope failure type

SF Type	**Geomorphic Category**						
	Slope Gradient	Slope Aspect	Slope Curvature	Precip	Rock Type	Trimline Position	Distance from fault
Avalanches	<0.001	<0.001	None	0.005	-	<0.001	0.05
Falls	<0.001	0.005	None	None	<0.001	None	None
Flows	<0.001	0.005	None	<0.001	<0.001	<0.001	<0.001
Slides	<0.001	<0.001	None	<0.001	<0.001	None	None

Slope gradient, slope aspect, rock type, and slope curvature stand out as four geomorphic characteristic as having a clear or negligible effect on slope failure distribution for each type of slope failure. Chi-square testing of precipitation rendered somewhat more mixed results with strong patterns for avalanches, flows, and slides, but not rock falls. Avalanches and debris flows showed similar strong associations for above trimline positions and to a lesser extent with moderate and short distances from the Teton Fault, respectively. Rock falls and rock slides

appeared to not have significant deviances from the local trimline and distance to fault characteristics, i.e. the expected result.

5.3b Chi-square testing for geomorphic characteristics of individual canyons

Chi-square analysis of geomorphic characteristic in individual canyons was undertaken as well. The most common observed values for each geomorphic characteristic in each canyon are listed in Table 5.57. P-value results from chi-square testing are listed in Table 5.58.

Table 5.57: Most common or dominant value for individual canyons and their geomorphic characteristics

Canyon	**Geomorphic Category**						
	Slope Gradient (deg.)	Slope Aspect	Slope Curvature	Precip (in./y)	Rock Type	Trimline Position	Distance from fault (m)
Cascade	36-40.9	N	Concave	50-54.9	Xmo	Above	1001-2000
Death	36-40.9, 51-55.9, 61-65.9 (tie)	N	Concave	55-59.9	Wgm	Above	4001-5000, 5001-6000 (tie)
Garnet	56-60.9	S	Convex	60-64.9	Xmo	Above	2001-3000
Granite	41-45.9	SE	Concave	40-44.9	Wr	Above	1001-2000
Paintbrush	31-35.9, 41-45.9, 51-55.9, 61-65.9 (tie)	N	Concave	55-59.9	Wag	Above	3001-4000

Table 5.58: Chi-square testing results for individual canyons in Grand Teton National Park.

Canyon	**Geomorphic Category**						
	Slope Gradient	Slope Aspect	Slope Curvature	Precip	Rock Type	Trimline Position	Distance from fault
Cascade	<0.001	<0.001	None	None	None	<0.001	<0.001
Death	<0.001	0.01	None	None	<0.001	None	None
Garnet	<0.001	<0.001	None	0.005	None	None	0.01
Granite	<0.001	<0.001	None	<0.001	<0.001	None	<0.001
Paintbrush	<0.001	None	0.05	0.025	<0.001	<0.001	None

Slope gradient values for each canyon displayed a distinct departure from the expected values in each canyon, suggesting a strong association between slope gradient values and slope

failure distribution. Slope aspect p-values also showed a strong departure from local expected values in Cascade, Death, Garnet, and Granite canyons, although curiously not in Paintbrush Canyon. Conversely, slope curvature chi-square testing revealed little variance from the local expected values in Cascade, Death, Garnet, and Granite canyons but 95% chance of variance from expected values in Paintbrush Canyon. Rock type p-values were all or nothing as Death, Granite, and Paintbrush canyons had the lowest possible value whereas Cascade and Garnet canyons did not achieve statistical significance. Cascade and Paintbrush canyons saw strong associations with above trimline positions and statistically significant chi-square results, but the other three canyons did not achieve statistical significance from chi-square testing despite strong associations with above trimline positions. Testing for precipitation values in individual canyons yielded strong levels of significance in Garnet, Granite, and Paintbrush canyons but not in Cascade and Death canyons.

5.3c Discussion and comparisons with Sections 5.1 and 5.2

Strong patterns emerged for slope gradient and slope aspect values for slope failure types as well as individual canyons, and these patterns were backed by strongly significant chi-square testing results for all slope failure types and canyons with the except of Paintbrush canyon for slope aspect. Interestingly, both comparatively high and low slope gradient values were considered statistically significant for Death and Paintbrush canyons, which may reflect the trends of debris flows and snow avalanches tending towards lower slope gradients and rock falls and rock slides tending towards higher slope gradients.

Slope curvature values possessed high levels of variability from the mean in the descriptive statistics and also appeared to have little variation from local expected characteristics for both slope failure types and individual canyons, suggesting little evidence for a link between

slope curvature and slope failure distribution in the study area. Rock type patterns for slope failures exhibited a clear departure from local expected characteristics in chi-square testing, suggesting a high level of importance for rock type in rock fall, rock slide, and debris flow distributions, but testing for individual canyons revealed less conclusive results with all-or-nothing p-values for the five canyons. Testing of precipitation data revealed strong statistical significance for avalanches, flows, and slides, as well as in Garnet, Granite and Paintbrush canyons, but not for rock falls or Cascade and Death canyons.

Although a clear pattern for above trimline positioning exists for all slope failure types and individual canyons, chi-square testing revealed all-or-nothing results in regards to observed values departing from expected local conditions. Cascade and Paintbrush canyons had strong p-values of <0.001, and so did debris flows and snow avalanches. Considering the high numbers of debris flows and snow avalanches in Cascade Canyon and the high number of snow avalanches in Paintbrush Canyon, one might consider the lack of statistically significant trimline results in Granite Canyon to be a curious aberration from strong patterns in the other two. Distance from the Teton Fault revealed similarly random results from chi-square testing for statistical significance. Cascade, Garnet, and Granite canyons as well as debris flows saw strong significance from chi-square testing and snow avalanches with a p-value of 0.05, but Death and Paintbrush canyons as well as rock slides and rock falls appeared to have little statistical significance to suggest trimline position as a potential explanatory factor in slope failure distribution.

Comparison with Study Hypotheses

- For slope gradient data of failures located in the five canyons, chi-square testing has disproved the null hypothesis for all slope failure types and all individual canyons.

- For slope aspect data of failures located in the five canyons, chi-square testing has disproved the null hypothesis for all slope failure types and all individual canyons except Paintbrush.
- For slope curvature data of failures located in the five canyons, chi-square testing has proved the null hypothesis for all slope failure types and all canyons except Paintbrush.
- For precipitation data of failures located in the five canyons, chi-square testing has disproved the null hypothesis for avalanches, flows, and slides, but has proved the null hypothesis for rock falls. It has also disproved the null hypothesis for slope failures located in Garnet, Granite, and Paintbrush canyons, but has proved the null hypothesis in Cascade and Death canyons.
- For rock type data of failures located in the five canyons, chi-square testing has disproved the null hypothesis for debris flows, rock falls, and rock slides, as well as slope failures located in Death, Granite and Paintbrush canyon. However, the null hypothesis was proven for slope failures located in Cascade and Garnet canyons.
- For trimline position data of failures located in the five canyons, chi-square testing has disproven the null hypothesis for snow avalanches and debris flows, but has proven the null hypothesis for rock falls and rock slides. The null hypothesis has been disproven for Cascade and Paintbrush canyons, but not for Death, Garnet, and Granite canyons.
- For distance from the Teton Fault data of failures located in the five canyons, chi-square testing has disproven the null hypothesis for snow avalanches and debris flows, but has proven the null hypothesis for rock falls and rock slides. The null hypothesis has been disproven for Cascade, Garnet, and Granite canyons, but the null hypothesis has been proven for Death and Paintbrush canyons.

5.4 Slope Failure Maps – With Human Structures

Campgrounds

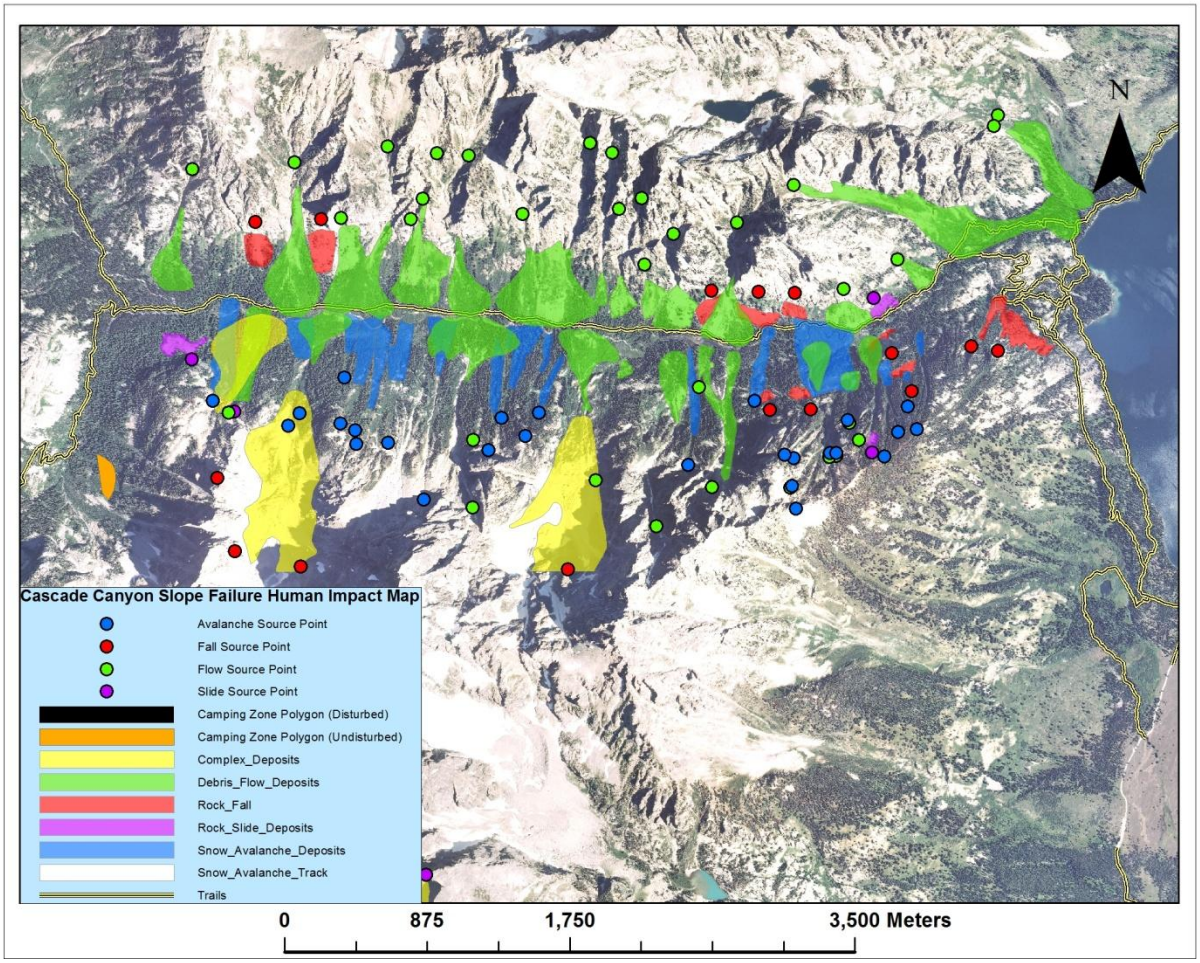

Figure 5.47: Slope failure human impact map for campgrounds in Cascade Canyon.

Table 5.59: Information for campgrounds present and affected by slope failures in Cascade Canyon.

Names of campgrounds present	Names of campgrounds affected	Total area of campgrounds (m^2)	Campground area impacted by slope failure deposits (m^2)	Percentage area of campgrounds impacted by slope failure deposits
Cascade South Fork	None	20,538	0	0

Slope failure impacts on campgrounds within the Cascade Canyon area and within 500 m of the final field sampling point were minimal, primarily because no major camping zones are

located within the first 5 km of the Cascade Canyon hiking trail. A small sliver of the South Fork Campground is within 500 m of the sample site cutoff line, but no noticeable slope failures appear to be present.

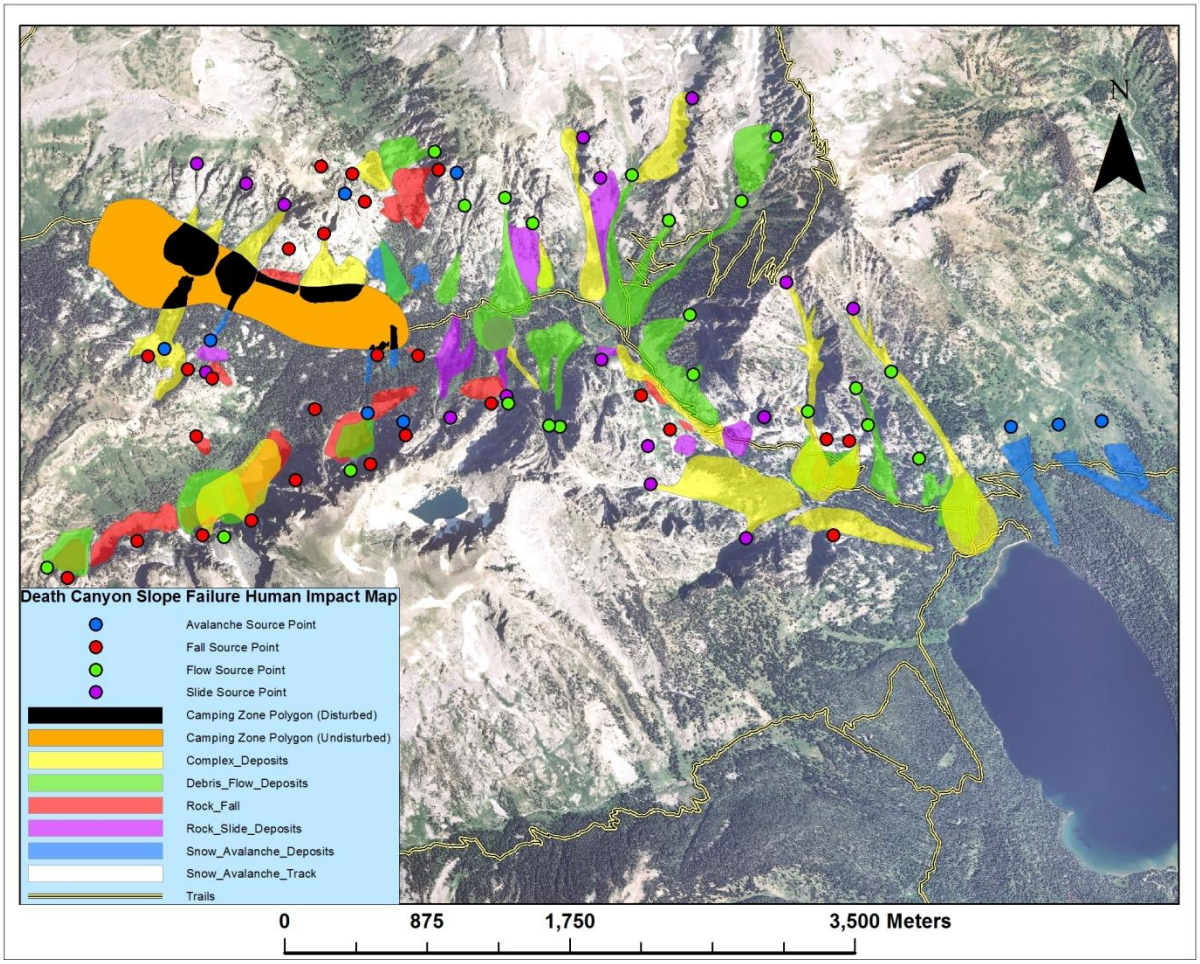

Figure 5.48: Slope failure human impact map for campgrounds in Death Canyon

Table 5.60: Information for campgrounds present and affected by slope failures in Death Canyon.

Names of campgrounds present	Names of campgrounds affected	Total area of campgrounds (m^2)	Campground area impacted by slope failure deposits (m^2)	Percentage area of campgrounds impacted by slope failure deposits
Death Canyon	Death Canyon	804,195	222,640	27.68%

Over one-quarter of the Death Canyon campground located on the western edge of Death Canyon has been impacted by past slope failures. Although complex slope failures appear to be the primary source of campground disturbance, fall and avalanche deposits are also present in the camping zone.

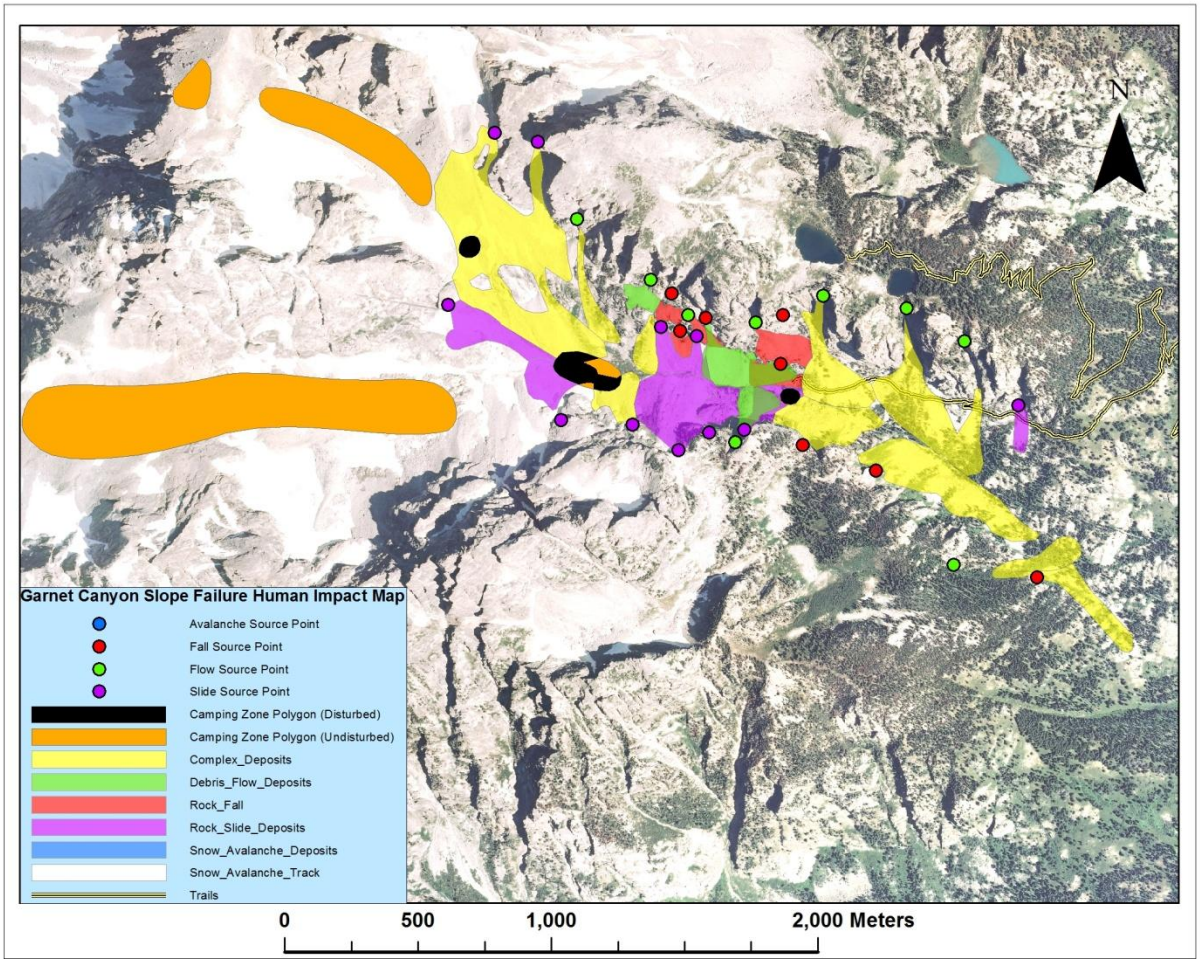

Figure 5.49: Slope Failure Human Impact Map for Campgrounds in Garnet Canyon

Table 5.61: Information for campgrounds present and affected by slope failures in Garnet Canyon.

Names of Campgrounds Present	Names of Campgrounds Affected	Total Area of Campgrounds (m^2)	Campground Area impacted by slope failure deposits (m^2)	Percentage area of campgrounds impacted by slope failure deposits
Garnet South Fork, Garnet Caves, Lower Saddle, Platforms, Meadows, Moraine	Meadows, Platforms, Garnet Caves	495,178	Meadows: 20,077; Platforms: 3,600; Garnet Caves: 5,227	Meadows: 76.96%; Platforms: 100%; Garnet Caves, 100%; Total: 5.84%

Camping zones directly inside the slope failure study areas have been heavily impacted by past slope failures. The tiny camping zones of Garnet Caves and Platforms were completely engulfed by complex slope failures and rock slides, respectively. Meadows camping zone at the southwest edge of Garnet Canyon is intersected by two large complex deposits and a rock slide deposit. Although no slope failures were mapped for South Fork, Lower Saddle, and Moraine camping zones that does not mean that no slope failure activity was present, instead merely that no slope failures were mapped outside of the study area. Given the high activity level of slope failures in Garnet Canyon, visitors in Meadows, Platform, and Garnet Caves camping zones should exercise much caution when camping there.

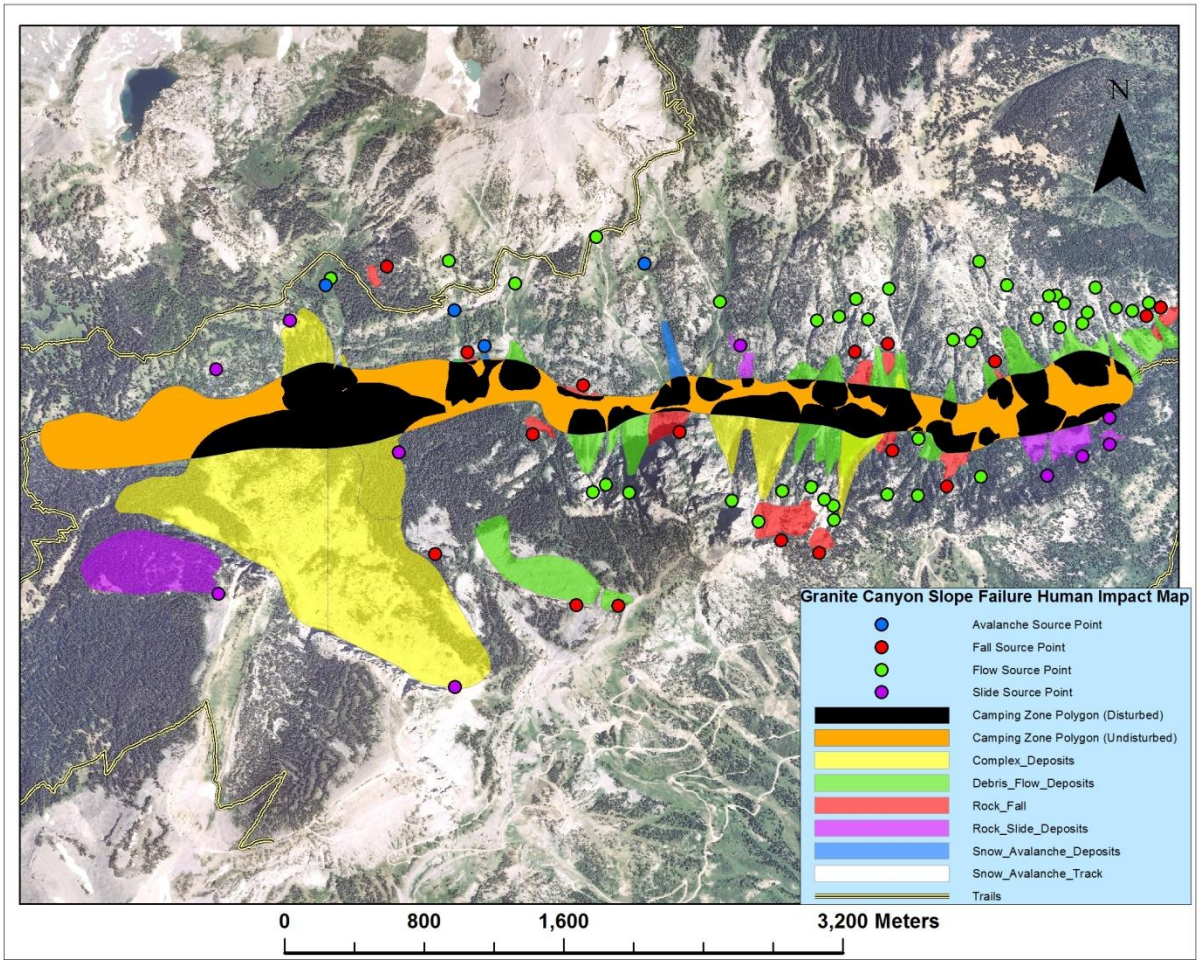

Figure 5.50: Slope failure human impact map for campgrounds in Granite Canyon

Names of campgrounds present	Names of campgrounds affected	Total area of campgrounds (m^2)	Campground area impacted by slope failure deposits (m^2)	Percentage area of campgrounds impacted by slope failure deposits
Granite Lower	Granite Lower	1,880,671	1,116,320	59.36%

Table 5.62: Information for campgrounds present and affected by slope failures in Granite Canyon.

Just under two-thirds of the long, snake-like Granite Lower camping zone has been impacted by various slope failure deposits. All five types of slope failure deposits intersect this camping zone, although debris flows and complex deposits are the most common types breaching the zone. Only the extreme western edge of the camping zone is spared from slope

failure impacts within a kilometer. Given the ability of debris flows and complex deposits with debris flow components to reoccur in similar areas over time, Granite Canyon should be considered a potential high hazard zone for slope failure impacts on campers.

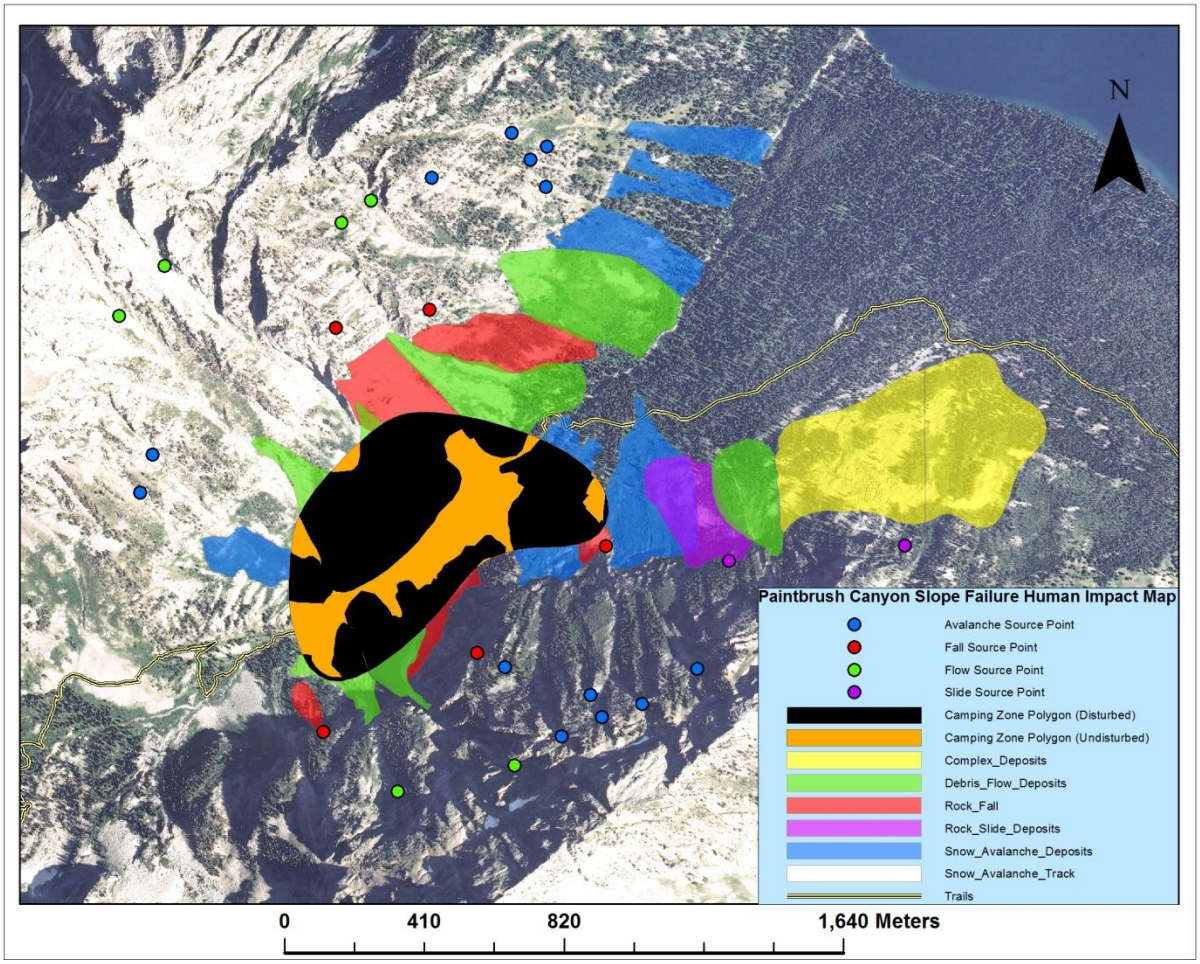

Figure 5.51: Slope failure human impact map for campgrounds in Paintbrush Canyon

Table 5.63: Information for campgrounds present and affected by slope failures in Granite Canyon.

Names of campgrounds present	Names of campgrounds affected	Total area of campgrounds (m^2)	Campground area impacted by slope failure deposits (m^2)	Percentage area of campgrounds impacted by slope failure deposits
Paintbrush Lower	Paintbrush Lower	440,040	324,665	73.78%

Paintbrush Canyon's Lower camping zone is the second largest camping zone impacted by slope failure deposits and also contains the second largest area of camping zone intersected by slope failures behind Granite Lower. However, Paintbrush Lower has an even higher percentage area intersected by slope failures than Lower Granite at ~ 74%. Debris flows, rock falls, and snow avalanches are the primary types of slope failures that have intersected Paintbrush Lower in the southwestern edge of Paintbrush Canyon. Given the ability of snow avalanches and debris flows to reoccur in similar areas over time, Paintbrush Lower should be considered a high hazard zone for visiting campers.

Trails

Table 5.64: Length and percentage of trail segments intersected by the five categories of slope failure deposits in the five canyon study area in GTNP

Canyon name	Length (m) intersected by avalanches	Length (m) intersected by falls	Length (m) intersected by flows	Length (m) intersected by slides	Length (m) intersected by complex deposits	Total length of canyon (m)	Total length (m) and percentage intersected
Cascade Canyon	445	182	3,263	2	0	6,875	3,892, 56.61%
Death Canyon	571	274	3,121	250	2,611	16,554	6,827, 41.24%
Garnet Canyon	0	50	8	61	615	1,813	734, 40.49%
Granite Canyon	456	208	1,265	8	856	8,076	2,793, 34.58%
Paintbrush Canyon	498	0	440	0	0	7,028	938, 13.35%

Over half of the trail length of Cascade Canyon traveled in this study was intersected by slope failures, and a large portion of those intersections was dominated by debris flow deposits. Snow avalanches and debris flows comprised minor segments of Cascade Canyon intersections. Death and Garnet Canyons had intersection rates of close to 40 percent, although the slope

failure category intersection rates were very different between the two. Death Canyon is primarily intersected by debris flows and complex deposits with minor intersections of avalanches, falls, and slides, whereas Garnet Canyon intersections are dominated by complex deposits. Approximately 35% of Granite Canyon was intersected, with flows and complex deposits comprising the most significant intersecting categories with minor avalanche and fall intersection lengths. Paintbrush Canyon curiously had a comparatively low intersection rate of 13.55%, which stands in stark contrast to the ~74% intersection rate for the Paintbrush Lower camping zone. The Paintbrush trail is intersected only by flow and avalanche deposits, the two most common reoccurring slope failure categories. Therefore, although Paintbrush Canyon's trails are comparatively safe, those lengths should be considered potentially hazardous areas. Maps displaying trails intersected by slope failures can be found in Figures 5.1, 5.6, 5.11, 5.16, and 5.21.

5.4 Field Work Results

Selby system sampling of local geomorphic characteristics was undertaken at a rate of every .5 kilometers. RMS values were calculated using Intact Strength Ratings via a Schmidt Hammer and the Selby System for Rock Mass Strength (Figure 4.1). Rock Mass Strength values for all sites in a specific canyon were averaged together to determine the average RMS value for each individual canyon.

5.4a RMS Values

Rock mass strength averages for all five canyons fell under *moderate* strength ratings based on the Selby system as outlined in Figure 4.1. Little variance existed between the means, with Cascade, Death, Garnet, and Granite Canyons especially registering values in close proximity to one another. Low sample sizes for Garnet and Paintbrush Canyons were caused by

the relative shortness of the canyon trail before encountering cirque or boulder field terrain. Data for Granite Canyon site #10 were too incomplete to calculate an RMS rating because of high tree cover preventing an uninhibited view of the canyon wall

Table 5.65: Rock mass strength values for each 0.5 kilometer sample site, with cumulative RMS averages for each canyon.

Canyon	Site #1	Site #2	Site #3	Site #4	Site #5	Site #6	Site #7	Site #8	Site #9	Site #10	Average
Cascade Canyon	75	61	79	67	65	61	67	77	77	69	70
Death Canyon	71	65	61	66	75	66	63	67	61	61	66
Garnet Canyon	60	74	71	-	-	-	-	-	-	-	68
Granite Canyon	68	64	62	77	68	70	65	69	74	-	69
Paintbrush Canyon	58	77	54	53	-	-	-	-	-	-	61

CHAPTER 6 – CONCLUSIONS

The primary aims of this project were to take a comprehensive look at locations, geomorphic conditions, and potential human impacts of slope failures in Grand Teton National Park (GTNP). The results convey that all five canyons analyzed in this study area have experienced numerous past slope failures and will likely continue to do so in the future. All five canyons contain all five types of slope failure deposits: snow avalanches, debris flows, rock falls, rock slides, and complex deposits that mix the four categories—with the notable exception of snow avalanches in Garnet Canyon. The vast majority of area in the bottoms of each canyon is occupied by slope failure deposits that can travel from near the top of the canyon face down to the trails and streams below. Rock mass strength values for all five canyons appear to fall into the moderate category, suggesting that rock strength is neither too weak nor strong, yet numerous slope failures persist in these deglaciated canyons.

Strong patterns in slope conditions at the sites of source points for slope failures have emerged for all four categories of slope failures. Snow avalanches and debris flows occur most often on gentle, north-facing, flat to convex slopes; debris flows are most common on gentle, south-facing, flat to convex slopes; rock falls and rock slides are most common on steep slopes near 55º and both favor north- and south-facing slopes. Chi-square analysis of these data, however, has only proven to be statistically significant for slope gradient and slope aspect data. Slope curvature data for rock falls and rock slides are variable and inconclusive due to its lack of statistical significance in chi-square testing. Strong statistical significance has been shown for rock falls being associated with Mount Owen quartz monzonite and associated pegmatite deposits, slope failures in Death Canyon and all rock slides with layered gneiss and migmatite deposits, slope failures in Granite Canyon and all debris flows with Rendezvous metagabbro

deposits, and slope failure deposits in Paintbrush Canyon with augen gneiss deposits. All slope failure types and slope failures in all five canyons showed a clear tendency towards beginning above an established trimline, but only slope failures in Cascade and Paintbrush canyons as well as all avalanche and debris flow source areas showed statistical significance when tested for variance from the local expected conditions. Precipitation values vary by canyon but appear to be a potentially important control of slope failure distribution for all slope failure types except rock falls as well as slope failures in all canyons except Cascade and Death. Finally, geomorphic data for slope failures that occurred less than 2000 m from the Teton Fault appeared to have statistically significant departures from expected local distance conditions but results become much less conclusive for slope failures occurring further away from the Fault.

Human structures in all five canyons are impacted by slope failures. Thirty-five percent or more of trail lengths are intersected by past slope failures in all canyons but Paintbrush. Camping zones in all canyons but Cascade are directly intersected by past slope failure deposits, suggesting the potential for more conflict between hikers and nature in the future. Although debris flows and snow avalanches are more dependable in occurring in the same place repeatedly, the correct combination of slope conditions and precipitation may cause future rock slides and falls in areas of human activity.

6.1 Avenues for Future Research

This is an introductory look into the average geomorphic conditions for slope failures in five canyons of Grand Teton National Park and an inventory on slope failure locations in the study area. Although patterns of slope conditions for slope failures may provide a first look at what might be behind the formation of these events, it is not a comprehensive system for predicting where and when future failures will occur. Advances in data availability and

technology should be used in creating a statistical analysis of all available geomorphic data that can be analyzed via multivariate regression and incorporated into a GIS model that predicts the spatial and temporal likelihood for future slope failure locations. *In situ* verification and expansion of geomorphic characteristics of individual slope failures would also provide a more comprehensive view of slope failures in GTNP. An unavoidable shortcoming of this project was that determining the absolute exact locations of source points of slope failures and/or paths feeding into slope failure deposits proved to be impossible; the locations used in this study are the most educated of estimates possible given satellite imagery and GIS technology. *In situ* verification of source sites would thus provide a superior understanding of geomorphic conditions of slope failure source areas. Additional future research from the author to bolster the GIS and statistical results from this study will include hazard maps and assessments of each canyon using the chi-square tests of local geomorphic characteristics, curvature testing for planiform and profile raster layers, and zonal statistics for slope gradient values of slope failure polygons as well as skewness and kurtosis data and box and whisker plots for frequency distributions and summary statistics, respectively.

Another unavoidable shortcoming of this study was a lack of ability to verify the temporal characteristics of past slope failure deposits in the study area. More comprehensive monitoring of the times and conditions under which an active slope failure occurs in the study area could be essential in developing a further understanding of slope failure dynamics in GTNP. Precipitation values during periods of failure activity could be monitored via real time rain gauges, and failure events may be monitored by ground-level vibration sensors near areas of previous slope failure activity. Although implementing an electronic preventative and/or real time warning system for slope failures in GTNP for park visitors is likely not socially or

economically feasible, non-intrusive vibration sensors may improve the understanding of the National Park Service in observing and predicting present and future slope failure activities. More in-depth studies of individual or groups of slope failures should be undertaken in the study area of this project as well. Intact rock strength (IRS) values from Schmidt hammer testing were taken from rocks close to the trails of sample sites, so taking IRS samples from the canyon walls themselves may be a more accurate representation of the data set. Additionally, field validation of joint spacing, orientation, width, and other Selby values may provide a more statistically rigorous validation of rock mass strength data in these five canyons.

6.2 Recommendations

Park officials now armed with the knowledge generated by this study, the work of Marston et al. (2011), and Case (1989) can take proactive steps to better inform the public about the potential risks they face when backpacking and climbing through Cascade, Death, Garnet, Granite, and Paintbrush Canyons. Any human structures directly in the way of a past avalanche or debris flow deposit should be considered areas of high risk for future slope failures, and human structures near slope sites with conditions conducive for rock falls and rock slides could potentially be considered risk zones as well. Signage for hikers warning them of the potential for flows, falls, and slides may raise awareness of their potential for destruction and hazard to personal health, promoting more responsible backcountry behaviors.

Camping zones that have been heavily impacted in the past by slope failures, especially debris flows or multiple falls and slides from the same slope face, should be given extra warning signage for hikers and climbers. Camping at or near the base of large debris flow deposits should be actively discouraged or even prohibited. Of course, the decision-making process for

determining any future camping zones should take into account the potential hazards of the local terrain.

The choice of how to use the data and findings from this study ultimately rests with the National Park Service and interested park visitors who want to learn more about slope failures in GTNP. Grand Teton National Park is one of the most breathtaking and widely visited national parks in the United States, and it is also a source of excitement and intrigue for geomorphologists. Slope failures will continue to be active processes in deglaciated canyons in GTNP; and with the combination of GIS and remote sensing technology as well as *in situ* data, the boundaries for future geomorphic research are seemingly limitless.

REFERENCES

Abanco, C., Hurlimann, M., Fritschi, B., Graf, C., and Jose Moya, 2012. Transformation of ground vibration signal for debris-flow monitoring and detection in alarm systems. *Sensors* 12: 4870-4891.

Alexander, D. 1993. *Natural Disasters.* Chapman and Hall Publishers, New York, NY. pp. 185, 255.

Armstrong, B., and K. Williams, 1986. *The Avalanche Book.* Fulcrum Publishers, Inc., Golden, Colorado, pp. 1, 38-40.

Bates, R. L., and J. A. Jackson, 1984. *Dictionary of Geologic Terms* (3rd edition). American Geologic Institute, New York, NY. 571 pp.

Bovis, M. J., and M. Jakob, 1999. The role of debris supply conditions in predicting debris flow activity. *Earth Surface Processes and Landforms* 24: 1039-1054.

Brocklehurst, S. H., and K. X. Whipple, 2002. Glacial erosion and relief production in the eastern Sierra Nevada, California. *Geomorphology* 42: 1–24, doi:10.1016/S0169-555X(01)00069-1.

Bromhead, E. N. (2004). Landslide slip surfaces: their origins, behaviour and geometry. in: *Landslides: Evaluation and Stabilisation, Proceedings of the 9th International Symposium on Landslides.* Balkema Publishers, London, UK. v.1, pp. 3-22.

Butler, D. R., 1983. Rockfall hazard inventory, Ram River, Mackenzie Mountains. *The Canadian Geographer* 27 (2): 175-178.

Butler, D. R., 1989. Snow-avalanche hazards in Glacier National Park, Montana: meteorologic and climatologic aspects. *Physical Geography* 7: 72-87.

Butler, D. R., 1990. The geography of rockfall hazards in Glacier National Park, Montana. *The Geographical Bulletin* 32 (2): 81-88.

Butler, D. R., and G. P. Malanson, 1985. A reconstruction of snow avalanche characteristics in Montana, U.S.A., using vegetative indicators. *Journal of Glaciology* 31(108): 185-187.

Butler, David R., 1986. Snow-avalanche hazards in Glacier National Park, Montana: meteorologic and climatologic aspects. *Physical Geography* 7 (1): 72-87.

Butler, D. R. and G. P. Malanson, 1992. Effects of terrain on excessive travel distance by snow avalanches. *Northwest Science* 66: 77-85.

Butler, D. R., and G. P. Malanson, 1996. A major sediment pulse in a subalpine river caused by debris flows in Montana, USA. *Zeitschrift für Geomorphologie* 40(4), 525-535.

Butler, D.R., and S. J Walsh, 1990. Lithologic, structural, and topographic influences on snow-avalanche path location, eastern Glacier National Park, Montana. *Annals of the Association of American Geographers* 80 (3): 362-378.

Butler, D. R., and S. J. Walsh, 1994. Site characteristics of debris flows and their relationship to alpine treeline. *Physical Geography* 15 (2): 181-199.

Butler, D. R., G.P. Malanson, and S. J. Walsh, 1992. Snow-avalanche paths: conduits from the periglacial-alpine to the subalpine-depositional zone. In: *Periglacial Geomorphology*, pp. 185-202. John Wiley and Sons, ltd.

Butler, D. R., G. P. Malanson, F. D. Wilkerson, and G. L. Schmid, 1998. Late Holocene Sturzstroms in Glacier National Park, Montana, U.S.A. In: J. Kalvoda and C. Rosenfeld (Eds.), *Geomorphological Hazards in High Mountain Areas*, Geojournal Library, Kluwer Academic Publishers, Dordrecht, The Netherlands, pp. 149-166.

Case, J.C., 1989, Wyoming landslide classification scheme. Geologic Hazards Section, Wyoming State Geological Survey. www.wrds.uwyo.edu (Last accessed July 2010).

Coe, J. A., J. W. Godt, M. Parise, and A. Moscariello, 2003. Estimating debris-flow probability using fan stratigraphy, historic records, and drainage-basin morphology, Interstate 70 highway corridor, central Colorado, U.S.A. In: D. Rickenmen and C. Chen (Eds.), *Debris-Flow Hazards Mitigation: Mechanics, Prediction, and Assessment*. Millpress, Rotterdam, The Netherlands.

Corominas, J., Remondo, J., Farias, P., Estevao, M., Zezere, J., Diaz de Teran, J., Dikau, R., Schrott, L., Moya, J., Gonzales, A., 1996. Debris Flow. In Landslide Recognition: Identification, Movement and Causes, Dikau, R., Brundsen, D., Schrott, L., Ibsen, M.-L (Ed). John Wiley & Sons, pp. 161-180.

Costa, J., 1984. Physical geomorphology of debris flows. In: I. Douglas (Eds.), *Developments and Applications of Geomorphology*. Springer-Verlag, Berlin, Heidelberg, Germany. pp. 268-312

Cruden, D. M., 1976. Major rock slides in the Rockies. *Canadian Geotechnical Journal* 13 (1): 8-20.

Cruden, D.M., and D. J. Varnes, 1996: Landslide types and process: In: A.K. Turner and R. L. Schuster (Eds.), *Landslides: Investigation and mitigation.* Special Report 247, Transportation Research Board, National Research Council, Washington, DC, (673 pp.): pp. 36-75.

Department of the Interior, August 2010. Grand Teton National Park and John D. Rockefeller, Jr. Memorial Parkway: Geologic Resources Inventory Report. Natural Resource Report NPS/NRPC/GRD/NRR—2010/230.

Dirks, R. A., and B. E. Martner, 1982. *The climate of Yellowstone and Grand Teton National Parks.* U.S. Department of the Interior/National Park Service Occasional Paper Number Six.

Ellen, S. D. and R.K. Mark, 1993. Mapping debris flow hazard in Honolulu using a DEM, *1993 Hydraulic Engineering Conference Proceedings* 2: 1774-1779.

Erschbamer, B., 1989. Vegetation on avalanche paths in the Alps. *Vegetation* 80: 139-146.

Flageollet, J. C., and D. Weber, 1996. Fall. In: Dikau, R., Brunsden, D., Schrott, L., and Ibsen, M. L. (Eds.), *Landslide recognition: Identification, Movement, and Causes*. John Wiley and Sons Ltd., Chichester, UK. pp 13-28.

Forest Service, n.d.. "A Brief History of the Gros Ventre Slide Geological Site." http://www.fs.usda.gov/Internet/FSE_DOCUMENTS/stelprdb5340454.pdf (Last accessed August 26, 2012).

Foster, D., S. H. Brocklehurst, and R. L. Gawthorpe, 2010. Glacial-topographic interactions in the Teton Range, Wyoming. *Journal of Geophysical Research* 115: F01007, doi:10.1029/2008JF001135.

Fryxell, F. M., and L. Horberg, 1943. Alpine mudflows in Grand Teton National Park, Wyoming. *Bulletin of the Geological Society of America* 54: 457-472.

Geonex Program Development, Inc., 1992. Geology of Grand Teton National Park and surrounding area. *U.S. Department of the Interior, National Park Service, Grand Teton National Park, Science and Resource Management, GIS Office.* Geospatial Dataset-1034504.

Gerrard, J., 1994. The landslide hazard in the Himalayas: geological control and human action. *Geomorphology* 10: 221-230.

Goudie, A. S. 2006. The Schmidt Hammer in geomorphological research. *Progress in Physical Geography* 30 (6): 703-718.

Guzzetti, F., P. Reichenbach, and G. F. Wieczorek, 2003. Rockfall hazard and risk assessment in Yosemite Valley, California, USA. *Natural Hazards and Earth System Sciences* 3: 491-503.

Hallet, B., L. Hunter, and J. Bogen (1996), Rates of erosion and sediment evacuation by glaciers: A review of field data and their implications, *Global Planet. Change* 12: 213 – 235. doi:10.1016/0921-8181(95)00021-6.

Hampel, R. 1977. Geschiebewirtschaft in WildbaÈchen. *Zeitschrift des Vereins der Diplomingenieure der Wildbach und Lawinenverbauung sterreichs*, 4: 53-144.

Harp, E.L., R.C. Wilson, and G. F. Wieczorek, 1981. Landslides from the February 4, 1976, Guatemala Earthquake, *U.S. Geological Survey Professional Paper 1204-A.*

Harvey, A., 2012. *Introducing Geomorphology*. Dunedin Academic Press, Ltd., Edinburgh, Scotland, UK. pp. 65

Hopfinger, E. J. 1983. Snow avalanche motion and related phenomena. *Annual Review of Fluid Mechanics* 15: 47-76.

Hungr, O., 2007. Dynamics of Rapid Landslides. In: Sassa, K., Fukuoka, H., Wang, F., and G. Wang (Eds.), *Progress in Landslide Science*. Springer, Berlin, Heidelberg, Germany; New York, NY. pp. 47-57.

Hungr, O., G. C. Morgan, and R. Kellerhals, 1984. Quantitative analysis of debris torrent hazards for design of remedial measures. *Canadian Geotechnical Journal* 21: 663-677.

Ikeya, H., 1981. A method of designation for areas in danger of debris flow, in Erosion and sediment transport in Pacific Rim steeplands. *International Association of Hydrological Sciences, Christchurch, New Zealand* 132: 576-587.

Ikeya, H. and T. Mizuyama, 1982. Flow and deposit properties of debris flow. *Public Works Research Institute, Tsukuba, Japan*, Report 157-2: pp. 88-153.

Jakob, M., and O. Hungr, 2005a. Classification and terminology of debris flows and avalanches, in *Debris-flow Hazards and Related Phenomena*. Praxis Publishing, Ltd., Chichester, UK., pp. 9-16.

Jakob, M., and O. Hungr, 2005b. *Debris-flow Hazards and Related Phenomena.* Praxis Publishing, Ltd., Chichester, UK., pp. 37.

Jakob, M., Bovis, M., and M. Oden, 2005. The significance of channel recharge rates for estimating debris-flow magnitude and frequency. *Earth Surface Processes and Landforms* 30 (6): 755-766.

Jobes, P. 1992. Population and social characteristics in the Greater Yellowstone Ecosystem. *Society and Natural Resources* 6: 149-163.

Johnson, A. M., 1970. *Physical processes in geology*. Freeman, Cooper, and Co., San Francisco, California. pp. 576

Johnson, A.M., and J. R. Rodine, 1984. Debris Flow. In *Slope Instability*, Brunsden, F., Prior, D.B., (Eds.), John Wiley and Sons, New York, NY. pp. 257-361.

Johnson, P. A., R. H. McCuen, and T. V. Hromadka, 1990. Magnitude and frequency of debris flows. *Journal of Hydrology* 123: 69-82.

Keefer, D. K., 1994. The importance of earthquake-induced landslides to long-term slope erosion and slope-failure hazards in seismically active regions. *Geomorphology* 10: 265-284.

Keefer, D. K., 2002. Investigating landslides caused by earthquakes – a historical review. *Surveys in Geophysics* 23: 473-510.

Kronfellner-Kraus, G. 1982. Torrent erosion and its control in Europe and some research activities in the field in Austria. *SABO – The Erosion-Control Engineering Society of Japan* 3: 33-44.

Lacroix, P., J. R. Grasso, J. Roulle, G. Giraud, D. Goetz, S. Morin, and A. Helmstetter, 2012. Monitoring of snow avalanches using a seismic array: Location speed estimation, and relationships to meteorological variables. *Journal of Geophysical Research* 117: F01034.

Lageson, D.R. and Spearing, D.R. 1991. *Roadside Geology of Wyoming*. *2nd ed.* Mountain Press Publishing Co., Missoula, Montana. pp. 271.

Lindstrom P. 2005. Precipitation grid for Grand Teton NP, John D. Rockefeller Jr. MP, and Yellowstone NP, WY, MT, ID, 1971-2002. *U.S. Department of the Interior, National Park Service, Grand Teton National Park, Science and Resource Management, GIS Office.* Geospatial Dataset-1036862.

Love, J. D., J. C. Reed, Jr., and A. C. Christiansen., 1992. (Reprinted 2000). Geologic map of Grand Teton National Park, Teton County, Wyoming (scale 1:62,500). *Miscellaneous Investigations Series Map I-2031*. U.S. Geological Survey, Reston, Virginia, USA.

Love, J. D., J. C. Reed, Jr., and K. L. Pierce., 2003. Creation of the Teton landscape: A geological chronicle of Jackson Hole and the Teton Range. *Grand Teton Natural History Association*. Moose, Wyoming, USA.

Luckman, B. H., 1977. The geomorphic activity of snow avalanches. *Geografiska Annaler* 59 (1): 31-48.

Luckman, B. H., 1978. Geomorphic work of snow avalanches in the Canadian Rocky Mountains. *Arctic and Alpine Research* 10(2); 261-276.

Mahaney, W.C., 1990. Neoglacial chronology and floristics in the Middle Teton area, central Teton Range, Western Wyoming: *Journal of Quaternary Science* 1: p. 53-66.

Malanson, G. P., and D. R. Butler, 1984. Transverse patterns of vegetation on avalanche paths in the northern Rocky Mountains, Montana. *Great Basin Naturalist* 44: 453-458.

Malanson, G.P., and D. R. Butler, 1986. Floristic patterns on avalanche paths in the Northern Rocky Mountains, U.S.A. *Physical Geography* 7 (3): 231-238.

Marston, R. A., B. J. Weihs and W. D. Butler, 2010. Slope failure and cross-valley profiles, Grand Teton National Park, Wyoming. *University of Wyoming-National Park Service Research Center 33rd Annual Report 2010*. pp 51-64.

Matsuoka, N., H. Kazuomi, T. Watanabe, W. Haeberli, and F. Keller, 1998. The role of diurnal, annual and millennial freeze-thaw cycles in controlling alpine slope instability. *Permafrost – Seventh International Conference (Proceedings), Yellowknife (Canada), Collection Nordiana No. 55,* 711-717.

Mears, A. I., 1975. Dynamics of dense-snow avalanches interpreted from broken trees. *Geology* 3: 521-523.

Mizuyama, T. 1982. Analysis of sediment yield and transport data for erosion and control works. *Recent Development in the Explanation and Prediction of Erosion and Sediment Yield, Proceedings of Exeter Symposium, International Association of Hydraulics Research* 137: 177-182.

Montgomery, D. 2002. Valley formation by fluvial and glacial erosion. *Geology* 30: 1047-1050.

Moon, B. P. 1984. Refinement of a technique for determining rock mass strength for geomorphological purposes. *Earth Surface Processes and Landforms* 9: 189-193.

Moon, B. P., and Selby, M. J. 1983. Rock mass strength and scarp forms in southern Africa. *Geografiska Annaler.* 65 A (1-2): 135-145.

National Atlas of the United States. "Landslide Types and Processes." Adapted from July 2004 *USGS Fact Sheet 2004-3072, Version 1.0.* http://nationalatlas.gov/articles/geology/a_landslide.html#one (Last accessed 8/20/2012).

National Park Service. "National Park Service Visitor Summary Report Total Recreation Visits for December, 2010." http://www.nature.nps.gov/stats/viewReport.cfm?selectedReport=SystemYTDByPark.cfm (Last accessed March 11, 2011).

National Park Service, February 25, 2011. "Backcountry Skier Injured in Slab Avalanche in Granite Canyon." http://www.nps.gov/grte/parknews/backcountry-skier-injured-in-slab-avalanche-in-granite-canyon.htm (Last accessed August 25, 2012).

National Park Service, June 17, 2011. "Late Season Avalanche Hazard Cause for Concern in Snowy Teton Range." http://www.nps.gov/grte/parknews/avalanche-hazard.htm (Last accessed August 25, 2012).

National Park Service, March 8, 2012. "Rangers Recover Bodies of Two Missing Backcountry Skiers." http://www.nps.gov/grte/parknews/news-release-12-14a.htm (Last accessed August 25, 2012).

National Park Service, March 9, 2012. "More Details Emerge in Death of Backcountry Skiers." http://www.nps.gov/grte/parknews/news-release-12-15.htm (Last accessed August 25, 2012).

National Park Service, July 6, 2012. "Injured Man Rescued from the Grand Teton." http://www.nps.gov/grte/parknews/news-release-12-50.htm (Last accessed August 25, 2012).

Owen, G., J.A. Matthews, and P. G. Albert. 2007. Rates of Holocene chemical weathering, 'Little Ice Age' glacial erosion and implications for Schmidt-hammer dating at a glacier-foreland boundary, Fåbergstølsbreen, southern Norway. *The Holocene* 17 (6): 829-834.

Parise, M., 2002. Landslide hazard zonation of slopes susceptible to rock falls and topples. *Natural Hazards and Earth System Sciences* 2: 37-49.

Patten, R. S. and D. H. Knight. 1994. Snow avalanches and vegetation pattern in Cascade Canyon, Grand Teton National Park, Wyoming, U.S.A. *Arctic and Alpine Research* 26 (1): 35-41.

Porter, S. C. and Orombelli, G., 1981. Alpine rockfall hazards. *Am. Scientist* 69: 67–75.

Schumm, S. A., and R. W. Lichty. 1965. Time, space, and causality in geomorphology. *American Journal of Science* 263: 110-119.

Selby M. J. 1980. A rock mass strength classification for geomorphic purposes: with tests from Antarctica and New Zealand. *Zeitschrift für Geomorphologie* 24: 31–51.

Selby, M. J. 1982. Rock mass strength and the form of some inselbergs in the Central Namib Desert. *Earth Surface Processes and Landforms* 7: 489-497.

Sidle, R. C., and H. Ochiai, 2006. Landslides – Processes, Prediction, and Land Use. *American Geophysical Union*, 26-29 pp.

Smith, R.B., J. R. Pelton, and J. D. Love, 1976. Seismicity and the possibility of earthquaked related landslides in the Teton-Gros Ventre-Jackson Hole area, Wyoming. *Contributions to Geology* 14 (2): 57-64.

Stiny, J., 1910. *Die Muren.* Verlag der Wagner'schen Universtäts-buchhandlung, Innsbruck. *Debris Flows* (English translation by M. Jackob and N. Skermer, 1997, pp. 106). EBA Engineering Consultants, Vancouver, Canada.

Stoffel, M., I. Lievre, D. Conus, M.A. Grichting, H. Raetzo, H. W. Gartner, and M. Monbaron., 2005. 400 years of debris-flow activity and triggering weather conditions: Ritigraben, Valais, Switzerland. *Arctic, Antarctic, and Alpine Research* 37 (3): 387-395.

Stroeven, A. P., C. Hättestrand, J. Heyman, J. Harbor, Y. K. Li, L. P. Zhou, M. W. Caffee, H. Alexanderson, J. Kleman, H. Z. Ma, and G.N. Liu, 2009. Landscape analysis of the Huang He headwaters, NE Tibetan Plateau – Patterns of glacial and fluvial erosion. *Geomorphology* 103: 212-226.

Takahashi, T., 1981. Estimation of potential debris flows and their hazardous zones: soft countermeasures for a disaster, *Journal of Natural Disaster Science*, 3: 57-89.

Thomas, D.S.G. and A. Goudie, (eds), 2000. A *dictionary of physical geography*. 3rd edition. Blackwell Publishers Ltd, Malden, MA.

Thurber Engineering Ltd. 1983. Debris torrent and flooding hazards, Highway 99, Howe Sound. *Report to Ministry of Transportation and Highways*. British Columbia, Vancouver.

Topal, T., M. K. Akin, and M. Akin., 2012. Rockfall hazard analysis for an historical castle in Katamonu (Turkey). *Natural Hazards* 62: 255-274.

U.S. Geological Survey (USGS), 2004. Landslide Types and Processes. *U.S. Geological Survey Fact Sheet 2004-3072,* Version 1.0.

VanDine, D. F. 1985. Debris flows and debris torrents in the southern Canadian Cordillera. *Canadian Geotechnical Journal* 22: 44-67.

Vankat, J.L., 1979. *The Natural Vegetation of North America*. Krieger Publishing, Malbar (FL).

Varnes, D.J., 1958. Landslide types and processes. In: E. B. Eckel (Ed.), Landslides and engineering practice. *Highway Research Board, Special Report* 29, 20-47.

Varnes, D.J., 1978. Slope movement types and processes. In: R.L. Schuster and R.J. Krizek (Eds.), *Landslide analysis and control.* Transport Resource Board Special Report 176. Washington D.C.: National Academy of Sciences, 11-33.

Vaughn, D. M., 1997. A major debris flow along the Wasatch Front in northern Utah, USA. *Physical Geography* 18 (3): 246-62.

Viles, H., A. Goudie, S. Grab, and J. Lalley, 2011. The use of Schmidt Hammer and Equotip for rock hardness assessment in geomorphology and heritage science: a comparative analysis. *Earth Surface Processes and Landforms* 36 (3): 320-333.

Walsh, S. J., and D. R. Butler, 1997. Morphometric and multispectral image analysis of debris flows for natural hazard assessment. *Geocarto International* 12 (1); 59-70.

Walsh, S. J., Butler, D. R., Brown, D. G., and L. Bian, 1990. Cartographic modeling and snow avalanche path location within Glacier National Park, Montana. *Photogrammetric Engineering and Remote Sensing* 56 (5): 615-621.

Whalley, W. B., 1984. Rockfalls. In: D. Brunsden, and D. B. Prior, (Eds.), *Slope Instability*. John Wiley and Sons Ltd., Chichester, UK. pp. 217-256.

Whitlock, C. 1993. Postglacial vegetation and climate of Grand Teton and Southern Yellowstone National Parks. *Ecological Monographs* 63 (2): 173-198

White, B. J. P., Smith, R. B., Husen, S., Farrell, J. M., and I. Wong, 2009. Seismicity and earthquake hazard analysis of the Teton-Yellowstone region, Wyoming.

Wilkerson, F. D., 2004. The spatial and temporal hazard of debris flows in Glacier National Park, Montana. Dissertation, Texas State University – San Marcos Department of Geography.

Youssef, A. M., and N. H. Maerz, 2012. Development, justification, and verification of a rock fall hazard rating system. *Bull. Eng. Geol. Environ.* 71: 171-186.

APPENDIX A - STUDY SITE PHOTOGRAPHS

Figure A-1: Cascade Canyon, south-facing slope, study site #1
Latitude: 43.45896 N **Longitude:** 110.44959 W **Elevation:** 2147 m

Figure A-2: Cascade Canyon, south-facing slope, study site #2
Latitude: 43.45939 N **Longitude:** 110.45314 W **Elevation:** 2247 m

Figure A-3: Cascade Canyon, south-facing slope, study site #3
Latitude: 43.45799 N **Longitude:** 110.45650 W **Elevation:** 2285 m

Figure A-4: Cascade Canyon, south-facing slope, study site #4
Latitude: 43.45818 N **Longitude:** 110.46096 W **Elevation:** 2286 m

Figure A-5: Cascade Canyon, south-facing slope, study site #5
Latitude: 43.45805 N **Longitude:** 110.46419 W **Elevation:** 2295 m

Figure A-6: Cascade Canyon, south-facing slope, study site #6
Latitude: 43.45806 N **Longitude:** 110.46803 W **Elevation:** 2316 m

Figure A-7: Cascade Canyon, south-facing slope, study site #7
Latitude: 43.45834 N **Longitude:** 110.47179 W **Elevation:** 2325 m

Figure A-8: Cascade Canyon, south-facing slope, study site #8
Latitude: 43.34868 N **Longitude:** 110.47553 W **Elevation:** 2343 m

Figure A-9: Cascade Canyon, south-facing slope, study site #9
Latitude: 43.45876 N **Longitude:** 110.47937 W **Elevation:** 2355 m

Figure A-10: Cascade Canyon, south-facing slope, study site #10
Latitude: 43.45871 N **Longitude:** 110.48344 W **Elevation:** 2365 m

Figure A-11: Death Canyon, south-facing slope, study site #1
Latitude: 43.39327 N **Longitude:** 110.48484 W **Elevation:** 2061 m

Figure A-12: Death Canyon, south-facing slope, study site #2
Latitude: 43.39375 N **Longitude:** 110.48880 W **Elevation:** 2091 m

Figure A-13: Death Canyon, south-facing slope, study site #3
Latitude: 43.39509 N **Longitude:** 110.49235 W **Elevation:** 2223 m

Figure A-14: Death Canyon, south-facing slope, study site #4
Latitude: 43.39635 N **Longitude:** 110.49577 W **Elevation:** 2341 m

Figure A-15: Death Canyon, south-facing slope, study site #5
Latitude: 43.39867 N **Longitude:** 110.49770 W **Elevation:** 2389 m

Figure A-16: Death Canyon, south-facing slope, study site #6
Latitude: 43.40020 N **Longitude:** 110.50105 W **Elevation:** 2400 m

Figure A-17: Death Canyon, south-facing slope, study site #7
Latitude: 43.39889 N **Longitude:** 110.50474 W **Elevation:** 2409 m

Figure A-18: Death Canyon, south-facing slope, study site #8
Latitude: 43.39889 N **Longitude:** 110.50858 W **Elevation:** 2455 m

Figure A-19: Death Canyon, south-facing slope, study site #9
Latitude: 43.39921 N **Longitude:** 110.51251 W **Elevation:** 2482 m

Figure A-20: Death Canyon, south-facing slope, study site #10
Latitude: 43.40036 N **Longitude:** 110.51590 W **Elevation:** 2519 m

Figure A-21: Garnet Canyon, south-facing slope, study site #1
Latitude: 43.43412 N **Longitude:** 110.46222 W **Elevation:** 2612 m

Figure A-22: Garnet Canyon, south-facing slope, study site #2
Latitude: 43.43488 N **Longitude:** 110.46571 W **Elevation:** 2669 m

Figure A-23: Garnet Canyon, south-facing slope, study site #3
Latitude: 43.43517 N **Longitude:** 110.46918 W **Elevation:** 2736 m

Figure A-24: Granite Canyon, south-facing slope, study site #1
Latitude: 43.37036 N **Longitude:** 110.49097 W **Elevation:** 2058 m

Figure A-25: Granite Canyon, south-facing slope, study site #2
Latitude: 43.36906 N **Longitude:** 110.49477 W **Elevation:** 2139 m

Figure A-26: Granite Canyon, south-facing slope, study site #3
Latitude: 43.36906 N **Longitude:** 110.49873 W **Elevation:** 2168 m

Figure A-27: Granite Canyon, south-facing slope, study site #4
Latitude: 43.36958 N **Longitude:** 110.50.237 W **Elevation:** 2212 m

Figure A-28: Granite Canyon, south-facing slope, study site #5
Latitude: 43.37001 N **Longitude:** 110.50614 W **Elevation:** 2253 m

Figure A-29: Granite Canyon, south-facing slope, study site #6
Latitude: 43.36968 N **Longitude:** 110.50999 **Elevation:** 2295 m

Figure A-30: Granite Canyon, south-facing slope, study site #7
Latitude: 43.36972 N **Longitude:** 110.51443 W **Elevation:** 2310 m

Figure A-31: Granite Canyon, south-facing slope, study site #8
Latitude: 43.36991 N **Longitude:** 110.51833 W **Elevation:** 2348 m

Figure A-32: Granite Canyon, south-facing slope, study site #9
Latitude: 43.37030 N **Longitude:** 110.52211 W **Elevation:** 2382 m

Figure A-33: Paintbrush Canyon, south-facing slope, study site #1
Latitude: 43.48221 N **Longitude:** 110.45368 W **Elevation:** 2291 m

Figure A-34: Paintbrush Canyon, south-facing slope, study site #2
Latitude: 43.48134 N **Longitude:** 110.45687 W **Elevation:** 2295 m

Figure A-35: Paintbrush Canyon, south-facing slope, study site #3
Latitude: 43.48003 N **Longitude:** 110.46017 W **Elevation:** 2387 m

Figure A-36: Paintbrush Canyon, south-facing slope, study site #4
Latitude: 43.47881 N **Longitude:** 110.46349 W **Elevation:** 2429 m